1969

An experimental transfer function relating oxyhemoglobin concentration to blood flow rate in the canine hind limb and its use in controlling an artificial heart

Robert Allan Peura
Iowa State University

AN EXPERIMENTAL TRANSFER FUNCTION RELATING OXYHEMOGLOBIN CONCENTRATION TO BLOOD FLOW RATE IN THE CANINE HIND LIMB AND ITS USE IN CONTROLLING AN ARTIFICIAL HEART

by

Robert Allan Peura

A Dissertation Submitted to the

Graduate Faculty in Partial Fulfillment of

The Requirements for the Degree of

DOCTOR OF PHILOSOPHY

Major Subjects: Electrical Engineering
Biomedical Engineering

Approved:

Signature was redacted for privacy.

In Charge of Major Work

Signature was redacted for privacy.

Head of Major Department

Signature was redacted for privacy.

Dean of Graduate College

Iowa State University
Ames, Iowa

1969

TABLE OF CONTENTS

INTRODUCTION

The purpose of this research was twofold. The chief purpose was to characterize the transient (dynamic) response involved in the autoregulation of blood flow in skeletal muscle. A transfer function was determined relating arterial oxyhemoglobin concentration (% saturation of hemoglobin with oxygen) as the input, to blood flow rate as the output. Autoregulation is a local mechanism by which the tissues of the body govern their own blood flow rate independent of central nervous system control. Blood oxyhemoglobin concentration (% HbO_2) has been documented as an important controlling parameter involved in the autoregulation of tissue blood flow especially in skeletal and cardiac muscle (39). Much work has been done in characterizing the steady state relationships between % HbO_2 and flow rate, but little work has been done in measuring the dynamic response of these parameters.

The second purpose of this investigation was to determine the feasibility of using the experimental transfer function, described above, in the design of a control system for an artificial heart. The objective of Part II of the dissertation was to determine the <u>in vitro</u> dynamic characteristics of the artificial heart power and control systems. A transfer function was found relating the input control signal of the artificial heart to the artificial ventricle output flow rate. The objective of Part III of the dissertation was to design and test an artificial heart control system which utilizes arterial oxyhemoglobin concentration level as the input control signal. A series of experiments

was designed to test the feasibility of using this type of artificial heart control system. Various degrees of whole body hypoxia were used as perturbations to the animal-machine system.

PART I. AN EXPERIMENTAL TRANSFER FUNCTION RELATING ARTERIAL OXYHEMOGLOBIN CONCENTRATION TO BLOOD FLOW RATE IN THE CANINE HIND LIMB

REVIEW OF THE LITERATURE

Autoregulation of Blood Flow

Autoregulation is a local mechanism by which the tissues of the body govern their own blood flow independent of central nervous system control.

The genesis of the concept of local autoregulation is based on the experiments of Bayliss in 1902 (3). He observed that the vascular bed in a denervated limb tends to change its resistance to maintain a constant flow rate in response to changes in perfusion pressure.

Roy and Brown in 1879 were the first to suggest that the regulation of blood flow in tissue beds might be determined by the nutrient demands of the local tissue bed (66). They postulated that the local blood flow was regulated according to the tissue needs for oxygen or other important nutrient constituents.

Nicoll and Webb (55) in 1955 observed microscopically the physiological behavior of capillaries in the bat wing. They found that neural control was not fundamental for the regulation of adequate capillary conditions. In individual terminal arterioles active vasomotion established alternate periods of vigorous flow and reduced flow or no flow. They found that local chemical and physical conditions in the environment of the terminal arterioles regulated the magnitude and frequency of the vasomotor activity observed. The availability of oxygen was a prime determinant in the activity of the precapillary sphincters. Unanesthetized bats with denervated wings were subjected to various O_2 concentrations of the respiratory gas. The duration and magnitude of the contraction phase of the sphincters was sharply reduced with oxygen poor mixtures, as

compared to 100% O_2 rich gas. When 100% helium was used, the sphincters appeared to lose their ability to constrict.

Two recent review papers on autoregulation of blood flow by Walker (80) and Johnson (44) summarize the present status and current theories concerning the subject. Autoregulatory activity has been observed in skeletal muscle (39), kidney (72), myocardium (58), brain (64), intestine (43) and liver (5).

Guyton et al. (39) have found a high degree of correlation between the local regulation of blood flow and oxygen demand of the tissues.

Crawford et al. (17) used a perfusion system which provided either venous blood, arterial or various mixtures of these, at a constant pressure to the isolated canine hind limb. They found that when the level of blood oxygen saturation (%HbO_2) was altered between completely arterial blood and completely venous blood that the flow rate always increased when changing toward venous %HbO_2 levels. The flow rate always decreased when changing toward arterial %HbO_2 levels. The change in flow began immediately and reached a maximum or minimum stable level in approximately 2 minutes. When the %HbO_2 was changed from 91 to 30 the flow rate increased an average of 2.08 times the control value.

By decreasing the %HbO_2 level in gradual steps from completely arterial to completely venous blood they found a progressive increase in flow as the blood was desaturated. The blood flow increased an average of 2.5 times as the %HbO_2 was changed from 100 to 30. However, they showed that the oxygen availability (flow rate times %HbO_2) when the %HbO_2 was 30 had only decreased to 75% of the control value. It should be noted that oxygen availability is an exact indication of oxygen transport from the

blood to the tissues only for the case when the venous saturation level is maintained at a constant level. A more accurate indication of the exact amount of oxygen transported from the blood to the tissues is found by multiplying the flow rate by the $\%HbO_2$ arteriovenous difference. Crawford et al. concluded that the autoregulatory reaction compensated for the decrease in oxygen availability that would have occurred had the reaction not taken place.

In another group of animals the effect of carbon dioxide changes on the rate of blood flow in the perfused hind limb was studied. These animals, under spinal anesthesia, breathed 20% carbon dioxide with mixtures of oxygen and nitrogen for one hour. No appreciable increase in blood flow rate was observed. Since the carbon dioxide concentration did not affect the blood flow rate in the hind limb, it was concluded that the increase in flow rate observed when the blood oxygen saturation was changed from completely arterial to completely venous was due solely to the change in $\%HbO_2$ and not to the excess carbon dioxide of the venous blood.

Since some investigations indicated that vasodilator factors exist in venous blood, Ross et al. (65) using deoxygenated arterial blood instead of venous blood, perfused the same type hind limb preparation as that o Crawford et al. (17), described above. Using a double-lumen catheter th two lungs were respirated separately. The left lung was respirated with a mixture of oxygen and nitrogen. In this way the $\%\ HbO_2$ for the perfused hind limb was decreased, in a stepwise fashion, between 100 and 0. The right lung was used to oxygenate the blood for the rest of the animal's circulation. The dogs with total spinal anesthesia demonstrated an increase in flow 3.4 times normal as the $\%\ HbO_2$ was changed from 100 to 10.

For normal dogs (no spinal anesthesia) an increase in flow of 3 times normal was observed as the % HbO_2 was changed from 100 to 0.

Their results supported the findings of Crawford et al. (17) both qualitatively and almost exactly quantitatively. The results obtained with normal dogs and dogs with total spinal anesthesia were essentially the same. The conclusion might be drawn that the oxygen lack vasodilator effect is essentially independent of nervous system control.

Carrier et al. (10, 11) investigated the role of oxygen in the control of local blood flow. Isolated arterial segments from minute coronary, mesenteric and skeletal muscle arteries were perfused with blood in which the arterial Po_2 was in the normal physiologic range. The results of their experiments indicated that changes in arterial oxygen tension between 100 and 30 mmHg caused the blood flow to rise 1.76 times the control level in skeletal muscle vessels, to 1.58 times control in the coronary vessels, and to 1.47 times control in the mesenteric vessels. Since no tissue other than the isolated blood vessel was involved, these experiments demonstrated that the vasodilation was due to the effect of oxygen lack per se and not a vasodilation substance from the extravascular tissue. It was concluded that oxygen could be a major factor in the control of local blood flow.

Reactive hyperemia has been studied by Fairchild et al. (31). Using the same lung oxygenator and hind limb preparation as Ross et al. (65), reactive hyperemia was initiated by occluding the arterial inflow to the hind limb for 3 to 10 minutes. With blood perfusion of zero %HbO_2 the blood vessels remained dilated, indicating no recovery from reactive hyperemia. However, when the perfusion blood was reoxygenated, complete

recovery from reactive hyperemia took place. These experiments indicate that oxygen is essential for the blood flow to return to the control level during reactive hyperemia. Fairchild et al. postulated that the smooth muscle of the resistance vessels relax in reactive hyperemia because of either insufficient oxygen to maintain adequate contraction, or because of the depletion of ATP or other oxygen-dependent energy substrates in the smooth muscle cells.

Walker and Guyton (81, 82) determined the pressure-flow curves of isolated dog hind limbs for various levels of oxygen content. The perfusion pressure was varied between 25 to 175 mmHg and the flow rate for various oxygen content levels was observed when equilibrium was reached.

Two types of experiments were performed, hyperbaric and normobaric. In the hyperbaric experiments, the isolated hind limb was perfused with Tyrode's solution, to which 6 percent dextran had been added. The oxygen content of this solution was varied by changing the atmospheric pressure of the solution. The results of the hyperbaric experiments showed that an increased oxygen content was associated with a decreased flow rate.

The normobaric experiments were conducted using blood supplied by a support dog. The $\%HbO_2$ level was varied by adjusting the concentration of nitrogen in the inspired air of the support dog. Walker and Guyton noted that the flow rate change in response to a change in $\%HbO_2$ was asymptotic, reaching equilibrium in approximately 3 minutes.

Figure 1 shows the averaged composite pressure-flow curves for 7 isolated hind limb preparations. These curves show that between the

perfusion pressure ranges of about 50 to 150 mmHg, the flow rate does not change appreciably for a given $\%HbO_2$ level. This plateau region represents an attempt of the vascular bed to maintain a constant flow rate irrespective of the perfusion pressure. The fact that the plateau region of the pressure-flow curves rose with lower levels of $\%HbO_2$ indicates that the vascular resistance is dependent on the arterial oxygen content.

From their experimental results, Walker and Guyton (81, 82) concluded that within the ranges of about 50-150 mmHg perfusion pressure and 100-60 arterial $\%HbO_2$, the adjustments in flow rate were very nearly what would be required to assure a constant delivery of oxygen to the local tissue vascular bed.

Detar and Bohr (23) have found that oxygen tension is an important determinant of the contractile tension developed in isolated strips of rabbit aorta. The contractile response to epinephrine was found to be linearly related to Po_2 level of the bath solution between the levels of 100 mmHg and less than 1 mmHg. The tension decreased for a decrease in the Po_2 level. Detar and Bohr measured the time constant of contractile tension for rapid increases and decreases in oxygen tension. A time constant was defined to be the time in minutes from the beginning of the recorded Po_2 change to the point where 63% of the maximal steady state mechanical tension was reached. The input Po_2 changed exponentially, reaching steady state in approximately one minute. For a decrease in oxygen tension from 100 mmHg to a lower steady state value, during sustained contraction produced by epinephrine, the time constant for the decreased contractile tension was less than 4 minutes. For the case where the smooth muscle was stimulated with epinephrine near the end of a 15 minute

hypoxic period an increase in Po_2 to 100 mmHg caused the contractile tension to increase with a time constant less than 2.5 minutes, provided that the Po_2 during hypoxia was greater than 5 mmHg.

Detar and Bohr assumed that the dependence of contractile tension on Po_2 is based on the assumption that oxygen plays a metabolic role within the smooth muscle cells mitochondria. The oxygen acted as the final electron acceptor in the respirator chain.

One theory explaining the mechanism by which autoregulation of blood flow due to the lack of oxygen per se is discussed by Guyton (36). The small arterioles, meta-arterioles and capillaries of a local tissue bed have strong, sparse and highly active smooth muscle fibers. The vascular smooth muscle of the capillary is the precapillary sphincter located at the origin of the capillary. As mentioned previously in the discussion of Nicoll and Webb's experiment (55), active vasomotion of alternate periods of vigorous flow and reduced flow or no flow is found in capillary beds. Neural control was not found to be necessary for regulation of this vasomotor activity but the local chemical and physical conditions in the environment regulated the vasomotor activity. The strength of contraction of the vascular smooth muscle increases with increased oxygen concentration and vice versa.

The tissue cells and the vascular smooth muscle are in competition for the available oxygen in the extravascular space. If this available oxygen should decrease due to either high utilization of oxygen by the local tissue cells or low flow rates, then the vascular smooth muscle will dilate increasing the flow rate. More oxygen will become available for

both the local tissue cells and vascular smooth muscle. With this increase in oxygen availability, the vascular smooth muscle will contract causing a decrease in the flow rate to the local tissue bed and thus another vasomotor cycle will be initiated. Guyton (36) further suggests that when many capillaries supply a local tissue bed that the cyclic nature of the precapillary sphincters will not occur, but rather that a certain portion of the spincters will remain open while the rest remain closed. The number of capillaries that remain open is proportional to the oxygen concentration approximately midway between that necessary to cause closure of the precapillary sphincters and that required to cause them to open. In this manner the autoregulation of local blood flow could be accomplished by alterations in the oxygen availability.

Transfer Functions Measured in the Cardiovascular System

There has been a limited amount of research concerning the measurement of transfer functions describing the cardiovascular system as a feedback regulator. In a recent review article, Katona (47) has summarized the various attempts to describe the cardiovascular system in engineering terms. Most of this effort has been concentrated on describing the regulation of blood pressure by the baroreceptor reflex.

Warner (83, 85) examined the frequency-dependent nature of blood pressure regulation by the carotid sinus pressoreceptors. An electrical analog of the pressure regulating mechanism was connected in parallel to the dog's natural pressure regulating system. This artificial system acted as an amplifier of the carotid sinus function. The activity of the natural pressure regulator was evident from the fact that amplification

of carotid sinus function increased the amplitude of the pressure excursions for given forcing functions.

Warner and Cox (86) investigated the effect on the heart rate of stimulation of sympathetic and vagus efferent nerves to the heart. A nonlinear model relating the dynamic relationship between heart rate and the frequency of stimulation of the nerves was derived.

The effects of carotid sinus stimulation on peripheral resistance was studied by Scher and Young (70). Sinusoidal and squarewave pressures were applied to the carotid sinus and the resultant systemic pressure changes were measured. They modeled the efferent side of the system as a pure delay followed by either a first or second order system.

Levison et al. (53) examined in great detail the nonlinear aspects in the regulation of blood pressure by the baroreceptor reflex. A wide variety of inputs were used to examine the nonlinear aspects of the reflex. The model simulating the input-output behavior of the baroreceptor reflex consisted of linear and nonlinear cascade blocks. The input linear section provided high frequency emphasis. The next series block was a rectifier which yielded zero output for inputs less than a given level. A second nonlinear element in the form of a second order system was used to simulate the observed nonlinear behavior of the physiological system. Levison et al. used two additional series linear networks to improve the sinusoidal response of the model.

Katona et al. (48) investigated the segment of the blood pressure regulatory system which changes heart rate due to changes in blood pressure. The normal control loop was not broken, i.e. a closed loop condition was present. Blood pressure disturbances were introduced by

blowing up and then releasing a balloon inserted in the abdominal aorta. The resulting changes in heart rate were recorded and the data was processed using both an analog and digital computer. A nonlinear model was found relating the pressure input to the heart rate.

Clarke et al. (15) in a recent paper have proposed a model of the carotid sinus baroreceptor which relates the nerve spike frequency to the intrasinus pressure. They have correlated the model parameters with specific biologic elements. The model consists of a mechanical filter, a receptor membrane and a digital encoder.

Warner (84) using an R,L,C network analog of the large arteries found transfer functions relating aortic arch pressure to radial, bronchial and femoral arterial pressures in humans and dogs.

Transfer functions relating cerebral perfusion pressure and systemic arterial pressure have been measured by Sagawa et al. (68, 69). A linearized small signal analysis was made of the ischemic response system. The model that was found, using the classical Nyquist and Bode techniques, consisted of a transport lag associated with either a first or second order system. Sagawa et al. found that the cerebral ischemic pressor response was unstable under certain conditions.

Fleischli and Bellville (32) examined the cardiovascular control system by using sinusoidal norepinephrine infusions. Fleischi and Bellville were able to obtain a Bode plot relating peripheral resistance change, as the input, to systemic blood pressure, as the output.

Using a Fourier series transformation of the upstream and downstream indicator-dilution curves, Coulam et al. (16) have found time domain transfer functions for various segments of the circulatory system.

In the preceding discussion it has been shown that much qualitative and quantitative work has been done in examining the static characteristics of the autoregulation of blood flow due to blood oxygen saturation, but there has been little if any work performed concerning the dynamic characteristics of this phenomenon. The sections that follow in this dissertation describe the experimental protocol, the computer program, and the results of the transfer function relating oxyhemoglobin concentration to blood flow rate in the canine hind limb.

APPARATUS

The objective of this portion of the thesis research was to design a constant pressure perfusion system which would allow for changing the blood $\%HbO_2$ levels, in a step wise fashion, from arterial to venous levels and vice versa, using both large and small input $\%HbO_2$ changes. A transfer function relating $\%HbO_2$ as the input, to blood flow as the output, in the canine hind limb was desired. The input-output sampled functions were analyzed as both first and second order systems using a continuous time system identification program.

The perfusion circuit, modified from that of Crawford et al. (17) consisted of a mixing chamber, a constant pressure pump, a rotameter flow-meter, a heat exchanger, a pressure transducer and an oximeter. Figure 2 is a block diagram showing the hind limb perfusion setup.

Blood compatible tubing (3/16"i.d.x5/16"o.d.)[1] was used for the perfusion apparatus. The glass "Y" connectors used were coated with a silicone compound.[2]

The following cannulations were made, the right carotid artery for the animal's systemic pressure, the right femoral artery both centrally and peripherally, the left femoral artery peripherally and ligated centrally, and the right atrium via the right jugular vein.

A shunt section of tubing was inserted between the central and peripheral right femoral artery catheters, to insure that the perfused

---

[1] S-50-HL. Tygon tubing, U.S. Stoneware Inc., Akron, Ohio

[2] Siliclad, Clay Adams Inc., New York, New York

hind limb circulation would only be interrupted only during the short period of the cannulation procedure. When the extra-corporeal perfusion circuit and all the surgery was completed, the shunt section of tubing was closed and the extra-corporeal perfusion circuit instituted.

Two inputs to the mixing chamber were necessary; one for venous blood from the right atrium and the other for arterial blood from the central right femoral artery catheter. Figure 3 is a photograph of the mixing chamber. These two inputs (a is the arterial input and c is the venous input in Figure 3) were mixed to any desired $\%HbO_2$ level, between arterial and venous blood, by means of ten parallel flow paths. To facilitate mixing, small diameter tubes (f in Figure 3) were used to drop the arterial pressure to approximately venous pressure levels.

A typical parallel flow path consisted of small diameter medical grade Silastic[1] tubes, which varied in size from .030"i.d.x.125"o.d. to .078"i.d.x.125"o.d. These tubes were fitted over Luer stub adapters[2] at both ends. These adapters were attached to 4 way stopcocks[3] which were glued to polyethylene "T" connectors[4]. For arterial $\%HbO_2$ levels, a larger diameter Tygon tube (e in Figure 3) was used in the parallel circuit. This tube was attached directly to the "T" connectors. The "T" connectors were attached to each other with short sections of Tygon tubing.

---

[1] Dow Corning., Midland, Michigan

[2] #A-1030/20, A-1030/18, A-1030/15, Clay-Adams Inc., New York, New York

[3] #R62, Travenol Laboratories, Inc., Morton Grove, Illinois

[4] #15-316, Fisher Scientific Co., Chicago, Illinois

For completely venous $\%HbO_2$ levels of perfusion all parallel paths were closed; the Silastic tubes by means of the stopcocks and the arterial parallel path by a tubing hemostat. The venous input tube to the mixing chamber was clamped with a tubing hemostat, and the arterial parallel path was opened for completely arterial $\%HbO_2$ levels of perfusion. A desired level between completely arterial $\%HbO_2$ and venous $\%HbO_2$ was obtained by opening the venous line, closing the arterial parallel path and opening a number of parallel tubes.

In addition to the mixing chamber output leading to the roller pump (d in Figure 3), another output of the mixing chamber supplies the peripheral left femoral artery catheter (b in Figure 3). This output provides for continuous flow through the central right femoral artery catheter, even when the perfusion $\%HbO_2$ is venous blood.

The roller pump[1] occlusion was set for minimum damage to the blood elements according to the directions of the manufacturer. The roller pump was converted from a pulsating constant flow pump to constant pressure source by connecting a Starling's Resistor in shunt with the pump.

Figure 4 is a photograph of the Starling's Resistor. It consists of a lucite tube 6" long X 1"o.d. X 3/4"i.d. inside of which is a concentric 1/4" latex Penrose drainage tube[2]. Each end of the drainage tube was tied to a tapered 1/4"o.d.X3/16"i.d. lucite tube. These lucite tubes were glued[3]

---

[1]Model 3500 Roller Pump, Sarns Inc., Ann Arbor, Michigan

[2]#9787, Davol Rubber Co., Providence, R.I.

[3]#84C3199, Epoxy glue, Montgomery Wards Co., Kansas City, Missouri

to aluminum plugs which served as caps for the 1" lucite tube. These caps were also glued to the lucite tube. The lucite tube was drilled and tapped for a 3/16" brass hose connector. Air pressure was maintained inside the lucite tube by means of a pressure bulb, a pressure bottle and a pressure gauge.

The operation of the Starling's Resistor is analogous to an electrical diode operating in the forward biased region. No fluid will flow through the drainage tubing until the fluid pressure is equal to or greater than the air pressure outside the flexible latex tube. The air pressure at which the Starling's Resistor is set will determine the maximum perfusion pressure of the pump.

The pump speed must be set such that the pump will be able to supply sufficient flow, at the desired perfusion pressure, when maximum vasodilitation occurs in the hind limb. With this pump setting and the Starling's Resistor operating, the systolic pressure level at the output of the pump will be maintained at the Starling's Resistor air pressure for all perfusion flow rates.

The pump pulsations were effectively eliminated by means of six 50cc shunt air filled syringes.[1] The plunger position was fixed by "U" shaped steel rods threaded at both ends. The rods were placed through a pair of diametrically opposed holes in the plunger and the syringe body. The rods were fastened with brass nuts.

Figure 2 shows the placement of the syringes. They act as a hydraulic capacitance. This shunt capacitance with the series resistance

---

[1]Disposable plastic syringe, Becton Dickinson and Company, Rutherford, N.J.

acts as an excellent low pass filter which eliminates the high frequency pulsations of the roller pump.

The blood next flowed through a rotameter flowmeter[1]. A transducer monitor coupler[2] unit was necessary in order to connect the rotameter into the polygraph recorder[3]. A shunt tube around the rotameter was used to facilitate cleaning of the rotameter without interrupting the blood flow.

The blood temperature was maintained at 37± 0.5 C by means of a heat exchanger unit. A proportional temperature controller utilized a thermistor in the blood line as the feedback element. The temperature of the hind limb was maintained at 37± 0.5 C by means of a heating pad placed beneath the hind limb and a water blanket placed over the whole animal. The water blanket circulation was connected in series with the heat exchanger water jacket. The hind limb temperature was monitored with a thermistor probe[4] placed in the muscle.

A bubble trap consisting of a glass "Y" connector was connected to the blood output of the heat exchanger. Pressure at the hind limb was measured using a strain gauge pressure transducer.[5]

The $\%HbO_2$ level of the perfusing blood was continually measured by a two wave length reflection oximetry system utilizing fiber optic transmission lines. The optical portion of the reflection oximetry system is

---

[1]#93-201-70, #93-202-70, and #93-203-72, E and M Instruments Co. Inc., Houston, Texas

[2]T-M-C Unit, E and M Instrument Co., Inc., Houston, Texas

[3]Model #5 or #7, Grass Instrument Co., Quincy, Mass.

[4]Type 423, Thermistor probe, Model 43TA, Tele-Thermometer, Yellow Springs Instrument Co., Inc., Yellow Springs, Ohio

[5]Type P23AC, Statham Physiological Transducers, Inc., Puerto Rico

similar to that described by Erickson et al. (29, 30, 28).

Figure 5 is a schematic diagram for the optical and electrical portions of the reflection oximetry system. It consists of a light source, three optical channels in a fiber optic bundle, one of which transmits light from the source to the blood stream, the other two bundles return this reflected light to a pair of filter-photocell combinations and an operational amplifier. One narrow band pass filter is at 660mμ and the other at 805mμ. The ratio of the reflected light intensity at 805 and 660mμ is a linear function of the oxygen saturation as determined by refection oximetry (27, 46, 62). The resistance vs. illumination curve for the matched pair of photocells[1], is essentially linear over the operating range of the oximeter. Thus the ratio of photocell resistances for light reflected at 805 and 660mμ is linearly related to the $\%HbO_2$ level.

Erickson et al. (28, 29, 30) connected these photocells as two arms of a Wheatstone bridge. Because of the nonlinear nature of the bridge output voltage, a linear relationship between the bridge output voltage and the $\%HbO_2$ level was not observed. However, in the present arrangement, the change in the ratio of photocell resistance is linearly detected using an operational amplifier circuit. Refer to Figure 5. The 805mμ photocell is the input resistor and the 660mμ photocell is the feedback resistor for the operational amplifier.[2]

---

[1]Type 640L, Clairex Corp., New York, New York

[2]Model PP65AU, Philbrick Research, Inc., Dedham, Mass.

A 1.35 volt mercury battery[1] serves as a voltage source. The 330Ω resistor and silicon diode combination drop the input voltage to 0.6 volts to insure that the amplifier doesn't overload. The output voltage, E_0 then is:

$$E_0 = 0.6 \frac{R660}{R805} \text{ volts} \tag{1.1}$$

where R660 and R805 are the photocell resistances of the 660mμ photocell and the 805 mμ photocells, respectively. Thus E_0 is linearly related to the $\%HbO_2$ level. The calibration procedure and experimental results for the oximeter are discussed in the next section.

---

[1] #RM502R, Mallory Battery Co., Tarrytown, New York

EXPERIMENTAL METHODS

Oximeter

The operation of the two wavelength oximetry system was described in the previous section. Erickson (28) has shown that this reflection oximetry system is essentially independent of linear velocity of flow (3-38cm/sec.), pulsatile flow and species variation between canine and ovine blood. Packed cell volume changes between 41 to 14 percent caused approximately a 5 percent change in the oximeter reading.

In the present studies, it was found that the warm-up time for the oximetry system was approximately 12 hours. This was believed to be due to the photocell warm-up time in reaching an equilibrium with respect to light and ambient thermal levels. Manufacturers of photocells recommend that because of the photocell's long-term time effects, that the cells should be preconditioned to light before sensitivity measurements are made on the cells (63). These long-term time effects result from previous levels of light exposure. It is common in some production testing to precondition the photocells to high light levels for 16 to 24 hours before making sensitivity tests.

The warm-up period for the operational amplifier was found to be an order of magnitude less than that of the total oximetry system. Accordingly, before an experimental run or an oximeter calibration procedure, the oximetry system was turned on the evening before, with the fiber optic bundle shining into a bottle of milk of magnesia[1], the

---

[1]The Charles H. Phillips Co., New York, New York

calibration standard used.

In vitro and in vivo calibrations were made for the oximeter. Approximately one liter of heparinized (24mg/liter) blood was obtained from canine donors. The calibration procedure was essentially that described by Erickson (28). The blood was divided into two portions. One portion was oxygenated by bubbling 100% O_2 through the blood, the other was deoxygenated by bubbling 100% N_2 through the blood. These two blood samples were mixed to a desired oxygenation level and pumped at a constant flow rate with a pumping system developed by Edgington and Cholvin (25). The pumping system was designed to provide a constant flow rate with minimum trauma to the blood. The flow rate used for all in vitro calibrations was 100ml/min. Two blood samples were taken at each $\%HbO_2$ level and the average of these taken as the $\%HbO_2$ value. The $\%HbO_2$ of the blood samples was determined spectrophotometrically[1], utilizing the method described by Edgington (24).

In vivo calibrations were performed during the course of the experimental transfer function determination runs. A 4-way stopcock attached to a "T" connector in series with the oximeter was used as a sampling port for drawing blood samples. The samples were drawn after a step change and an equilibrium $\%HbO_2$ level had been reached. This equilibrium level was determined by observing the output voltage of the oximeter operational amplifier with a digital voltmeter. These

---

[1] DU Spectrophotometer, Beckman Instruments Co., Inc., Fullerton, California

anaerobically obtained blood samples were handled in the same fashion as were those in the in vitro trials.

An in vivo calibration curve is shown in Figure 6.

Flowmeter

The rotameter flowmeter used was calibrated in vitro using approximately 1 liter of heparinized (24mg/liter) canine donor blood. A constant gravity flow system was used. Blood temperature was maintained at 37± 0.5C using the heat exchanger unit described in the previous section. Flow rate was determined by noting the time necessary for a graduated cylinder to fill.

The effects of packed cell volume on flow rate readings were observed for blood hematocrits between 45 and 20%. The effect of packed cell volume on flow rate readings was found to be negligible. This result compares with the findings of others (35, p. 106; 73; 88, p. 1304).

Figure 7 shows the nonlinear calibration curves for the rotameter. Four calibration curves are shown for various sensitivity settings of the polygraph recorder.

Surgical Procedure

Twelve mongrel dogs ranging in weight from 10.5 to 28.0kg were used in the transfer function determination experiments. The subjects were anesthetized with 30mg/kg sodium pentobarbital[1] to a surgical plane of

---

[1]Napental, S. E. Massengill Co., Bristol, Tennessee

anesthesia. Exposures were made for the right external jugular vein, the right common carotid artery, and both right and left femoral arteries. The trachea was cannulated and the dog allowed to breath room air unassisted. Complete hemostasis was achieved during the surgical procedure. Heparin was then administered, initially at the dose of 5mg/kg followed by 5mg/kg every 2 hours. This high level of heparin was administered because of the length and complexity of the extracorporeal circuit.

Prior to the beginning of the surgical procedure, the perfusion apparatus had been primed with 800cc of lactated Ringer's solution and in one case with cross-matched canine donor blood. At this time, the cannulations were made for the perfusion apparatus, cannulae being placed in the right atrium, right femoral artery in both directions and the left femoral artery in the peripheral direction. A cannula was placed in the right carotid artery to monitor the subject's systemic blood pressure. Following the right femoral artery cannulation, the shunt tubing connection between the central and peripheral catheters was opened to re-establish circulation in the right hind limb.

After checking to see that there were no bubbles present in the perfusion apparatus, the shunt connection was closed and the perfusion system inflow and outflow clamps simultaneously removed. The roller pump was also started at this time. Arterial blood was used as the initial perfusate until equilibrium conditions were reached.

The systemic blood pressure was measured with a strain gauge

pressure transducer[1]. The outputs of four transducers; rotameter, hind limb perfusion blood pressure, systemic blood pressure and reflection oximeter were recorded on a polygraph recorder.[2]

Experimental Protocol

The hind limb perfusion pressure was set 10 mm Hg higher than the systolic arterial pressure by means of the roller pump-Starling's Resistor combination. This minimized the contribution of blood flow to the hind limb from collateral channels. After allowing the hind limb temperature to reach an equilibrium level of 37$\pm$ 0.5 C the test sequence began.

Small and large changes were made in the input $\%HbO_2$ level, in both increasing and decreasing directions. A typical large change in $\%HbO_2$ would be from an arterial to a venous $\%HbO_2$ level, this would correspond to a $\Delta\%HbO_2$ of approximately 50. A typical small change in $\%HbO_2$ would be approximately 15-20. At the beginning of an experimental sequence the $\%HbO_2$ was changed from arterial to venous and back to arterial, equilibrium being reached at each level of $\%HbO_2$. Using the mixing chamber, the $\%HbO_2$ was then changed in small increments from arterial to venous $\%HbO_2$ levels, in a step-wise fashion. Having reached the venous $\%HbO_2$ level, the $\%HbO_2$ was changed in small increments to the arterial $\%HbO_2$ level. The perfusion at the arterial $\%HbO_2$ level was long enough to repay the oxygen debt incurred. At each $\%HbO_2$ level the flow rate was

---

[1]Model P23AC Statham Transducers, Inc., Hato Rey, Puerto Rico

[2]Model 5 or 7, Grass Instruments Co., Quincy, Mass.

allowed to reach an equilibrium state for approximately 5 to 8 minutes.

Periodically, packed cell volume readings were taken and the flowmeter zero level was checked. The flowmeter shunt tube was opened and the flowmeter flow stopped to check the zero flow condition. If after re-establishment of rotameter flow, the flowmeter reading didn't return to approximately that which existed prior to the flow stoppage, then this indicated that the rotameter float was sticking. This necessitated cleaning of the rotameter float and base.

The systemic arterial pressure was carefully observed and it was noted that when the mean systemic arterial blood pressure began to fall below approximately 100mm Hg that periodic blood pressure oscillations became apparent. The period of these oscillations was found to be between 20 and 40 seconds, a characteristic of vasomotor activity (36). This caused undesirable fluctuations in the hind limb flow observed. To diminish the vasomotor activity an elevated infusion bottle of lactated Ringer's solution was connected in parallel with the arterial pressure transducer. The height of the bottle was set such that the mean arterial pressure was maintained at a level above 100mm Hg.

DATA ANALYSIS

Data Handling

The input and output functions, $\%HbO_2$ level and blood flow rate, were digitized initially by hand, from the polygraph recordings, and in the later experiments by means of an analog to digital converter system.

The two channels of information were recorded on a magnetic tape recorder.[1] The tape recorder inputs were secured from jack J5 of the appropriate driver amplifiers[2]. Data compression was utilized by recording the data at 1 7/8 ips and playing it back at 7 1/2 ips. Figure 8 shows block diagrams of the data recording and analog to digital converter systems.

The analog to digital converter system consisted of a two channel sample and hold circuit, two automatic digital voltmeters[3] and an electro-mechanical digital recorder.[4] The digital recorder paper tape output was key punched on IBM cards. During the playback mode, the tape recorder output was monitored on the polygraph recorder.

The sample and hold circuit is used to sample the two information channels simultaneously. Figure 9 is a schematic diagram of the sample and

---

[1]Model FR1100, Ampex Corporation, Redwood City, California

[2]Model 7P1, Grass Instruments Co., Quincy, Massachusetts

[3]Model 405CR, Automatic digital voltmeter, Hewlett Packard Co., Palo Alto, California

[4]Model 561B, digital recorder, Hewlett Packard Co., Palo Alto, California

hold circuit. Basically the circuit consists of two identical two stage operational amplifier stages (6). The first stage provides amplification and an adjustable bias voltage. The bias was adjusted such that the output of the sample and hold circuit was between 1.00 and 9.99 volts, for a full range of input voltages from the tape recorder. This feature eliminated the problem of digital voltmeter ranging and consequential printer malfunction. The second stage consists of an operational amplifier operating in two modes, in one mode as an inverting amplifier and in the other as an integrator. The mode of the operation is determined by the state of the field effect transistor (FET) switch[1]. With the FET switch closed, the output of the operational amplifier follows the input, i.e. it samples the input. At the instant when the FET switch is opened, by a negative pulse applied to the gate terminal, the output of the operational amplifier is held by the storage capacitor, C_1.

The sampling rate of both digital voltmeters is controlled externally by an external trigger signal from a low frequency function generator[2], applied at jack J4. The sample and hold circuit is synchronized with the sampling rate of the digital voltmeters by a positive pulse of 110-145 ms duration supplied by the relay control multivibrator (pin 6, V9) of one of the digital voltmeters. This signal is attenuated and applied at point D (sample and hold circuit). Clamping this signal provides a

---

[1] #2N 4220 , Motorola Semiconductor Inc., Phoenix, Arizona

[2] Model 202A, Hewlett Packard Co., Palo Alto, California

negative pulse which opens the FET switches of both sample and hold circuits simultaneously. These "hold" voltage levels are then indicated by the digital voltmeters and printed on the paper tape. A 100 conductor cable was used to connect the digital voltmeter output (jack J3) to the printer input (jack J101 or J102). The print command for the printer was supplied by one of the digital voltmeters.

The sampling rate, taking into account the time compression of 4, was set between 0.1 and 0.5 cps, approximately 10 times the highest frequency of the output function. The time lags between input and output functions, due to blood circulation time, were removed manually before the paper tape data was key punched.

A recalibration subroutine was used to convert the punched card input-output sample values to the actual values of the $\%HbO_2$ and flow rate. This procedure was comprised of two steps. First, by using appropriate calibration procedures, linear equations relating polygraph deflection to the punched card value were found for both the input and output functions. In the second step, calibration curves relating the input function and the output function to polygraph deflection were used. These calibration curves were obtained according to the methods described in the previous section. Figures 6 and 7 show two such curves.

For the linear calibration curves, the slope and y-intercept were specified. The coordinates for 14 points were specified for each of the 4 nonlinear flow rate vs. polygraph deflection curves.

The recalibration subroutine algorithm used the slopes and y-intercepts from the linear equations relating $\%HbO_2$ to polygraph deflection and

polygraph deflection to punch card values in order to obtain a single linear equation relating $\%HbO_2$ to the punch card value. For the nonlinear curves, the subroutine used linear interpolation, between the 14 coordinates of the flow rate vs. polygraph deflection curves, to find the desired flow rate for a given punched card value. All computer operations were performed on the recalibrated input-output samples.

Since an incremental transfer function relating the change in flow rate to the change in $\%HbO_2$ level was desired, the initial values of the input-output samples were subtracted from the succeeding input-output samples.

Computer Program

The input and output sampled functions were analyzed as first and second order systems on an IBM 360-65 computer using a continuous time system identification program[1]. This program finds the parameters of a first order model of the system of the type discussed by Zadeh and Desoer (90, p. 281). It is based upon a technique for minimizing the mean square error in the input-output-state relation. This results in a system of linear equations whose solution gives the required set of parameters.

Zadeh and Desoer show that any transfer function can be realized by an interconnection of integrators and coefficient potentiometers. Figure 10 shows their realization of an n^{th} degree transfer function. For the

---

[1]Duven, Dennis, Ames, Iowa. Computer program. Private communication. 1968.

purposes of discussion, a 2nd order model will be used as an example of how the computer program works.

Figure 11 shows a second order transfer function with $b_2=0$ and $a_2=1$. The components of the state vector are taken to be the outputs of the two integrators. The state equations can then be written as follows:

$$\begin{aligned} \dot{x}_2 &= -a_1 y + b_1 u + x_1 \\ \dot{x}_1 &= -a_0 y + b_0 u \\ y &= x_2 \end{aligned} \tag{2.1}$$

These equations written in matrix form become:

$$\begin{bmatrix} \dot{x}_1 \\ \dot{x}_2 \end{bmatrix} = \begin{bmatrix} 0 & -a_0 \\ 1 & -a_1 \end{bmatrix} \begin{bmatrix} x_1 \\ x_2 \end{bmatrix} + \begin{bmatrix} b_0 \\ b_1 \end{bmatrix} \begin{bmatrix} u \end{bmatrix}$$

$$\begin{bmatrix} y \end{bmatrix} = \begin{bmatrix} 0 & 1 \end{bmatrix} \begin{bmatrix} x_1 \\ x_2 \end{bmatrix} \tag{2.2}$$

Equation 2.2 has the form:

$$\begin{aligned} \dot{\underline{x}} &= A\underline{x} + b\underline{u} \\ \underline{y} &= M\underline{x} \end{aligned} \tag{2.3}$$

Taking the Laplace transform of Equation 2.3

$$\begin{aligned} s\underline{X}(s) - \underline{x}(0) &= A\underline{X}(s) + b\underline{U}(s) \\ \underline{Y}(s) &= M\underline{X}(s) \end{aligned} \tag{2.4}$$

Solving for $\underline{X}(s)$

$$\begin{aligned} (sI-A)\underline{X}(s) &= x(0) + b\underline{U}(s) \\ \underline{Y}(s) &= M\underline{X}(s) \end{aligned} \tag{2.5}$$

$$\underline{X}(s) = (sI-A)^{-1}\, x(0) + (sI-A)^{-1}\, b\underline{U}(s)$$
$$\underline{Y}(s) = M\underline{X}(s) \tag{2.6}$$

The transition matrix in this case is given by:

$$(sI-A)^{-1} = \frac{\begin{bmatrix} s+a_1 & -a_0 \\ 1 & s \end{bmatrix}}{s^2 + a_1 s + a_0} \tag{2.7}$$

To simplify notation let:

$$C(s) = s^2 + a_1 s + a_0 \tag{2.8}$$

$$X_0(s) = x_1(0) + x_2(0)s \tag{2.9}$$

$$B(s) = b_0 + b_1 s$$

Then Equation 2.6 becomes:

$$C(s)\, \underline{Y}(s) = X_0(s) + B(s)\, U(s) \tag{2.10}$$

Dividing by s^2 results in:

$$(1 + a_1 s^{-1} + a_0 s^{-2})\, \underline{Y}(s)$$
$$= x_1(0)\, s^{-2} + x_2(0)\, s^{-1} + (b_0 s^{-2} + b_1 s^{-1})\, \underline{U}(s) \tag{2.11}$$

Taking the inverse Laplace transform of Equation 2.11 yields the time domain expression

$$[x_1(0)t + x_2(0)] + [b_0 u_2(t) + b_1 u_1(t)]$$
$$- [y(t) + a_0 y_2(t) + a_1 y_1(t)] = e(t) \tag{2.12}$$

where $e(t)$ is the error function, $y_i(t)$ denotes the i^{th} definite integral of $y(t)$ and $u_i(t)$ denotes the i^{th} definite integral of $u(t)$. The input, $u(t)$, and output, $y(t)$, functions are known, an estimate of $x_i(0)$, a_i and b_i are desired such that the integral of the squared error function is minimized i.e.

$$\int_0^T e^2(t)dt = \text{minimum} \tag{2.13}$$

where T = total time of input and output time functions.

A necessary but not sufficient condition that a relative minimum of a function $f(z_1,z_2,z_3, \cdots z_m)$ exists at the point $(c_1,c_2,c_3 \cdots c_m)$, is that the partial derivations with respect to the independent variables, at the point, are equal to zero, i.e.

$$\frac{\partial f(c_1,c_2,c_3 \cdots c_m)}{\partial z_i} = 0 \tag{2.14}$$

for i = 1,2, $\cdots$m.

The partial derivatives in this 2nd order example are:

$$\begin{aligned}
&\frac{\partial}{\partial b_m}\int_0^T e^2(t)dt = 2\int_0^T e(t)\,\frac{\partial e(t)}{\partial b_m}\,dt = 0 \\
&\frac{\partial}{\partial a_m}\int_0^T e^2(t)dt = 2\int_0^T e(t)\,\frac{\partial e(t)}{\partial a_m}\,dt = 0 \\
&\frac{\partial}{\partial x_m(0)}\int_0^T e^2(t)dt = 2\int_0^T e(t)\,\frac{\partial e(t)}{\partial x_m(0)}\,dt = 0
\end{aligned} \tag{2.15}$$

It should be noted that:

$$\begin{aligned}
&\frac{\partial e(t)}{\partial b_m} = u_{2-m}(t) \\
&\frac{\partial e(t)}{\partial a_m} = -\,y_{2-m}(t)
\end{aligned} \tag{2.16}$$

and

$$\frac{\partial e(t)}{\partial x(0)_m} = \frac{d^m}{dt}\,t$$

for m = 0,1

This leads in general to a set of 3n linear equations in 3n unknowns, where n is the order of the system. In the present case 6 equations in 6 unknowns result. These equations are expressed in matrix notation in Equation 2.17 shown in Figure 12.

Equation 2.17 can be simply written as:

$$Dz = E \tag{2.18}$$

The solution for z is desired. A linear equation solver subroutine is used to calculate the elements of the z vector.

It should be noted that the elements of the 6x6 matrix in Equation 2.17 are integrals of products of first and second integrals of the input function, output function and of the function t. The function t is generated internally in the computer by adding sampling period increments. If the input function is a step function, u(t), the first integral, $u_1(t)$, would be a ramp function and the second integral, $u_2(t)$, would be a quadratic function. The product of the first and second integrals of the step function would be a cubic, $u_1(t) \cdot u_2(t)$. These product functions are integrated over the total time period of the input-output samples. Once the elements of matrix have been calculated a generalized inverse matrix is found which yields the desired z vector elements.

A unique solution for Equation 2.18 exists if the determinant of D does not equal zero. The solution is:

$$z = D^{-1}E \tag{2.19}$$

where D^{-1} is the inverse of D. However, if the determinant is equal to zero, there is not a unique solution for z. Since these singular solutions occur, a method of finding the inverse of singular matrices is

necessary.

Penrose (59) showed that a generalized inverse matrix provides a "best" approximate solution for dependent systems of equations by the method of least squares. Rust et al. (67) have developed a simple algorithm for computing the generalized inverse of any matrix. For the case where the matrix is nonsingular the algorithm gives the ordinary inverse of the matrix. In the singular case the algorithm finds the shortest length vector $|z|$ defined by

$$z = D^{I}E \tag{2.20}$$

where D^{I} is the generalized inverse of the matrix D. The value of z, as defined in Equation 2.20 minimizes the distance

$$\rho(z) = |E - D(z)| \tag{2.21}$$

Many z vectors exist which minimize the distance $\rho(z)$ but the vector z is the shortest of all these.

The elements of the solution vector, z, consist of the values of the initial conditions of the integrators, and the coefficients of the numerator and denominator polynomials of the desired transfer function.

The roots of the numerator and denominator polynomials were found using a Newton-Raphson iterative technique. The final iterations on each root were performed using the original polynomial rather than the reduced polynomial to avoid the accumulation of errors in the reduced polynomial.

The computer program was checked by using known input-output samples of a first order system. The program identified data as both a first and second order system. The effects of the total number of samples and scaling of the sampling period on the system identification were determined.

The system identification in the first order case was within 10% of the actual when the total number of samples was equal to or greater than the time constant of the first order system identified. As the number of samples was increased above this number the identification approached the known solution.

Using the actual sampling period in the second order identification resulted in incorrect identifications. By scaling the sampling period down by a factor of 10 to 100, predictable results occurred. The reason for this problem was believed to be the large numbers in the D matrix of Equation 2.18 which resulted because the integrations were performed over relatively long periods of time. Scaling the sampling period decreased this total integration time by the scale factor. It was an easy matter to rescale the answers. The first order identification did not necessitate scaling of the sampling period. In the second order identification the sampling period was scaled by 0.01.

The second order identification of the first order system produced a pole-zero cancellation resulting in the actual first order system transfer function. This identification was within 10% of the actual when the total number of samples was equal to or greater than 1.5 times the time constant of the first order system. As in the first order identification, increasing the number of samples beyond this point improved the identification. The total number of samples for a given experimental determination was selected to be 1.5 to 2 times the average time constant.

RESULTS AND DISCUSSION

Much qualitative and quantitative work has been done in examining the static characteristics of the autoregulation of blood flow due to blood oxygen saturation (39). There has been almost no qualitative or quantitative work performed concerning the dynamic characteristics of this phenomenon. Consequently, the present findings have little if any previous criteria with which they can be compared.

Dynamic experiments in biological preparations are fraught with difficulties. One of the greatest difficulties is in isolating the physiological system. In this thesis research the dynamic relationships involved in the local autoregulation of blood flow due to $\%HbO_2$ were desired. Autoregulation is a local mechanism by which the tissues of the body govern the state their own vasculature. This control is independent of central nervous system control and dependent on the nutrient needs of the local tissue bed. In addition to the local autoregulatory control of blood flow rate, the central nervous system independently also controls the vasculature of the local tissue bed. This central nervous system control is important in maintaining the homeostasis of the entire circulatory system. The dual control of the peripheral circulation allows for vacular adjustments which direct blood flow to tissue beds whose immediate requirements are high from those tissue beds whose requirements are less (4).

The autonomic portion of the central nervous system mediates the control of blood flow at the local vascular bed. The smooth muscles of the peripheral blood vessels are in a continued active state of partial contraction. This vasomotor tone is controlled by vasoconstrictor fiber

innervation of the blood vessels' smooth muscles. The blood vessels controlling the vascular resistance are the arteries, small arteries, venules and small veins (36).

The central nervous system maintains the arterial pressure at a desired level by changing the vascular resistance of the various tissue beds of the body. Pressoreceptors, which sense the arterial pressure level, are located in the aortic arch and the carotid sinus area. The pressoreceptors not only respond to the general level of arterial pressure but also to the rate of change of pressure with respect to time. Many engineering studies have been made characterizing the dynamic response of this feedback mechanism (47).

It is quite common to observe oscillations in the arterial blood pressure waves in the order of 10 to 20mm Hg, with an average period of 26 seconds, during experimental animal trials. These oscillations are known by many names. The three most common are: vasomotor waves, Mayer waves and Traube-Hering waves (36). The usual cause for these oscillations is a positive feedback in one of the nervous system pressure regulators. Guyton states that these vasomotor waves are caused partially if not mainly by an oscillation of the pressoreceptor reflex (36). This positive feedback mechanism works in the following way. Low arterial blood pressure causes increased vasoconstriction activity raising the blood pressure. After a time delay, this high pressure excites the pressure receptors causing a decrease in vasoconstrictor activity which lowers the pressure. With this lowering of the blood pressure, a new cycle is initiated and the cycle continues. Guyton and Harris (37) found that the time delay of the carotid sinus reflex was approximately 13 seconds. This delay was close to

one half the average period of the sustained vasomotor oscillations they observed (25.2 seconds). They postulated that this time delay could be due to two factors. The first factor being the delay between the presso-receptors and the autonomic nerve endings at the smooth muscle of the blood vessels. And the second factor being the delay in the humoral response. In the experimental trials reported here, vasomotor activity usually appeared when the subject's systolic arterial blood pressure fell below approximately 100mm Hg. This vasomotor activity was superimposed on the normal autoregulatory response. Figure 13 illustrates typical input-output waveforms with the superimposed vasomotor activity present in the output waveform. As described in the previous section, it was found that the vasomotor activity could be diminished by maintaining the arterial pressure above the critical pressure level where vasomotor activity appeared. A hydrostatic reservoir was attached in shunt with the arterial system. This helped to diminish the vasomotor activity noise in the data. Figure 14 shows the effect of maintaining the arterial pressure constant above the critical level.

As a consequence of adding this pressure regulating system, the packed cell volume of the blood changed over the course of an experimental run. This decrease in the packed cell volume essentially results in a case of anemia. It has been observed that in acute hemodilution and chronic anemia that the cardiac output increases. Dedichen *et al.* (21) showed that the main factor for the increase in cardiac output was a reduction in the total peripheral resistance caused by decreased viscosity of the diluted blood. They produced acute isovolemic anemia in the dog by

dextran exchange hemodilution. A 70% increase in cardiac output resulted which was only partially reversed when the animals were subjected to hyperbaric oxygenation. Under these experimental hyperbaric conditions, the oxygen carried by the blood in physical solution corresponded to the oxygen volume (6 volumes per cent) normally extracted by the body tissues from the erythrocytes. They found that the cardiac output increased in acute isovolemic anemia under hyperbaric oxygenation. This indicated that the reduced hemoglobin content present in anemia was not the factor causing the increase in cardiac output. They concluded that the hemodynamic changes observed were probably due to the reduction of blood viscosity which decreased the total peripheral resistance.

The effect of the variation in the packed cell volume was noticeable in the hind limb preparation used in this report. For the same level of arterial blood saturation, the flow rate increased with hemodilution. The flow rate for arterial blood saturation as the input was selected as the control flow rate level. Data segments from a given experimental run were selected for analysis which did not vary more than $\pm 20\%$ from this control flow rate level. In all cases the packed cell volume was greater than 20%. It was observed in one case where cross matched blood was used in the arterial reservoir that the results were the same qualitatively as those in which lactated Ringer's solution was used in the reservoir. In another experiment where no arterial reservoir was used, and thus with essentially constant packed cell volume, the results were the same qualitatively as those obtained with the arterial reservoir.

As explained previously, the $\%HbO_2$ level was varied between arterial

and venous levels in large and small step input changes using the mixing chamber. Due to the nature of the mixing chamber, it was not possible to generate the same $\%HbO_2$ input levels each time. The resulting output flow rate showed a great deal of variability.

The "best" description of the biological system in terms of a transfer function was desired. It was noted previously that the computer program second order identification of a true first order system resulted in pole-zero cancellations in the factored form of the transfer function. This reduced transfer function was the same as the true first order system transfer function. Thus, with the order of the model assumed larger than the actual, the identification process will produce pole-zero cancellations. However, in the experimental data noise, in the form of vasomotor activity, is present which complicates the simple determination of the order of the model by pole-zero cancellations. When pole-zero cancellations occurred in the second order identification, and the remaining pole was approximately the same as that of the first order identification, then it was assumed that the system was of first order.

In order to see how well the resulting transfer function actually fit the data, a subroutine of the computer program simulated the output which resulted when the actual input samples were used as input to the identified transfer function. Another subroutine simultaneously plotted the actual input-output samples and the identified system output. This provided a visual check of how well the simulated transfer function modelled the actual input-output functions. Figure 15 shows typical actual input, actual output, and simulated output graphs.

In analyzing either a physical or biological system with control system techniques the linearity or range of linearity must be determined for the system under study. This is necessary since classical control techniques are only applicable to linear systems or to linear portions of nonlinear systems. Given an unknown system it is advantageous to study it as a linear one in order to determine what, if any, nonlinear discrepancies might exist. In the present study, the linearity was examined by applying large and small step inputs of $\%HbO_2$ between the arterial and venous saturation levels. For a linear system superposition holds and the basic output response should be the same regardless of the initial input level or magnitude of input change. Since the transfer function is the ratio of the output to the input function, it should be invariant for a linear system over all ranges of the input function. The results from these experiments and the conclusions drawn concerning the linearity of the system will be discussed below.

In the initial experiments large step changes in $\%HbO_2$ were used. The $\%HbO_2$ level was changed from the arterial to the venous level and then back to the arterial level. For the large changes in $\%HbO_2$ the arterial $\%HbO_2$ level ranged from 97 to 86%. The venous level ranged from 70 to 10%. Thus an input change in saturation level could be anywhere between the arterial or venous $\%HbO_2$ ranges. However, in general for high arterial levels of saturation the venous level was high and likewise for lower arterial levels the venous level was lower. A typical large change in $\%HbO_2$ would be in the order of 50%.

The first order system transfer function has the form

$$\frac{\Delta \text{ blood flow rate}}{\Delta \%HbO_2} = \frac{-k}{\tau s + 1} \tag{3.1}$$

where the units of k are

$$\frac{\text{ml/min/kg body weight}}{\%\text{ oxyhemoglobin saturation}}$$

and τ is in seconds.

The second order system transfer function has the form

$$\frac{\Delta \text{ blood flow rate}}{\Delta \%HbO_2} = \frac{-k\,(s+a)}{(s+b)(s+c)} \tag{3.2}$$

where k has the units of

$$\frac{\text{seconds (ml/min/kg body weight)}}{\%\text{ oxyhemoglobin saturation}}$$

and the constants b and c can be either real or complex numbers. The first order system identification resulted in left half plane poles. Singular solutions frequently resulted in the second order identification. The second order identification produced a number of pole-zero combinations. A left or right half plane zero resulted with the following pole locations: two real left half plane poles, one left half and one right half plane pole, and complex left half plane poles. In a number of cases (27%) pole-zero cancellations occurred in the second order identification with the resulting pole approximately equal to the first order identified pole. In these cases the system was most likely of first order. The results of a number of experiments will be discussed below.

Figures 15 to 20 show typical actual and simulated output responses for large $\%HbO_2$ input changes from the arterial to the venous saturation level. A first and second order identification for an input saturation level change from 87 to 63% is shown in Figures 15 and 16, respectively.

The first order identification resulted in a pole at -7.72×10^{-2} while the second order identification resulted in a singular solution with two poles, one located at -7.78×10^{-2} and the other at 2.16×10^{-3}, and a zero located at 2.17×10^{-3}. By cancelling the right half plane pole and zero of the second order transfer function a first order transfer function results having the same pole as that of the first order identified transfer function. The results of an input $\%HbO_2$ change from 89 to 45% are shown in Figures 17 (first order identification) and 18 (second order identification). Figures 19 and 20 show a first and second order identification, respectively, for an input $\%HbO_2$ change from 86 to 32%. The first order identification in Figures 17 and 19 resulted in a left half plane pole. In the second order identifications (Figures 18 and 20) singular solutions resulted with a left and a right half plane pole and a left half plane zero in the first case (Figure 18) and a right half plane zero in the second case (Figure 20). For the above cases it is observed that the initial conditions found were closer in general for the second order identification than in the first order identification. In the initial check of the computer program the initial conditions found were accurate for both the first and second order identifications. For the experimental data it was observed that the initial conditions found were not as accurate for noisy data as for data in which no noise was present.

Typical actual and simulated output responses for large $\%HbO_2$ input changes from venous to arterial saturation levels are shown in Figures 21 to 24. Figures 21 and 22 show a first and second order identification, respectively, for an input $\%HbO_2$ change from 53 to 86%. The first order

identification results in a pole located at -2.2×10^{-2} while the second order identification produces a singular solution of two poles located at -2.2×10^{-2} and 9.90×10^{-3} and a zero at 1.09×10^{-2}. The cancellation of the right hand plane pole and zero results in the transfer function found in the first order identification. The response to an input $\%HbO_2$ change from 26 to 87% is shown in Figures 23 (first order identification) and 24 (second order identification). The effects of moderate vasomotor activity on the output flow rate is shown in these figures. The first order identification produces a left half plane pole while the second order identification produces a pair of complex left half plane poles and a left half plane zero. It is noted from the above input-output, simulated output curves (Figures 15 to 24) that the improvement using the second order identification is not significant.

In addition to large $\%HbO_2$ input changes smaller step changes of $\%HbO_2$ levels were also used. The $\%HbO_2$ level was changed in a number of steps from the arterial $\%HbO_2$ level to the venous level and back again to the arterial level. As mentioned previously, it was difficult to control the exact level or magnitude of the small $\%HbO_2$ level changes. A small change in $\%HbO_2$ could range from 3 to 25%, while a typical small change would be in the order of 15 to 20%.

The response to smaller changes in the $\%HbO_2$ level is shown in Figures 25 to 34. Figures 25 and 26 show a first and second order identification, respectively, for an input $\%HbO_2$ change from 95 to 80%. The response to an input $\%HbO_2$ change from 84 to 71% is shown in Figures 27 (first order identification) and 28 (second order identification).

The effects of moderate vasomotor activity on the output flow rate is shown in these figures. The second order identification in the two above cases (Figures 26 and 28) produced two left half plane poles and one left half plane zero.

The response to small changes in $\%HbO_2$, as the $\%HbO_2$ level is increased, is shown in Figures 29 to 34. The first and second order identification for input saturation level changes from 63 to 88%, 57 to 61% and 34 to 49% are shown in Figures 29, 30, 31, 32, 33 and 34, respectively. The second order identified pole combinations which resulted were: two left half poles (Figure 30), complex left half plane poles (Figure 32) and one left and one right half plane pole (Figure 34). As with the large step inputs of $\%HbO_2$ the second order identification for small step inputs produced pole-zero cancellations with the resulting pole approximately equal to that found in the first order identification. From the results (Figures 25 to 34) obtained using the small $\%HbO_2$ inputs it can be observed that the second order identification is not appreciably better than that of the first order identification.

From the above discussion of the results obtained from both the large and small changes in $\%HbO_2$ it is concluded that the transfer function is most likely of first order. The reasons for this are as follows:

1. Pole-zero cancellations in the second order identification, with the resulting transfer function approximately equal to the first order identified transfer function, occurred in a significant number of cases (27%).

2. In most cases the second order identification was not significantly better than that of the first order. It was pointed out

previously that a higher order system will always fit noisy data better.

With the basic first order nature of the response established, an examination of the range of the gain constant, k, and the time constant, τ, of the first order system transfer function (Equation 3.1) should be examined. The variation in τ and k are shown in Figures 35 and 36. From these figures it is noted that there is a variation in both τ and k.

τ was found to be in the range 30 to 120 seconds (median value = 56 seconds, mean value = 85 seconds, SD = 107) for 86 of 121 experiments (70%) for 12 subjects and k was found to be in the range 0.04 to 0.16 (median value = 0.11, mean value = 0.12, SD = 0.07) for 84 of 121 experiments (70%) for 12 subjects. Regression techniques were used to determine whether the variations in τ and k were dependent on the $\%HbO_2$ level and the direction of change of the input $\%HbO_2$. No correlation could be found with the initial, final or mean value of the input $\%HbO_2$ level with either τ or k, for increasing or decreasing step input levels of $\%HbO_2$.

A dynamic nonlinearity was found. The flow rate response due to a decrease in the $\%HbO_2$ input level was slower than the response to an increase in the $\%HbO_2$ level. The median value of τ was 67 seconds for a decrease in the $\%HbO_2$ level, 45 seconds for an increase in the $\%HbO_2$ level, and 56 seconds for the combined data of increase and decrease $\%HbO_2$ levels.

Although the experimental preparation of Detar and Bohr (23), mentioned above, was dissimilar from that reported here, their observations of different values of time constant for increasing and decreasing

levels of oxygen tension indicate that they might have observed the same type of dynamic nonlinearity as reported here. For decreases in oxygen tension during sustained contraction produced by epinephrine, the time constant for the decrease in contractile tension was less than 4 minutes, while for the case where the vascular smooth muscle was stimulated with epinephrine near the end of a 15 minute hypoxic period an increase in oxygen tension caused the contractile tension to increase with a time constant less then 2.5 minutes.

From the steady data of Crawford et al. (17), in which the blood flow response was observed for the condition where the hind limb perfusion blood was changed gradually from the arterial to the venous $\%HbO_2$ level, values of the gain constant, k, can be obtained. The value of k (using 16.7kg as the average weight of their animals) for a gradual change in $\%HbO_2$ level from 100 to 55%, 100 to 42%, and 100 to 30% was calculated to be 0.042, 0.065, and 0.081, respectively. They also observed that with an abrupt change in the $\%HbO_2$ level from the arterial to the venous level that the transient flow rate took approximately 2 minutes to reach a stable level. If it is assumed that steady state is reached in 3 time constants, then the time constant, τ, which they observed would be in the order of 40 seconds. The values of k and τ calculated from the data of Crawford et al. (17) are within the 70% range of the values of k and τ, mentioned above.

The variation in τ and k was believed to be due to the fact that the system under study was not isolated from the influence of other controlling systems and other parameters. The changing physiological state of the

animal over the course of an experimental run also produced an effect. The vasomotor activity present in the output flow rate indicated that the central nervous system was sharing control of the hind limb vasculature with the desired local autoregulator response. The level of pH and Pco_2 present in the perfusing blood were two uncontrolled parameters which might have had an influence on the values of k and τ.

SUMMARY

The dynamic relationships involved in the local autoregulation of blood flow due to the blood oxygen concentration were determined in the canine hind limb. It was found that a first order transfer function best describes this system. The values of the gain constant, k, and the time constant, τ, were found for the first order transfer function given by Equation 3.1, repeated below.

$$\frac{\Delta \text{ blood flow rate}}{\Delta \%HbO_2} = \frac{-k}{\tau s + 1} \qquad (3.1)$$

where τ was found to be in the range 30 to 120 seconds (median value = 56 seconds, mean value = 85 seconds, SD = 107) and k was found to be in the range 0.04 to 0.16 (median value = 0.11, mean value = 0.12, SD = 0.07). The units of k are

$$\frac{\text{ml/min/kg body weight}}{\text{\% oxyhemoglobin saturation}}$$

A dynamic nonlinearity was found with respect to the value of τ and the direction of change of the input $\%HbO_2$ level. The linearity of the system with respect to the gain constant, k, could not be easily determined because of the variation in the values of k. No correlation was found between the input $\%HbO_2$ level and the resulting values of k and τ.

This thesis research is a preliminary study into the complex autoregulatory response. Much work remains to be done. A number of suggestions for extensions of this work can be made. The autoregulatory response of local tissue beds should be examined by using various types of input $\%HbO_2$

functions. Sinusoidal $\%HbO_2$ inputs would facilitate the data analysis by means of the Bode plot technique. A system to accurately measure the time delay (if any) between the input $\%HbO_2$ and output flow rate should be devised. An investigation into the dynamic autoregulatory response of other tissue beds should be performed.

PART II. *IN VITRO* ANALYTICAL STUDIES OF THE TRANSFER FUNCTION FOR THE ARTIFICIAL VENTRICLE POWER AND CONTROL SYSTEMS

INTRODUCTION

The transfer function found in the preceding section of this dissertation is not only useful in modeling the cardiovascular system autoregulatory response to blood oxyhemoglobin levels, but it also has potential value in the design of an artificial ventricle control system. This section of the dissertation concerns the dynamic analysis of the artificial heart control system. Transfer functions relating the artificial ventricle input control signal to the artificial ventricle output flow rate were found for various artificial ventricle parameter values.

A 1966 Hamilton Standard report submitted to the National Heart Institute indicates that there will be a need for 100,000 to 150,000 artificial heart operations per year in the year 1975 (52). By this time it is believed that a large scale artificial heart implantation program could start. This number of implantations is limited by various practical factors. The magnitude of an artificial heart program for this large group of people is not only justified from the point of saving human lives but it is a definite business proposition. The annual cost for the above proposed program would be in the neighborhood of 1.2 to 1.8 billion dollars with a net gain of 1.3 to 1.9 billion dollars in actual productive benefits to the nation because of the lives saved. Arteriosclerotic cardiac disease, including coronary artery disease, was found to be the primary condition justifying artificial heart consideration. The Artificial Heart Branch of the National Heart Institute has awarded contracts amounting to over 20 million dollars to private industry and academic institutions. These contracts are for work on various aspects of a complex artificial

heart system designed to replace a diseased natural heart which cannot be repaired or supported artificially.

Transplantation of homologous or heterologous hearts is one possible solution to the problem but the supply of potential donors for both of these sources does not come close to the number of heart replacements anticipated. In addition to this, the immunologic problem still remains as a great obstacle. Some heart transplant surgeons feel that the transplantation procedure is an intermediate stage to a mechanical artificial heart (22). The results of heart transplantation are useful to artificial heart research since a functioning transplanted heart is a denervated heart, devoid of autonomic nervous system control. Data from heart transplant patients could help establish the relative importance of neurological control of cardiac function.

REVIEW OF THE LITERATURE

The following section is a literature review in the area of artificial heart control systems. This literature review is designed to give the reader an idea of the various types of artifical heart control systems which have been used. This section does not attempt to evaluate the relative effectiveness of the various control systems. Uniform standarized experimental tests have not been proposed which evaluate the efficacy of the various artificial heart control systems. Consequently, each artificial heart group designs their own tests for examining the effectiveness of their artificial heart control system. Standardized criteria for *in vivo* and *in vitro* tests of artificial heart control systems would be a real contribution in this area.

An excellent review and analysis of the various methods of artificial heart control was recently given by Swift (75).

The control of cardiac output in the natural heart is a complex control system dependent on neural, chemical, hormonal and intrinsic mechanisms.

At present a majority of the artificial heart control systems regulate cardiac output by utilizing feedback control systems which are sensitive to venous or aterial pressures (2, 7, 8, 14, 41, 42, 56, 57, 61, 77, 89). This method of control follows Starling's law which states that venous pressure is maintained essentially constant by adjustments in the ventricular stroke volume, or in other words, the heart pumps all the returning blood without an appreciable increase in the venous pressure (36). Pierce *et al.* (61) selected venous pressure as the controlling variable

because studies had shown that in cases where hormonal and/or neural control were attenuated that venous pressure was the controlling variable which determined the cardiac output. Nosé (57) states that artificial heart control should be sensitive to venous pressure. This feedback control system would maintain the input pump (intra-atrial pressure) within a desired range. He further observed that a control system which maintains constant venous pressure would prevent venous pooling of blood. Kwan-Gett et al. (51) maintain that an acceptable artificial heart control system must be able to maintain the left and right atrial pressures within the normal physiological limits. With this method of control approximately equal average flows would result from the right and left hearts.

Most artificial heart control systems which utilize this method of control establish a constant reference pressure level as a set point for the control system. The venous pressure level is the input controlling signal. It is compared with the set point and an error voltage is generated which is proportional to the difference between these two levels. This error voltage adjusts the control systems such that the cardiac output will be changed in the appropriate direction in order to increase or decrease the venous pressure level.

Swift et al. (75, 76, 77) and Cholvin et al. (14) have used a slightly different approach to venous pressure control. A small reference zone of venous pressure was used as the reference input. If the venous pressure level was within this "dead" zone then no corrective control action would be initiated. For pressure levels outside the "dead" zone corrective action is taken by altering the stroke volume of the artificial ventricle to bring the venous pressure within the "dead" zone. This type of nonlinear

control system allows for normal small pressure fluctuations which result from respiration and other factors. A more detailed description of this control system and modifications that were made to it will be discussed in the next section of this dissertation.

Various types of artificial heart controllers have been used which utilize venous or atrial pressure as the control variable. The controller is that part of the control system which establishes the relationship between the control variable and the control system output.

Pierce et al. (61) used an integral controller which integrated the error signal with respect to time. They felt that by using an integral controller that the system response would be more stable than if they had used a proportional controller. An integral controller does not respond immediately to transient disturbances of the venous pressure level.

Wildevuur et al. (89) have used proportional, integral and proportional-plus-integral controllers in artificial heart animal trials. The proportional control system produces immediate corrective action to correct system disturbances. A finite steady state error exists in a proportional system. In contrast to this, the integral controller makes adjustments in a more gradual manner to correct system disturbances. It reduces the steady state error to zero. Both characteristics, the elimination of steady state errors and instantaneous response are combined in the proportional-plus-integral controller.

Venous pressure or atrial control has some inherent problems associated with this type of control. With this single control loop there is no provision that the arterial blood pressure level is within a

desired physiological range and that the ventricular flow rate is sufficient to supply the metabolic needs of the systemic tissue beds. It is believed by some researchers that venous pressure control is in itself adequate for controlling an artificial ventricle (57).

Some researchers have used venous pressure control in conjunction with other physiological variables. Kwan-Gett et al. (51) argue that if the regulation of arterial blood pressure is maintained by cardiac output and cardiac output governed by the amount of venous return to the heart, then arterial pressure control is not necessary. But if the cardiac output of the heart is mainly governed by the load into which it pumps, then arterial pressure control is necessary. Koch (49) proposed that cardiac output is regulated by means of arterial pressure receptors in order to maintain a constant arterial pressure level.

Topham (78, 79) has found a cause and effect relationship between the peripheral resistance level and cardiac output. He observed the effect of changing the peripheral resistance on cardiac output by inflating a balloon placed around the descending aorta. The cardiac output for resting values of resistance and for high resistance values due to balloon inflation was compared. Topham found that cardiac output was clearly dependent on the peripheral resistance level. With the animal exercising the usual 100 percent increase in cardiac output associated with the onset of exercise was essentially blocked. The cardiac output only increased by 10 percent when the resistance was held at the resting value. The decrease in vascular resistance during exercise is due to the vasodilation of the local tissue beds. This local autoregulatory effect is biochemical

in nature and dependent on the local tissue biochemical environment. In the first part of this dissertation it was shown that the $\%HbO_2$ level of the blood directly effects the vascular resistance of skeletal muscle tissue beds. Other substances, such as carbon dioxide, hydrogen ion concentration and metabolites from exercising muscle, might also have some effect on the vascular resistance.

Kwan-Gett et al. (51) have developed an artificial heart control system sensitive to atrial pressure and the output arterial pressure. Edwards and Bosher (26) also used a control system which was dependent upon both the venous and arterial pressures as the input controlling signals.

Erickson et al. (28, 29, 30) and Cholvin et al. (12, 13) have used an artificial heart control system which utilized three different methods of control. These were: 1) right ventricle controlled by the venous $\%HbO_2$ and the left ventricle by the left atrial input pressure; 2) right and left ventricles controlled by venous $\%HbO_2$; and 3) right ventricle controlled by the arteriovenous $\%HbO_2$ difference and the left ventricle by the left atrial input pressure. A maximum effort controller was used which utilized a "dead" zone similar to that described above. Perturbations of tissue temperature, inspired oxygen, and changes in the reference "dead" zone were used. They found that the most satisfactory method of control could be achieved by using the hybrid control system of venous $\%HbO_2$ as the control variable for the right ventricle and left atrial pressure as the control variable for the left ventricle. This method has the advantage that it tends to protect the pulmonary circulation from edema. Also, the venous $\%HbO_2$ level is a good prediction of the

adequacy of the tissue perfusion flow rates. Maintenance of the venous $\%HbO_2$ at a given level would insure adequate flow rates for the metabolic requirements of the tissue beds.

The second method of control, right and left ventricle control by venous $\%HbO_2$, was not satisfactory because this method of control did not have an awareness of the return blood flow rate.

The third method of control, arteriovenous $\%HbO_2$ difference as the control signal for the right ventricle and left atrial input pressure as the control signal for the left ventricle, was only effective under ideal conditions. The major problem was that the arterial $\%HbO_2$ level did not remain constant and thus a change in the arteriovenous $\%HbO_2$ difference could not be interpreted correctly for the proper direction of correction.

Sustained or slightly damped oscillations occurred in the stroke volume of both ventricles when continuous correction was applied using the first method of control described above. To alleviate this problem damping was applied by sampling the level of $\%HbO_2$ and thus the duration of the control response was limited.

Akutsu *et al.* (1) and Hall *et al.* (40) have used artificial heart control systems which utilize the natural pacemaker center of the heart. The input control signal is secured from electrodes implanted in the vicinity of the SA node. The advantage of this method of control is that the input control signal is dependent on the physiological state of the animal as reflected by the autonomic nervous system activity. One inherent problem with this method is that arrhythmias might occur which would cause erratic and unpredictable control system operation.

It appears that there has been a limited amount of work involved in examining the dynamic characteristics of both the artificial heart control system and the particular segment of the cardiovascular system being controlled. Without this basic dynamic information, in terms of a set of mathematical equations or transfer function descriptions, the performance of the animal-machine system can not be successfully predicted. However, with this information available, the stability and performance of the proposed system of control can be effectively evaluated. Compensation may be added, if necessary, to modify the response in order to meet the desired response criteria.

Oscillations and unstable artificial heart control system responses have been observed by a number of research groups (12, 30, 60, 73, 89). If the dynamics of the physiological system under control and dynamics of the artificial heart control system are found, and if through appropriate calculations it is determined that unstable results will occur, then necessary modifications can be made to the artificial heart controller which would eliminate these undesirable oscillations. The main difficulty with this approach is not in evaluating the dynamic characteristics of the artificial heart control system, but rather it is in determining the dynamic characteristics of the physiological system being controlled.

An example of this approach can be illustrated. Suppose that the cardiac output of an artificial heart was to be controlled by the systemic arterial pressure level. This negative feedback system would control the cardiac output in order that a reference arterial pressure level would be maintained. The information necessary to analyze the performance of such a system consists of two parts: 1) the dynamic characteristics of the

arterial heart control system (i.e., how is the cardiac output of the artificial heart related, in the dynamic sense, to the input control signal of the artificial heart controller) and 2) the dynamic characteristics of the physiological system being controlled, i.e., how is the systemic arterial pressure related, in the dynamic sense, to the cardiac output. This analysis should take into account all the system time lags. With the above information at hand, the stability of the proposed method of control can then be easily analyzed. Modifications to the artificial control system could be made to eliminate the presence of oscillations and possibly optimize the control function.

An approach similar to that outlined above has been used in this dissertation research. An attempt has been made to control an artificial ventricle by means of the arterial $\%HbO_2$ level. In the first part of this dissertation the dynamic characteristics relating the arterial $\%HbO_2$ level and the blood flow rate were found for canine skeletal muscle. The portion of the dissertation that follows describes the methods used to find the transfer function description of the artificial heart control system. In the last part of the dissertation one method of controlling the cardiac output of an artificial ventricle which is dependent upon the arterial $\%HbO_2$ level will be discussed.

APPARATUS

The artificial ventricle power and control system is a modified version of that used by Swift et al. (75, 76, 77). They used a maximum effort control system. In the present study a proportional control system was used. Both of these control systems regulate the stroke volume of a pneumatically powered artificial ventricle. The maximum effort system is not a continuous error correcting system. Rather, it makes use of a "dead" zone which allows for small variations in the control variable. One problem encountered with this nonlinear type system is a "hunting" or oscillator response which occurs when the machine's reponse time is not matched to that of the animal's. The gain of the system also has a direct effect on the stability of the system response.

A proportional control system is a continuous error correcting system. Proportional feedback control systems are also prone to unstable oscillatory conditions which result when the closed loop system gain is such that positive feedback occurs. The above discussion points out that the properties of the artificial heart controller should be carefully selected such that the animal-machine control system will be stable.

In order to appreciate the functions of the artificial ventricle and its associated power and control systems a brief description of these components will be given. Figure 37 shows a schematic diagram of the artificial ventricle power and control systems.

Cholvin et al. (14) and Swift (75) discuss the construction and operation of the extracorporeal artificial ventricle used. Basically, it consists of an air chamber and blood chamber separated by an elastic

diaphragm which, when filled with air under pressure, bulges, forcing blood out the exit port. Unidirectional flow is insured by two silicone rubber flap valves. The exit port valve prevents back flow into the blood chamber and the inlet port valve prevents back flow out of the blood chamber.

An artificial atrium was connected at the inlet port of the artificial ventricle to facilitate ventricle filling. The placement of this artificial atrium is shown in Figure 38. This small silicone rubber collapsable chamber absorbs the negative filling pressures which tend to collapse the great veins.

The stroke volume of the artificial ventricle is determined by the volume of air pulsing the ventricle. An electromechanical solenoid valve meters compressed air to the ventricle. The rate and duty cycle (fraction of cycle during which air enters ventricle) of the pulsations can be independently adjusted by relaxation oscillator circuits which operate the solenoid valve. The amount of pulse air reaching the ventricle's air chamber is determined by a bleeder valve which exhausts to the atmosphere. With the bleeder valve completely closed all the pulsed air of the source reaches the ventricle. With the valve open less pulsed air reaches the ventricle, the remainder of it is shunted to the atmosphere.

Ventricular output can be varied in four ways: 1) by varying the pressure of the compressed air supply; 2) by varying the frequency of pulses; 3) by varying the duty cycle; and 4) by changing the amount of bleed off in the air line. The last method mentioned was chosen for controlling the ventricular output. The position of the bleed-off needle

valve was controlled by a low rpm permanent magnet motor-tachometer[1] which was incorporated in the control circuit.

The proportional control system consists of a velocity servomechanism which controls the velocity with which the air bleeder valve turns. This, in turn, controls the amount of pulsed air which reaches the artificial ventricle and thus its stroke volume. Figure 37 shows a schematic diagram of the artificial ventricle control system. Basically, it consists of a dc amplifier driven motor-tachometer which controls the air bleeder valve. The operational power amplifier[2] is supplied by three inputs: 1) the input controlling signal; 2) the balance potentiometer input; and 3) the negative feedback from the tachometer. The input controlling signal is a voltage proportional to the control variable. This signal can be supplied directly by a physiological transducer or it can be derived from performing mathematical operations on a physiological signal. The balance input supplies a voltage which is used as a comparison or reference input. The negative tachometer feedback effectively eliminates the dead zone of the dc motor.

Swift (75) has examined the steady state performance of the artificial ventricles. Two sets of *in vitro* tests were performed with water as the pumped fluid. A family of curves was found relating the liquid output, with constant pulsed air pressure, to pressure head. The duty cycle, rate,

---

[1] #E-500 MGR, with 200:1 Thor speedway gearhead attached, dc servo motor, Electro-Craft Corporation, Minneapolis, Minnesota

[2] Model 440K Kit, Opamp Labs, Los Angeles, California

input filling pressure and air bleeder valve position were maintained constant. The ventricle was found to be load sensitive, i.e. the output flow rate of the ventricle was inversely related to the pressure head for any given air pressure level.

In another set of experiments data were obtained relating the liquid output, with constant pulsed air pressure, to the input filling pressure. The duty cycle, rate, pressure head and air bleeder valve position were maintained constant. These tests showed that the input filling pressure did not significantly alter the fluid output of the artificial ventricle for a given level of pulsed air pressure, as the input filling pressure was varied from -10.0 to 15.0mm Hg.

EXPERIMENTAL METHODS

In addition to the steady state characteristics of the artificial ventricle, the dynamic characteristics of the artificial ventricle and its associated power and control systems should be known. In the present project the dynamic as well as the steady state characteristics of the artificial ventricle were defined in terms of a transfer function relating the control system input to the fluid output of the artificial ventricle. Transfer functions were found for three values of duty cycle (32%, 44%, 56%) and rate (60 b/min, 73 b/min, 84 b/min), where b/min = beats/minute, for the condition of constant input filling pressure and constant output pressure head.

Figure 38 is a diagram of the test circulation which was used to determine the transfer function of the artificial ventricle power and control systems. A standard blood analog, 36.7% by volume of glycerine in water, which approximates the viscosity of blood, was used as the pumping fluid (88). The output of the artificial ventricle and the overflow from the constant level filling reservoir were returned to the supply reservoir. The fluid from the supply reservoir was pumped to the constant level filling reservoir which maintained the input filling pressure at approximately 1mm Hg. The height of the column of fluid pumped determined the end diastolic pressure. This pressure head level was set at 60mm Hg. The artificial ventricle air pressure, the output fluid pressure and the input filling pressure were continuously monitored by

means of three strain gauge pressure transducers[1]. The frequency response for these pressure transducers is essentially flat from zero to 20 Hertz. These three pressure signals were recorded on a polygraph recorder.[2]

Calibration curves relating the output flow rate of the artificial ventricle to the fluid output pressure and the pulsed air pressure were found. Figures 39 and 40 show typical calibration curves. The maximum or systolic pressure values were used in determining the calibration curves. The flow rate was found by determining the length of time necessary to fill a calibrated graduated cylinder. These calibration curves were then used in the dynamic tests discussed below.

As mentioned above, the dynamic tests consisted of finding the transfer function for the artificial heart and its associated power and control systems. The transfer function input is the input to the control system and the output is the artificial ventricle flow rate. The effects of the heart rate and duty cycle on this transfer function were examined. The method of obtaining the desired transfer function consisted of using the frequency analysis method. In this method constant amplitude sinusoidal signals are applied to a system and the resulting sinusoidal output variations are recorded. The output amplitude and phase variations provide the necessary information needed for the Bode amplitude and phase plots. Low frequency (0.01 to 0.50 Hertz) constant amplitude signals were applied

---

[1]One #PR23-1D-300 for input filling pressure and two #P23AC for air pressure and output fluid pressure, Statham Instruments, Incorporated, Hato Rey, Puerto Rico

[2]Grass Model 7 Polygraph, Grass Instruments Company, Quincy, Massachusetts

to the control system input by means of a low frequency function generator.[1] The output sinusoidal pressure variations were recorded. A calibration curve was found for each transfer function determination, in which the values of a parameter were changed. Using the corresponding calibration curve, the variations in output flow rate were found from the fluid output pressure variations. In addition to the recordings of the three pressures mentioned above, the input to the control system and the tachometer feedback voltage (proportional to motor shaft velocity) were attenuated and recorded on the polygraph recorder. Figure 41 shows a typical recording taken during one of these experiments. The apparent distortion of the sinusoids is created by the curvilinear recording of the polygraph. Recordings are shown for three input sinusoidal control frequencies, 0.015, 0.05 and 0.15 Hertz. It should be noted that the tachometer output, linearly related to the motor shaft velocity, does not show any attenuation with an increase in frequency. The significance of this result will be explained below.

In order to standardize the transfer function tests the air bleeder valve position was adjusted such that the maximum pulsed air pressure was 150mm Hg when the input sinusoidal control signal was at its maximum value and decreasing. This point is shown as point A in Figure 41. The output fluid pressure and consequently the output flow rate would oscillate about this operating point. The input balance potentiometer of the operation amplifier (Figure 37) was adjusted such that the motor voltage was zero

---

[1] Model HP202A, Hewlett-Packard Corporation, Palo Alto, California

at the operating point. This insured that the maximum and minimum values of the output flow rate would not drift from one cycle to the next. The amplitude of the input control signal was maintained constant at one value of voltage for all transfer function tests. This value of voltage was chosen such that operation was limited to the most nearly linear portion of the calibration curves.

The effects of using a thicker artificial ventricle membrane on the calibration curve and transfer function was determined. The thicker membrane was 0.02" while the membrane for the previous tests was 0.01" thick. Higher values of pulsed air pressure were used for the thicker membrane. The operating point for the transfer function determination was 300mm Hg of pulsed air pressure.

RESULTS AND DISCUSSION

This section deals with the results of the *in vitro* artificial ventricle calibration curve and the transfer function experiments.

Figures 42 through 45 show the results of the calibration curves. These figures display families of curves relating output flow rate to the pulsed air pressure (Figures 42 and 44) and the output flow rate to the fluid output pressure (Figures 43 and 45) for three values of duty cycle and three values of artificial ventricle rate.

The effect of the duty cycle on the output flow rate for a given value of pulsed air pressure is exhibited in Figure 42. For values of pulsed air pressure less than 300mm Hg an increase in duty cycle increases the fluid output. This is due to the fact that an increase in duty cycle, by definition, increases the fraction of the pumping cycle during which the artificial ventricle pumps. For the 56% duty cycle curve an interesting effect occurred. For pulsed air pressures above 300mm Hg an increase in pulsed air pressure caused a decrease in the output flow rate. This effect was most likely due to inadequate ventricular filling because of the combination of the high duty cycle and high pulsed air pressures. It is obvious that a characteristic curve of this type should be avoided since the control of the artificial ventricle output is based upon the premise that an increase in pulsed air pressure will increase the fluid output. In this particular calibration test an increase in air pressure could cause a decrease in the output flow rate, an undesirable result.

The effect of the artificial ventricle rate on the graph of the output flow rate versus pulsed air pressure is shown in Figure 44. It is noted

that higher values of output flow rate result from the low values of heart rate. The apparent reason for this decrease in flow rate with an increase in heart rate is that as the rate is increased the ventricular filling volume is decreased and thus the stroke volume per cycle is decreased. Although the heart rate has increased, the total output flow rate (stroke volume times heart rate) decreased because the decreasing stroke volume effect was greater then the increase due to the heart rate.

The family of curves relating the output flow rate to the fluid output pressure for three values of duty cycle and for three values of artificial ventricle rate are displayed in Figures 43 and 45, respectively. In each case the output flow rate increased as the fluid output pressure increased.

Figure 40 shows the calibration curve for the thicker (0.02") membrane. In comparing this calibration curve to that of Figure 39 (membrane - 0.01"), it is noted that the artificial ventricle flow rate can be significantly increased by using the thicker (0.02") membrane with higher values of pulsed air pressure.

The transfer function of the artificial ventricle power and control system was found to be essentially an integrator of the form $\frac{K}{s}$ where K is the system gain = $\frac{\Delta \text{ output flow rate in ml/min}}{\Delta \text{ input control signal in volts (peak-peak)}}$. The integrator nature of the transfer function is due to the nature of the air bleeder control valve. This is clearly demonstrated by the fact that the output flow rate increases directly with time for a constant valve of input control signal voltage. Essentially this is the method of operation of an integrator. With zero input control signal applied the motor and air bleeder valve velocity are zero. This results in a fixed amount of

pulsed air pressure at the artificial ventricle. With a constant voltage applied a constant motor shaft and air bleeder valve velocity is reached. This would result in an output flow rate which would increase linearly with time, provided that two conditions hold. A linear relationship between the amount of pulsed air pressure reaching the artificial ventricle and the air bleeder valve position is required. This appears to hold true for the particular air bleeder needle valve used. A linear relationship between the output flow rate of the artificial ventricle and the amount of pulsed air pressure reaching the ventricle is also necessary. This requirement can be examined in Figures 42 and 44. It is observed that this requirement is met for fairly wide ranges of pulsed air pressure.

Bode amplitude plots for three values of heart rate and duty cycle are shown in Figures 46 and 47, respectively. With the amplifier gain set for 25, the transfer functions for the three values of heart rate were all found to be approximately $\frac{1.25 \text{ ml/min}}{\text{volt (p-p)}}$/S. This incremental transfer function can be found by observing on the Bode amplitude plot (log-gain vs. log-frequency) that the slope is essentially -1 and the value of gain at ω = 1 radian/sec is equal to 1.25. The reason for essentially the same transfer function gain for the three values of heart rate is seen in the calibration curves. These curves (Figures 44 and 45) show that the slopes of the curves for the three values of heart rate at the operating point chosen, are essentially the same and thus approximately equal incremental transfer function gains would be expected.

Figure 47 shows that the incremental transfer function gain varies with the value of the duty cycle. The gain was found to be 1.5, 1.25, and

1.15 for duty cycle values of 56%, 44%, and 32%, respectively. The reason for this variation can be seen in the slope of the calibration curves (Figures 42 and 43) at the operating point chosen. The slope of the calibration curves increased as the value of duty cycle was increased. Thus for a given change in the input control signal the resulting pulsed air pressure caused a larger change in the output flow rate for higher values of duty cycle.

The transfer function for the thicker membrane (0.02") resulted in a significant increase in the incremental gain over that found for the thinner membrane (0.01") discussed above. The incremental transfer function was found to be 3.25/S for the 0.02" thick membrane (Figure 48).

It was observed that the phase shift between the input control signal and the output pressure was approximately 90^{o} over the frequency range used. This result verifies the simple integrator nature of the transfer function found from the Bode amplitude plot.

The effect of the motor time constant was not observed in the Bode amplitude plot or the phase relationships between the input and output functions. Also, as mentioned above, there was not any noticeable attenuation in the tachometer voltage (proportional to motor shaft speed) over the operating range of frequencies. This is to be expected at the low frequencies at which the analysis tests were performed. For this closed loop dc motor velocity control system a time constant of less than 100 milliseconds would be expected, which would mean an angular frequency of greater than 64 radians/sec, much greater than the frequency range examined here.

SUMMARY

Using the frequency analysis technique, transfer functions were found for the artificial heart power and control systems. These transfer functions relate the change in input control signal to the change in fluid output flow rate. These incremental transfer functions were found to have the form of an integrator, K/S, where K is the incremental gain, $\frac{\Delta \text{ ml/min}}{\Delta \text{ volts}}$. The value of K was found to be dependent upon the duty cycle value but not significantly upon the artificial ventricle rate. The thickness of the artificial heart membrane had a direct effect on the value of K. With the 0.01" thick membrane K was found to be 1.5, whereas with essentially the same test conditions, but with 0.02" thick membrane the value of K was found to be 3.25. In order to supply adequate flow rates for the normal sized dog the thicker membrane was used in the *in vivo* artificial heart studies described in the next section of this dissertation. However, with a more efficient design for an artificial ventricle it would be desirable to use a thinner membrane with the associated lower air pressure levels.

PART III. *IN VIVO* ARTIFICIAL HEART CONTROL STUDIES

INTRODUCTION

The first part of this dissertation was concerned with finding a transfer function relating arterial oxyhemoglobin concentration and blood flow rate in the canine hind limb. From this basic information, an extrapolated transfer function relating the arterial oxyhemoglobin level to the flow rate needs of the total body is proposed. The second portion of the dissertation dealt with a dynamic analysis of the artificial heart power and control systems. A transfer function was found relating the input control signal of the artificial heart to the artificial ventricle output flow rate.

This last portion of the dissertation describes an attempt to use the extrapolated transfer function and the artificial heart transfer function to control the cardiac output of an artificial ventricle with the arterial oxyhemoglobin concentration level as the control signal. A series of experiments was designed to test the feasibility of using this type of artificial heart control system. Various degrees of whole body hypoxia were used as perturbations to the animal machine system.

LITERATURE REVIEW

This literature review section is concerned with two topics. First, cardiovascular system models whose cardiac output regulation depend upon changes in the peripheral resistance will be discussed. The second portion is concerned with cardiovascular system responses to total body hypoxia.

Cardiovascular System Models

As discussed previously, Topham (78, 79) and Warner *et al.* (87) have shown that cardiac output is controlled by the peripheral resistance. From experimental observations of exercising dogs in which the peripheral resistance was changed by the inflation of a baloon which compressed the aorta, they found a cause-effect relationship between the peripheral resistance and the cardiac output. Cardiac output was dependent upon the peripheral resistance. They proposed that vasodilatation, which occurs during exercise, was probably due to decreased tissue oxygen concentration or increased carbon dioxide concentration or the presence of other metabolites. They proposed that the baroreceptor reflex reacted to the decrease in systemic pressure, due to the fall in peripheral resistance, by increasing the cardiac output and thus bringing the systemic pressure back to "normal".

The block diagram which they proposed for the cardiac output control system during exercise is shown in Figure 49. Exercise arouses the animal and affects the local biochemical environment of the muscles. Local autoregulation occurs due to the decreased oxygen availability due to other biochemical or metabolic products. The vasodilatation causes a drop

in the peripheral resistance. The arterial pressure level and a reference level of systemic pressure is compared in the central nervous system. The systemic pressure reference level can be modified by the arousal level of the animal. The error signal is positive at the onset of the exercise. This results in an increase in sympathetic and a decrease in vagus activity. The heart rate will increase and the stroke volume will be affected to some degree. They found that the stroke volume was determined primarily by the mechanical impedance change of the aorta. The increase in heart rate causes the cardiac output to increase. This in turn causes an increase in the arterial pressure toward its resting value. The increased blood flow provides a more effective transportation of metabolic substances to and from the local exercising muscles.

Grodins (34) has proposed a model of the cardiovascular system which depends upon chemostatic control of cardiac output. Grodins proposes that the systemic arterial pressure indirectly regulates the cardiac output. The peripheral resistance varies with the local tissue biochemical environment. This local autoregulation is independent of central nervous system control. If the peripheral resistance should be reduced by changing the local biochemical composition (decrease in the oxygen availability) at the local tissue level the arterial pressure (cardiac output X resistance) will decrease. This decrease in the systemic pressure will in turn increase the cardiac output via the baroreceptor mechanism. Thus the arterial pressure will increase to a level sufficient to supply the necessary blood flow levels for the metabolic needs of the local tissue beds.

Guyton et al. (38) propose that the phenomenon of local autoregulation

due to low oxygen levels determines the level of cardiac output by venous return control of cardiac output. Guyton (35) states that, "the tissues themselves possibly regulate their own blood flow in proportion to their own blood flow, they also regulate the tendency for blood to return from the systemic circulation to the heart and thereby the cardiac output".

Cardiovascular System Response to Hypoxia

As mentioned previously, the peripheral circulation is under a dual control. The central nervous system maintains the homeostasis of the entire cardiovascular system while the local tissue beds control their own vasculature. This latter control is dependent on the biochemical conditions in the local tissue environment. This dual control allows for a number of vascular adjustments which enable the body to direct blood flow to those areas where it is needed most and away from areas whose immediate requirements are less (4). The degree of dominance of the intrinsic or extrinsic control mechanisms depends on the local tissue bed. In the control of the blood supply to the two vital structures, the heart and brain, the intrinsic flow-regulating mechanisms dominate.

The control of the blood supply to skeletal muscle is governed by an interplay between the intrinsic and extrinsic mechanisms. During rest the neural control governs, while the intrinsic mechanism takes over control during exercise. As previously mentioned, anticipation of exercise brings an increase in the blood flow to the skeletal muscles. After the onset of exercise, the local intrinsic mechanisms assume control with local vasodilatation occurring due to low oxygen availability or metabolic by-products.

The chemoreceptors (carotid and aortic bodies) are small highly vascular bodies which are sensitive to changes in the Po_2, pH and Pco_2 of the blood bathing them (9). They are primarily concerned with respiratory system regulation. The carotid and aortic bodies respond to a hypoxic stimulus by increasing the depth and rate of respiration. They also influence the extrinsic control mechanism of the peripheral vascular resistance. It is felt that this vasoconstrictor response occurs, because of the interaction between the respiratory and vasomotor centers, in the brain. This chemoreceptor response to hypoxia can modify or diminish the local intrinsic autoregulatory mechanisms associated with hypoxia. In the first part of this dissertation it was demonstrated that local hypoxia of the skeletal muscle bed produced vasodilatation.

Litwin et al. (54) examined the chemoreceptor influence on the perfused hind limb of dogs. They found that vasoconstriction of the perfused hind limb resulted in animals breathing 5 percent oxygen. This response was almost entirely due to the stimulation of the chemoreceptors by the low blood oxygen levels.

Gorlin and Lewis (33) subjected dogs to varying degrees of hypoxia. They found that with arterial saturations down to 60%, that the only effects were on the vascular resistance. An immediate systemic vasoconstriction and hypertension with no cardiac output change was observed.

Kahler et al. (45) found an increase in systemic vascular resistance with hypoxia localized in the carotid arterial bed. With systemic hypoxia and chemoreceptor denervation a decline in systemic vascular resistance was observed. Their results indicated that the direct effect of hypoxia

is in arteriolar dilation but that this response is masked by the arteriolar constriction mediated by the chemoreceptor reflex arc.

To complicate the circulatory response to hypoxia further, it has been proposed that the sympatheticoadrenal system also has an effect. Daugherty et al. (19) found that oxygen and carbon dioxide were locally vasoactive when the fore limb and coronary vascular tissue beds were investigated individually. In another series of experiments Daugherty et al. (20) observed the active changes in the caliber of the blood vessels in the dog fore limb during generalized hypoxia and hypercapnia. They found that the degrees of hypoxia and hypercapnia used produced little active change in the caliber of the blood vessels. They felt that the local actions of hypoxia and hypercapnia on the fore limb vasculature were antagonized by remote actions. Daugherty et al. (20) proposed that one of the remote systems might be the sympathicoadrenal system. They attempted to directly verify the participation of the sympathicoadrenal system in the fore limb responses. Bilateral adrenalectomy was performed on a group of animals. A comparison between these animals and the normal ones could not be made because the vascular resistance of the bilateral adrenalectomic animals was too low.

Secondary reflexes associated with lung stretch receptors have been found to have a direct effect on the observed effects of systemic hypoxia. Daly and Scott (18) found a secondary reflex caused by hypoxic chemoreceptor stimulation. They found in the spontaneously breathing dog that the not infrequently observed cardiac acceleration, due to chemoreceptor stimulation, was due to a secondary reflex arising from the

lungs and not a primary reflex from the carotid bodies.

Kontos et al. (50) in a series of generalized hypoxia experiments found that the circulatory response to systemic hypoxia could be characterized by a decrease in limb and systemic vascular resistances and an increase in cardiac output, and tachycardia. They also found, in contrast, that during hypoxia with ventilation fixed by means of a respiratory pump and skeletal muscle paralysis that the cardiac output remained the same, heart rate decreased, systemic vascular resistance increased, and limb vascular resistance did not change. Kontos et al. proposed that in spontaneously breathing dogs the response to hypoxia is dependent on the associated increase in ventilation.

The local vasodilatory effects of systemic hypoxia have been observed by a number of researchers (74, 50). Smith and Crowell (74) examined the influence of hypoxia on the mean circulatory pressure and cardiac output in dogs. They observed that in a comparison of their results from normal animals and animals deprived of their circulatory reflexes that the degree of vasodilatation due to hypoxia was much greater without the influence of reflexes. Thus, they concluded that the intense arteriolar vasodilatation initiated by hypoxia in the normal dog is partially counterbalanced by the sympathetic nervous system which prevents the fall in the arterial pressure.

Kontos et al. (50) summarize the various differing circulatory responses to systemic hypoxia. Systemic hypoxia directly affects the blood vessels, the heart and the chemoreceptors. It also affects the central nervous system and the increased release of catecholamines from the

adrenal gland. Systemic hypoxia also has a direct affect on the increase in ventilation. Systemic vasodilatation, increase in cardiac output and tachycardia result from some of these effects. Whereas, systemic vasoconstriction, decrease in cardiac output, and bradycardia result from others. Thus, it is seen that the circulatory response to systemic hypoxia can be quite complex depending upon the experimental preparation used.

APPARATUS

This section of the dissertation will be concerned with a method of controlling the cardiac output of an artificial ventricle with arterial oxyhemoglobin concentration as the control variable. It should be mentioned that this single variable control is not sufficient by itself, but rather it could act as one control loop of a multiple variable control system. The other variables for such a control system might include; atrial or venous pressures, arterial pressure, the electrical activity from the intact pacemaker of the heart, venous oxyhemoglobin concentration, and other biochemical variables.

In order to test the validity of using the proposed artificial heart control system, its effectiveness must be tested both as a single variable controller and as one component of a multiple variable control system. The evaluation of the artificial heart control system with single variable control was chosen as the first step of evaluation.

The transfer function found in the first part of this dissertation related arterial oxyhemoglobin concentration to the blood flow rate in the canine hind limb. An extrapolated transfer function relating arterial oxyhemoglobin concentration to the total blood flow needs of the body tissues can be found by scaling the gain constant of the transfer function found for the hind limb.

Local autoregulation due to oxygen concentration has been demonstrated to occur in skeletal muscle (17, 65, 81, 82) cardiac muscle (10, 11), and intestine vesseis (10, 11). On the basis of mass muscle is the major component (4). It represents the largest vascular bed and thus the

participation of its vasculature plays an important role in the total peripheral resistance of the body. To find the extrapolated transfer function it was assumed that the total body vasculature behaved in a similar fashion, with respect to arterial oxyhemoglobin concentration levels, as the hind limb vasculature did. At the termination of three experimental trials the canine hind limb was removed and weighted. The weight of the hind limb was found to be approximately 10 percent of the animal's total weight. The mean value of k for the hind limb experiments was 0.12ml/min/oxyhemoglobin concentration - Kg of body weight. Assuming a linear relationship, the value of the gain constant K for the whole body would be 10k = 1.2ml/min/oxyhemoglobin concentration -Kg of body weight.

Although it was observed in the first part of this dissertation that the value of k is dependent upon the direction of change of the $\%HbO_2$ level, for the purposes of simplification only one value of k was used.

The time constant for the extrapolated transfer function was assumed to be the same as that found for the hind limb (mean value of $\tau = 85$ seconds). The extrapolated transfer function then becomes

$$\frac{\Delta \text{ flow rate}}{\Delta \%HbO_2} = \frac{-1.2}{85\,S + 1} \tag{4.1}$$

An immediate first approach to the problem of controlling the cardiac output of an artificial ventricle would be to connect the system as a negative feedback control system. This system is shown in Figure 50. This arrangement utilizes a transfer function which relates the change in flow rate as the input to the change in the arterial oxyhemoglobin concentration level as the output. This transfer function is assumed to be

the reciprocal of the transfer function given in Equation 4.1. From a purely engineering point of view this should work for a bilaterally linear system, but an examination of the physiology of the system shows that the system is unidirectional and nonlinear. Thus, this proposed method of control can not be used.

An alternate method of control is shown in Figure 51. This method of control is an open loop control system. With this controller it is assumed that the animal's total blood flow needs for various levels of arterial oxyhemoglobin concentration can be predicted from the extrapolated transfer function. Thus the artificial heart control system is set up to supply the necessary total blood flow rate (cardiac output) from a knowledge of the arterial oxyhemoglobin concentration level.

For this control system the transfer function relating the artificial ventricle cardiac output to the arterial oxyhemoglobin concentration is the extrapolated transfer function. Figure 52 shows the schematic diagram of this artificial heart control system. As mentioned previously this system is an open loop control system with all the problems associated with this type system. For a control system of this type to perform effectively it would have to be incorporated as one control loop of a multiple loop control system. In order to test the feasibility of this control system, the single loop control will be analyzed and tested first.

Basically the system measures the arterial oxyhemoglobin concentration level by means of an oximeter and produces a cardiac output as determined by the extrapolated system transfer function. For a sudden change (step input) of arterial oxyhemoglobin concentration the output flow rate will

change exponentially to a new level as determined by the magnitude of the input change.

Refer to Figure 52. The fiber optic oximeter described in the first part of this dissertation was used to monitor the arterial oxyhemoglobin concentration. From previous calibration data the relationship between the arterial oxyhemoglobin concentration and the oximeter voltage output was known. Using this information, operational amplifiers[1] 1 and 2 were utilized to yield the $\%HbO_2$ level in terms of a corresponding voltage value from the oximeter voltage. Since an incremental transfer function is desired, the change in oxyhemoglobin concentration ($\Delta\%HbO_2$) is necessary. This is obtained by subtracting a given arterial oxyhemoglobin reference ($\%HbO_2$ ref.) level from the existing $\%HbO_2$ level. The input to amplifier 2 from potentiometer 3 provides this reference input signal. As shown in Figure 52 the output of amplifier 2 is the $\Delta\%HbO_2$ divided by 100. This gain reduction was necessary because the operational amplifiers saturate at $\pm$ 10 volts.

Amplifiers 3 and 4 are connected to provide the transfer function

$$\frac{Y}{X} = \frac{10S}{S + 0.0118} \qquad (4.2)$$

where X and Y are the input and output to amplifiers 3 and 4, respectively. The input to amplifier[1] 5 from balance potentiometer 6 allows adjustments to be made to the control system, such that for the case when the $\Delta\%HbO_2$

---

[1] TR20, Electronics Associates, Inc., West Long Branch, New Jersey

is zero, the control motor velocity is zero and thus the ΔFR is zero. The output of amplifier 5 is a constant value times the derivative of the change in flow rate ($\Delta \overset{\cdot}{F}R$). This voltage signal is then fed into the artificial heart control system, which was found to be essentially an integrator. This integration of the $\Delta \overset{\cdot}{F}R$ produces the change in the output flow rate (ΔFR).

In summary this artificial heart control system method is an open loop control system which supplies the necessary cardiac output as determined by the arterial oxyhemoglobin concentration level. For a 14.5kg dog the extrapolated transfer function found by scaling the mean value data found from the canine hind limb experiments is

$$\frac{\Delta FR}{\Delta \%HbO_2} = \frac{-17.4}{85S + 1} \tag{4.3}$$

The above proposed method of controlling the cardiac output of an artificial ventricle is similar in some respects, to the previously mentioned theories (34, 78, 79, 87) in which cardiac output is controlled by the peripheral resistance. In those studies the peripheral resistance affected the cardiac output level through the baroreceptor feedback mechanism or by means of the venous return to the heart. The method proposed in this dissertation takes a different but similar approach in that the cardiac output of the artificial ventricle is being controlled by means of a transfer function relationship which essentially supplies information concerning the peripheral resistance of the body tissue beds for a given level of arterial oxyhemoglobin saturation. The necessary flow rate is then supplied by the artificial ventricle from the knowledge of the peripheral resistance value of the body tissue beds.

EXPERIMENTAL METHODS

A left ventricle bypass procedure was used to test the feasibility of the proposed artificial heart control system. This method was chosen because the replacement or assist of the left ventricle has the most clinical significance for patients with severe heart damage.

Nine mongrel dogs ranging in weight from 10.0 to 14.5 kg were used. Anesthesia was induced in the dogs with a thiobarbituate[1] and maintained with nitrous oxide and methoxyflurane.[2] The lungs were ventilated with 100% oxygen by means of a positive-negative respirator[3] and the anesthetic agent was administered through an anesthetic machine[4] coupled to the ventilator equipment. In two experiments a closed chest preparation in which the animal was allowed to breath unassisted, was used.

The right femoral vein, the jugular vein and the left carotid artery were exposed. A left thoracotomy was then performed through the 5th intercostal space. At this point heparin was administered (3mg/kg body weight). An equal amount of heparin was administered every two hours.

A loose ligature was placed at the root of the aorta just distal to where the coronary arteries emerge. The femoral vein was cannulated in

---

[1]Surital, Parke, Davis and Co., Detroit, Michigan

[2]Metofane, Pitman Moore, Division of the Dow Chemical Co., Indianapolis, Indiana

[3]Model 8, Bird Corporation, Palm Springs, California

[4]Bennet Assistor, Model BA-2P, Bennet Respiator Products, Inc. Los Angeles, California

both directions and an oximeter was connected between these two catheters. The left carotid artery was cannulated for systemic pressure recordings. The descending aorta was exposed and the intercostal arteries were ligated. Umbilical tape was placed around the aorta. The aorta was quickly cannulated in both directions. The two catheters were connected by a stainless steel "T" connector which allowed blood to flow through the aorta.

The pericardial sac was incised. A loose purse string suture was placed in the apex of the left ventricle. The apex was punctured and a special catheter was inserted and tied in place with the purse string suture. The heart was then positioned for optimum left ventricular and systemic arterial pressure values. The ventricular pickup catheter was made from a 5 cc disposable syringe body into which approximately 10-1/8" diameter holes were drilled. This type catheter provided a better blood supply for the artificial ventricle than an arterial or a venous catheter since there was less of a chance for an occlusion in the catheter openings.

Next, the artificial heart perfusion apparatus was set in place adjacent to the animal. Figure 53 shows a schematic diagram of this extracorporeal blood flow system. The tubing[1] and associated equipment was primed in advance with cross matched canine donor blood (approximately 700cc). All air bubbles were carefully removed before artificial ventricle pumping was initiated. As shown in Figure 53 the blood source for the extracorporeal path is from the left ventricle. The blood then flows through the following apparatus; the buffer chamber, the artificial

---

[1] S-50-HL, Tygon, U.S. Stoneware Corporation, Akron, Ohio

ventricle, the bubble trap and the heat exchanger. Arterial oxyhemoglobin concentration was measured by inserting a fiber optic oximeter in a shunt segment of tubing in the output line of the artificial ventricle. Blood temperature was monitored by a thermistor probe inserted in the blood line[1]. It was maintained at 37.0±0.5 C by means of the hyperthermia unit described in the first part of this dissertation. The relative flow rate was measured using an electromagnetic flowmeter.

The control system and physiological variables with their associated transducers, that were used to evaluate the performance of the animal-machine system are listed below.

1. Left ventricular pressure - strain gauge pressure transducer[2]
2. Systemic pressure, carotid artery - strain gauge pressure transducer[2]
3. Right atrial pressure, jugular vein catheter into right atrium-strain gauge pressure transducer[3]
4. Artificial ventricle air pressure - strain gauge pressure transducer[2]
5. Relative flow rate - electromagnetic flowmeter.
6. Arterial oxyhemoglobin concentration - fiber optic oximeter
7. Venous oxyhemoglobin concentration - fiber optic oximeter

---

[1]Type 423, Thermistor probe, Model 43TA, Tele-Thermometer, Yellow Springs Instrument Co., Yellow Springs, Ohio

[2]Model P23AC, Statham Transducers, Inc., Hato Rey, Puerto Rico

[3]Model PR23-1D-300, Statham Transducers, Inc., Hato Rey, Puerto Rico

8. Electrocardiogram

9. Electroencephalogram

10. Control motor speed voltage

11. Blood temperature - thermister probe.

All the above variables were recorded on ink writing polygraph recorders[1].

Hematological and blood studies (pH, Pco_2 and hematocrit) were also used to evaluate the animal's condition during the course of the experiment.

It was necessary to establish a criterion to determine how well the artificial heart and associated control system were performing. The primary criterion was the ability of the artificial ventricle system to maintain the animal in a state of homeostasis, with respect to certain physiological variables, after pumping was initiated.

The animal was shifted from natural heart pumping to the artificial ventricle by slowly tightening the loose ligature placed around the aorta. With the ligature securely tied, the artificial heart was supplying the systemic system with the natural heart still supplying its own coronary arteries.

A number of system perturbations were tried with the artificial ventricle maintaining the systemic circulation. These perturbations were designed to test the feasibility of using the proposed artificial ventricle control system which uses arterial oxyhemoglobin concentration

---

[1]Model 5 and Model 7, Grass Instruments Co., Quincy, Massachusetts

as the control signal which causes the cardiac output of the artificial ventricle to change according to the extrapolated transfer function relating arterial oxyhemoglobin concentration to total blood flow. The perturbations consisted of changing the gas mixture which the animals breathed. The gas mixture was changed from 100% O_2 to a low oxygen content mixture and then back to 100% O_2. The low oxygen content gas mixtures used were: 15%O_2, 85%N_2; 10%O_2, 90%N_2; and 0%O_2 and 100%N_2. The low oxygen content mixtures were maintained from 5 to 8 minutes with the exception of the last mentioned one which was maintained for about 30 seconds.

In addition to the open chest experiments described above, two closed chest experiments were performed allowing the animal to respirate voluntarily. In addition to the above procedures used in the open chest experiments, a few special experimental procedures used in the closed chest experiments should be mentioned. After connecting the extracorporeal circulation and with the animal on total bypass, the chest was sewn together with four tubes (left ventricular catheter, two aortic catheters and one suction tube) protruding through the chest wall. Petroleum grease[1] was used to seal these tubes. The chest was aspirated with a syringe attached to the suction tube. When it appeared that all fluids were removed from the chest cavity and that all air seals were tight, respiration was switched to the voluntary mode of operation. Perturbations similar to those described above were also used in the closed chest experiments.

---

[1]Vaseline, Cheesebrough-Pond's, Inc., New York, N.Y.

RESULTS AND DISCUSSION

Experiments were designed to evaluate the feasibility of the proposed artificial heart control system.

Total body hypoxia was used as a perturbation to the animal-machine system. The resulting change in the arterial oxyhemoglobin saturation level was sensed by the arterial oximeter. This control signal of the artificial heart control system caused the cardiac output to change exponentially to a new cardiac output level as determined by the extrapolated transfer function relating arterial oxyhemoglobin concentration to total body blood flow rate.

In order to determine the effectiveness of this artificial heart control system a series of experiments were first performed to examine the cardiovascular system response of the animal-machine system to total body hypoxia without the control system in operation. A left ventricle bypass procedure was used with the animals under assisted or voluntary respiration. The system perturbations used were various mixtures of oxygen and nitrogen in the inspiration gas. This method was successful in changing the arterial oxyhemoglobin level. The inspiration gas mixture was changed from $100\%O_2$, $0\%N_2$ to: $15\%O_2$, $85\%N_2$; $10\%O_2$, $90\%N_2$; and $0\%O_2$, $100\%N_2$. The resulting arterial oxyhemoglobin saturation levels ranged from 97 to 85%, 80 to 50%, 77 to 44%, and 40 to 22% respectively.

The vascular response to total body hypoxia was determined in six animals in twenty experiments during assisted respiration. The relative vasoactive state of the vessels was determined by dividing the mean arterial pressure by the relative flow rate. This variable is the total

systemic vascular resistance. In response to decreased arterial oxyhemoglobin concentration levels hypertension always resulted with the relative flow rate decreasing, increasing or remaining at essentially the same value. The relative vasoactive response to total body hypoxia was net vasoconstriction. The arterial pressure and relative flow rate returned to approximately the pre-perturbation levels on return to $100\%O_2$ inspiration gas.

Figure 54 shows a typical total body hypoxia response curve for a change in the inspiration gas from $100\%O_2$, $0\%N_2$ to $10\%O_2$, $90\%N_2$ and then back to $100\%O_2$, $0\%N_2$. The resulting arterial oxyhemoglobin concentration was 87%, 31%, and 87%, respectively. With the decrease in the arterial oxyhemoglobin concentration the arterial pressure increased from 90/65 to 100/70 and the relative flow rate increased. When the oxyhemoglobin concentration was increased to the normal level the arterial pressure returned to 90/65 and the relative flow rate returned to approximately the pre-perturbation level. Calculations of the total systemic vascular resistance indicate that the vasoconstrictive response in certain beds dominate the local vasodilatory response in others.

In the literature review section the work of Kontos et al. (50) was cited in which it was found that generalized hypoxia in spontaneously breathing dogs resulted in systemic vasodilatation. In dogs maintained on a respiration pump, which fixed the animals respiration, it was found that systemic vasoconstriction resulted.

In an attempt to remove any possible adverse effects of non-voluntary respiration a series of eight experiments was performed on two animals

with unassisted respiration (closed chest). Relative vasoconstriction resulted when the animal-machine system was perturbed with decreased arterial oxyhemoglobin concentration levels. These findings were quantitatively similar to those found in the assisted respiration animals.

In summary then, a net vasoconstrictive response for the animal-machine system was observed during total body hypoxia without the artificial heart control system in operation. This result is opposite to that found for the local autoregulatory response in the canine hind limb. In the first section of this dissertation it was shown that local hypoxia resulted in a vasodilatory response. Daugherty et al. (19, 20) noted similar type results when they tried to compare the local hypoxic response to the total body hypoxic response they observed in the fore limb.

As a consequence of this effect, successful artificial heart control studies could not be performed with the load sensitive artificial heart system available. The response of the artificial heart control system to total body hypoxia would be in the wrong direction. As shown above, the physiological response to total hypoxia is one of hypertension and vasoconstriction. The artificial heart control system responds to a decrease in arterial oxyhemoglobin concentration by increasing the cardiac output. This would increase the arterial pressure to an even higher hypertensive state, an undesirable result.

Gorlin and Lewis (33) reported acute hypertension as the response to acute hypoxia. They found that during hypoxia the chemoreceptors were stimulated by the low Po_2 causing selective reflex vasoconstriction. In addition, they found that the cerebral and coronary vessels were dilated

by the direct autoregulatory action of the low Po_2. In this way hypertension served to insure the preferential blood supply to the most vital organs.

The experiments of Gorlin and Lewis point to the fact that, although the total body response to hypoxia is one of hypertension and vasoconstriction, the most autoregulatory tissue beds (brain, heart, and skeletal muscle) may still be benefitted. Increased flow can result in the autoregulatory tissues due to vasodilation of the local vascular beds and the hypertension.

A final conjecture might be made concerning the use of the proposed method of controlling an artificial ventricle by means of the extrapolated transfer function. In a clinical situation, one might use the proposed control system, but also superimpose upon the subject other conditions (such as partial adrenergic blockage, hypotensive drugs, etc.) which would tend to avoid the detrimental effects of severe hypertension and marked vasoconstriction (this leads to tissue hypoxia in the constricted beds). In this situation, the artificial heart would supply the necessary blood flow to the tissue beds according to their nutrient needs for oxygen.

SUMMARY

The primary purpose of this dissertation research was to examine the dynamic characteristics of the response involved in the autoregulation of blood flow. A transfer function was found relating arterial oxyhemoglobin concentration as the input to blood flow rate as the output. Up to this time most of the research in this area has dealt with an examination of the steady-state autoregulatory characteristics. That is, the researchers were interested primarily in the steady-state (non-transient) relationships between the autoregulatory parameters. There are perhaps two reasons for this. First, it seems that classical biologists do not have an appreciation for the information that can be obtained from a transient analysis of a biological system. Secondly, and perhaps the most important reason, is that it is a very difficult problem to analyze transient response data without the aid of sophisticated data analysis techniques, usually involving the aid of a computer. In this dissertation research, the data analysis was performed on an IBM 360-65 computer using a continuous time system identification program.

The experimental data were analyzed as first and second order systems to see which order system best described the biological system. It was concluded that the system transfer function was most likely of first order. In a significant number of cases (27%), pole-zero cancellations in the second order identification resulted in a transfer function approximately equal to the first order identified transfer function. Also, it was found that in most cases the second order identification was not significantly better than that of the first order one.

A dynamic nonlinearity was found with respect to the value of the first order system time constant, τ, and the direction of change of the input arterial oxyhemoglobin concentration. The linearity of the system with respect to the first order system gain constant, k, was not determined because of the variation in the values of k. No correlation was found between the input arterial oxyhemoglobin concentration level and the resulting first order system parameters k and τ.

The transfer function found, in addition to being useful in modeling the cardiovascular system local autoregulatory response, has potential value in the design of the control system for an artificial ventricle. In order to design a suitable artificial heart control system, the dynamics of both the system controlled (cardiovascular system) and the controller must be determined. In Part II of the dissertation the dynamics of the artificial heart controller were determined. In vitro tests were performed on the artificial heart power and control systems in order to determine the transfer function relating the change in the input control signal to the change in the artificial ventricle output flow rate. Using frequency analysis techniques, the transfer function was found to have the form of an integrator. The effects of the various operating artificial ventricle parameters on the transfer function gain were evaluated.

The basic information from Part I and Part II was used in Part III of this dissertation. A control system for an artificial ventricle was designed which utilized an extrapolated transfer function relating the arterial oxyhemoglobin concentration, as the input, to the total body blood flow rate needs, as the output. This extrapolated transfer function was

based on the assumption that the total body would respond to hypoxia in the same way as was found for the canine hind limb skeletal muscle. The feasibility of using this control system was examined for various degrees of whole body hypoxia.

In order to determine the effectiveness of this artificial heart control system, a series of experiments were first performed to examine the cardiovascular system response of the animal-machine system to total body hypoxia without the control system in operation. In these in vivo tests, a left ventricle bypass procedure was used with the animals under assisted or voluntary respiration. It was found that the total body response of the animal-machine system was one of hypertension and vasoconstriction. It was found that the total body hypertensive and vasoconstrictive response of the animal-machine system did not support the assumption that the total body response is the same as that found in the hind limb skeletal muscle. As a consequence of this effect, successful artificial heart control studies could not be performed with the load sensitive artificial heart system available.

FIGURES

Figure 1. Composite pressure-flow curves for 7 preparations (Walker and Guyton 82, p. 507)

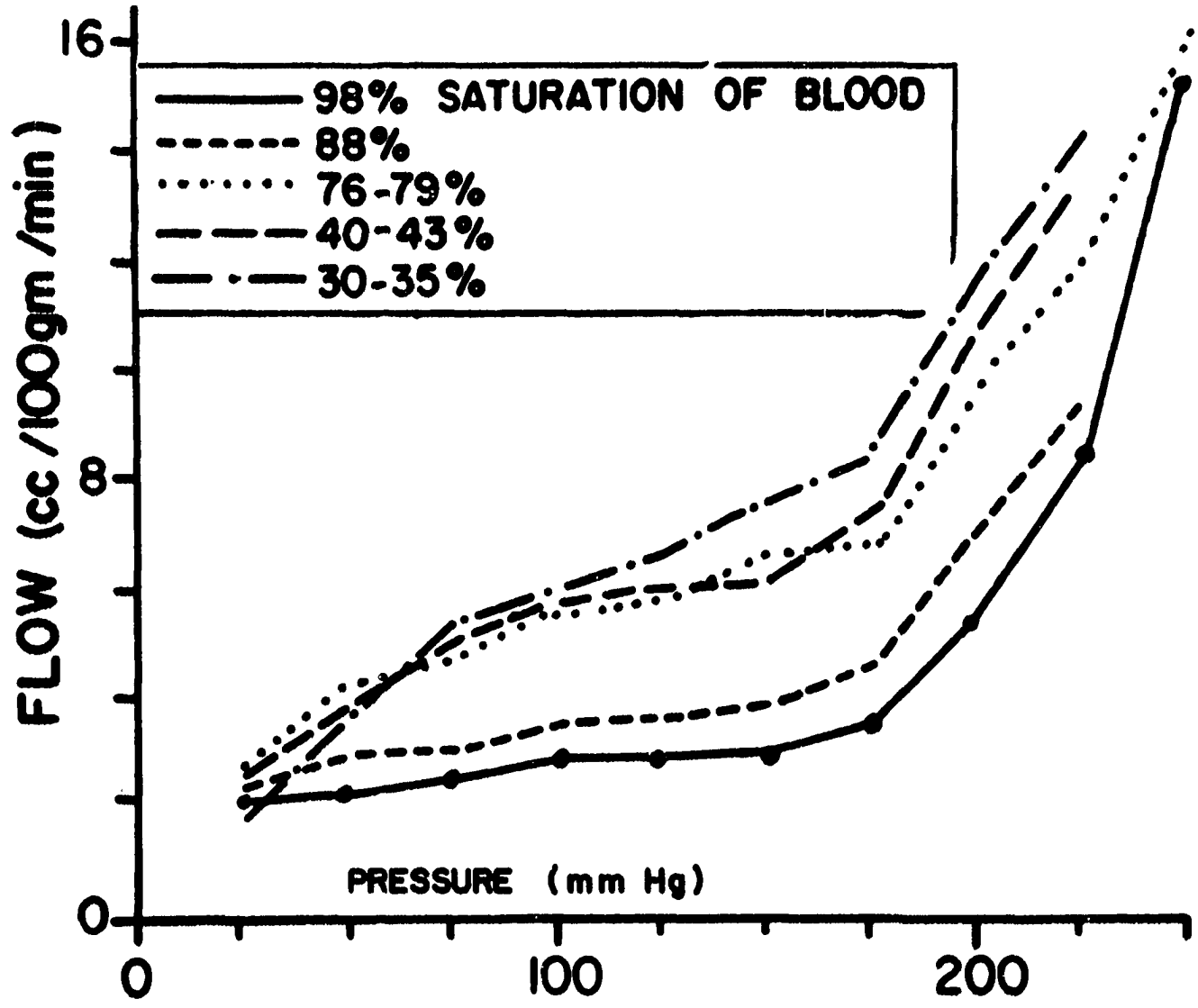
16
8
0
FLOW (cc/100gm/min)
98% SATURATION OF BLOOD
88%
76-79%
40-43%
30-35%
PRESSURE (mm Hg)
0
100
200

Figure 2. Diagram of hind limb perfusion setup

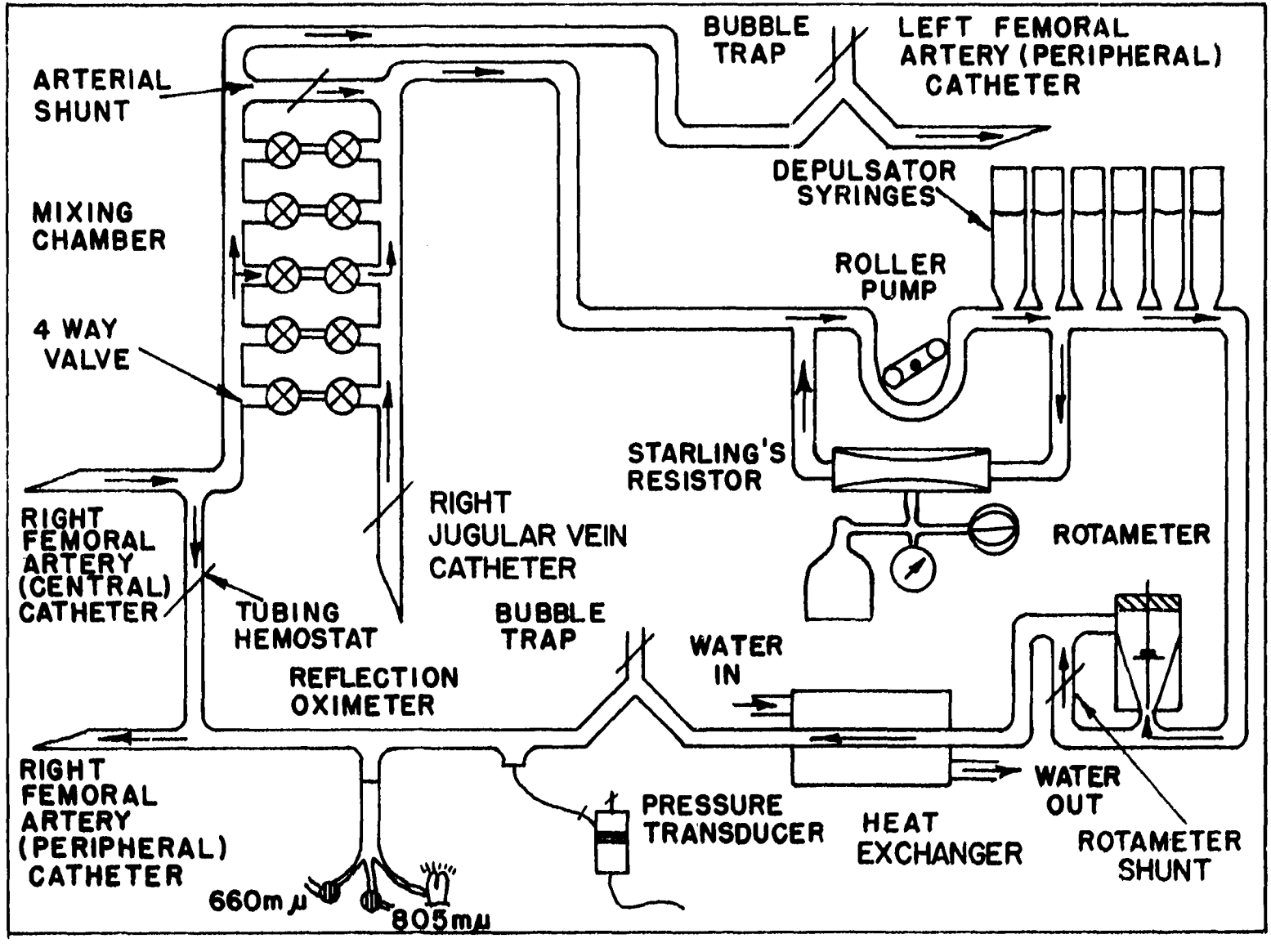
BUBBLE TRAP
LEFT FEMORAL ARTERY (PERIPHERAL) CATHETER
ARTERIAL SHUNT
DEPULSATOR SYRINGES
MIXING CHAMBER
ROLLER PUMP
4 WAY VALVE
STARLING'S RESISTOR
RIGHT FEMORAL ARTERY (CENTRAL) CATHETER
RIGHT JUGULAR VEIN CATHETER
ROTAMETER
TUBING HEMOSTAT
BUBBLE TRAP
WATER IN
REFLECTION OXIMETER
RIGHT FEMORAL ARTERY (PERIPHERAL) CATHETER
PRESSURE TRANSDUCER
WATER OUT
HEAT EXCHANGER
ROTAMETER SHUNT
660mμ
805mμ

Figure 3. Mixing chamber

a. arterial input to mixing chamber
b. mixing chamber output to femoral artery of opposite hind limb
c. venous input to mixing chamber
d. mixing chamber output to roller pump
e. large diameter parallel tube used for arterial $\%HbO_2$ perfusion levels
f. small diameter parallel mixing tube

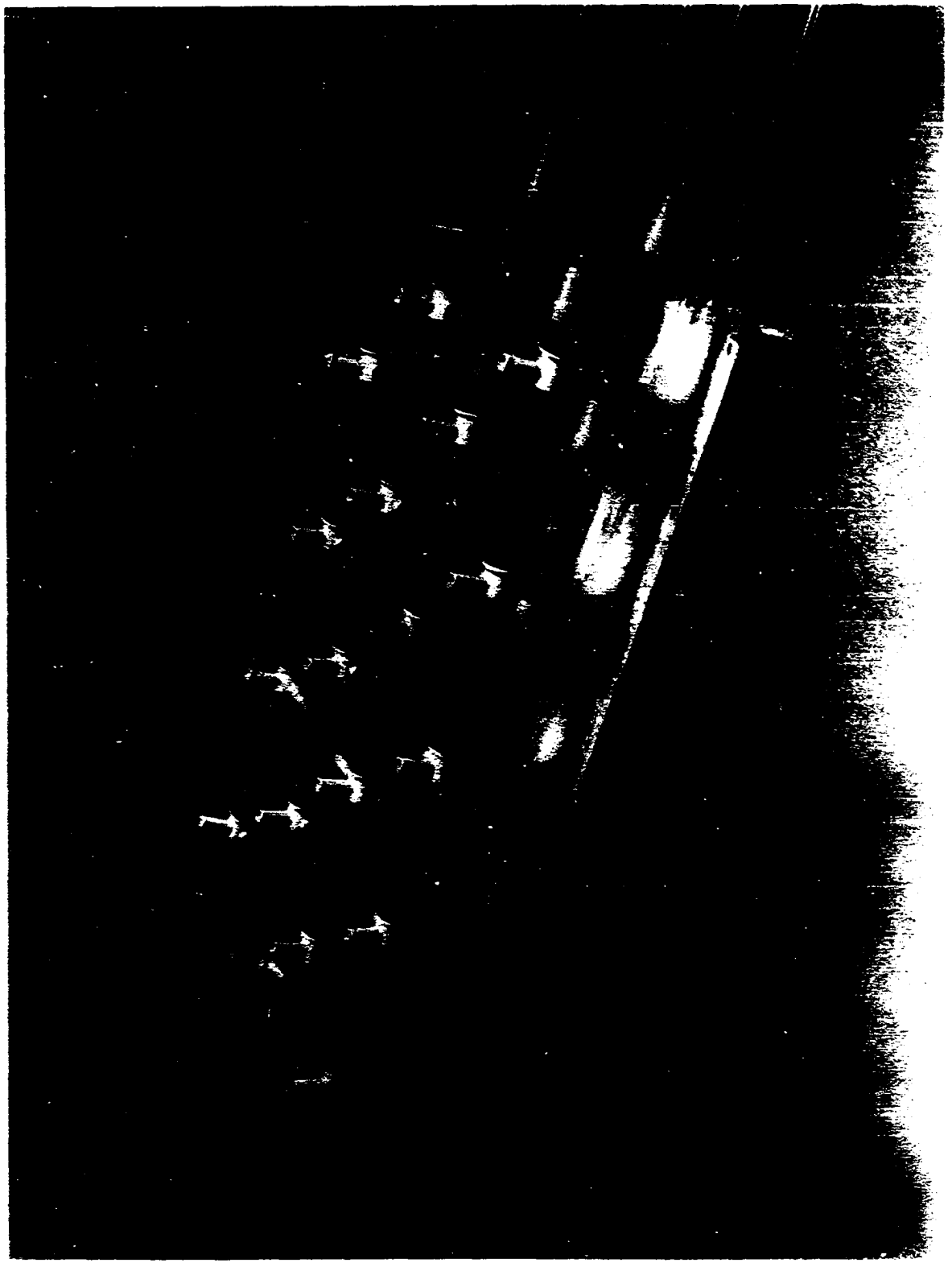

Figure 4. The Starling's Resistor system showing the Starling's Resistor in the foreground with the pressure bulb, pressure bottle and pressure gauge

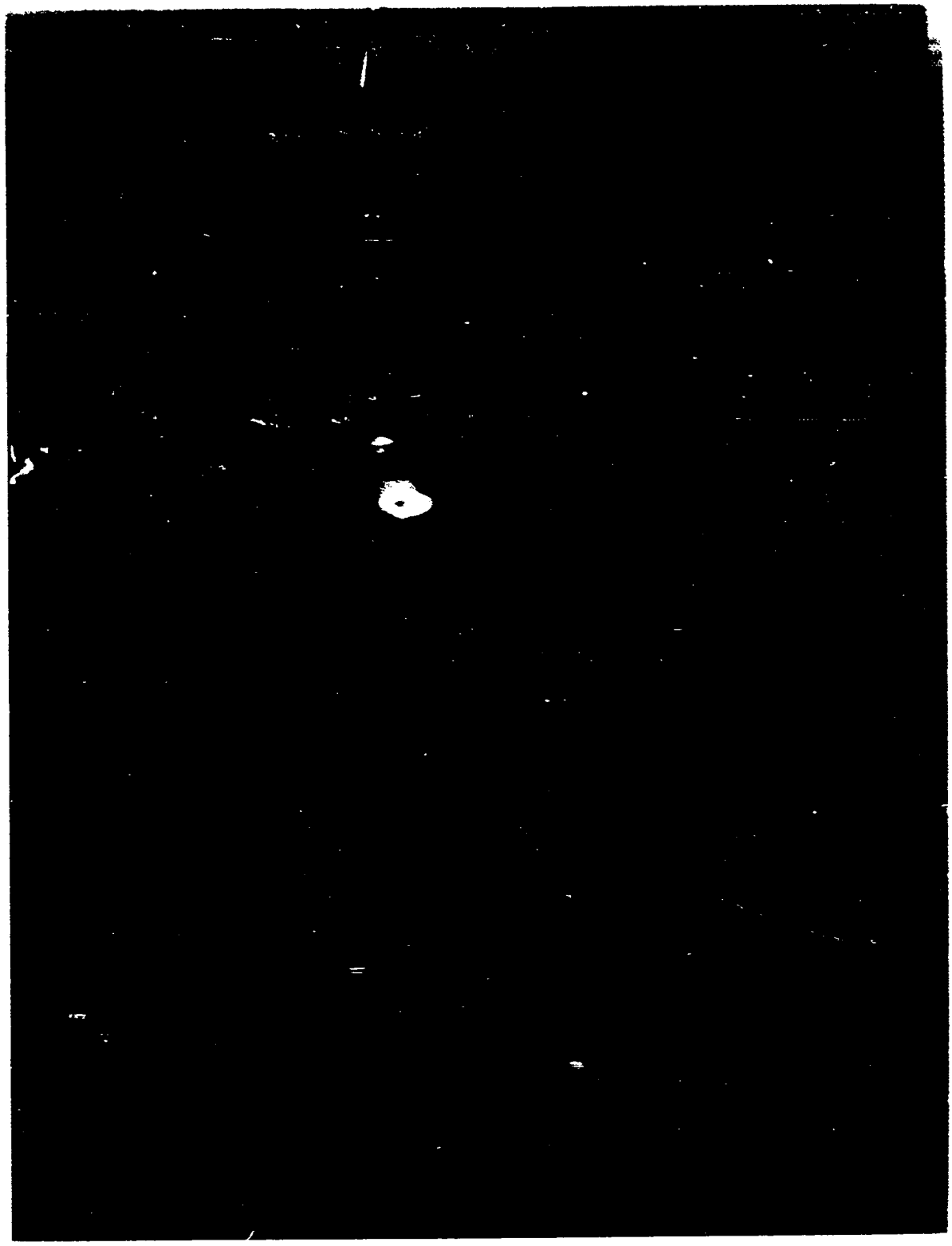

Figure 5. Schematic diagram for optical and electrical portions of the reflection oximetry system

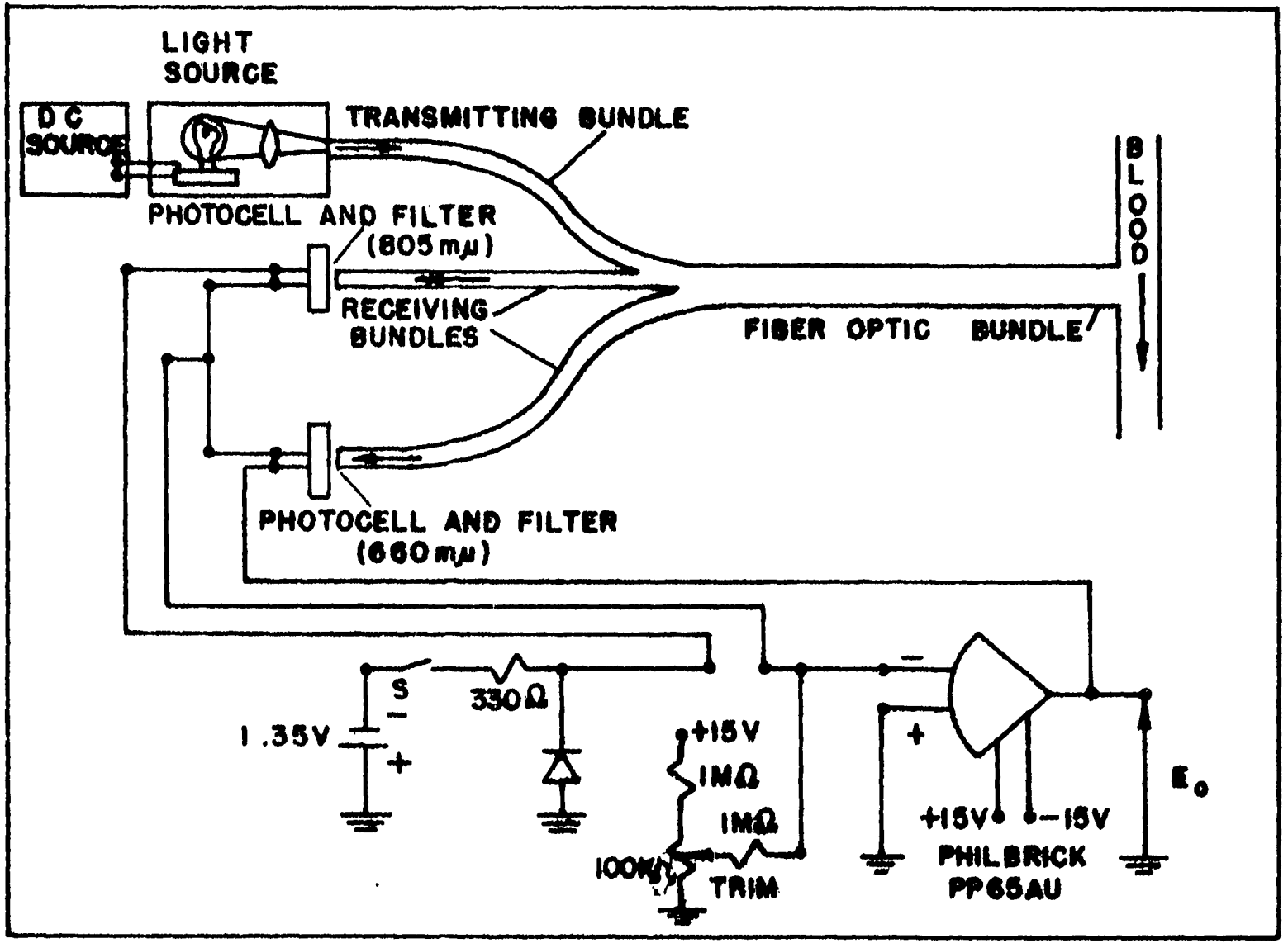
LIGHT
SOURCE
D C
SOURCE
TRANSMITTING BUNDLE
BLOOD
PHOTOCELL AND FILTER
(805 mμ)
RECEIVING
BUNDLES
FIBER OPTIC BUNDLE
PHOTOCELL AND FILTER
(660 mμ)
S
330Ω
1.35V
+15V
1MΩ
1MΩ
100KΩ
TRIM
+15V
−15V
PHILBRICK
PP65AU
E₀

Figure 6. In vivo oximeter calibration curve

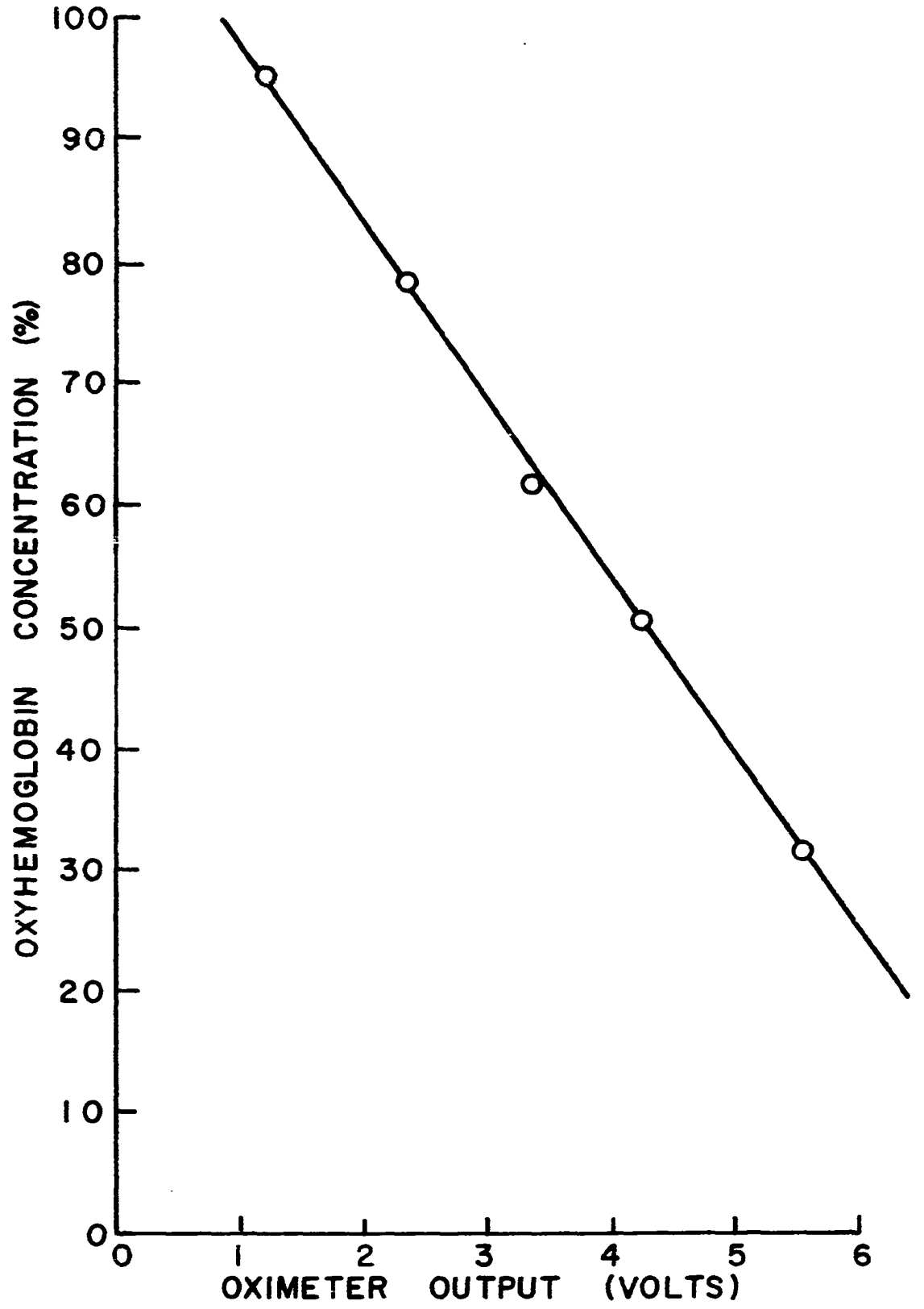
100
90
80
70
60
50
40
30
20
10
0
OXYHEMOGLOBIN CONCENTRATION (%)
0
1
2
3
4
5
6
OXIMETER OUTPUT (VOLTS)

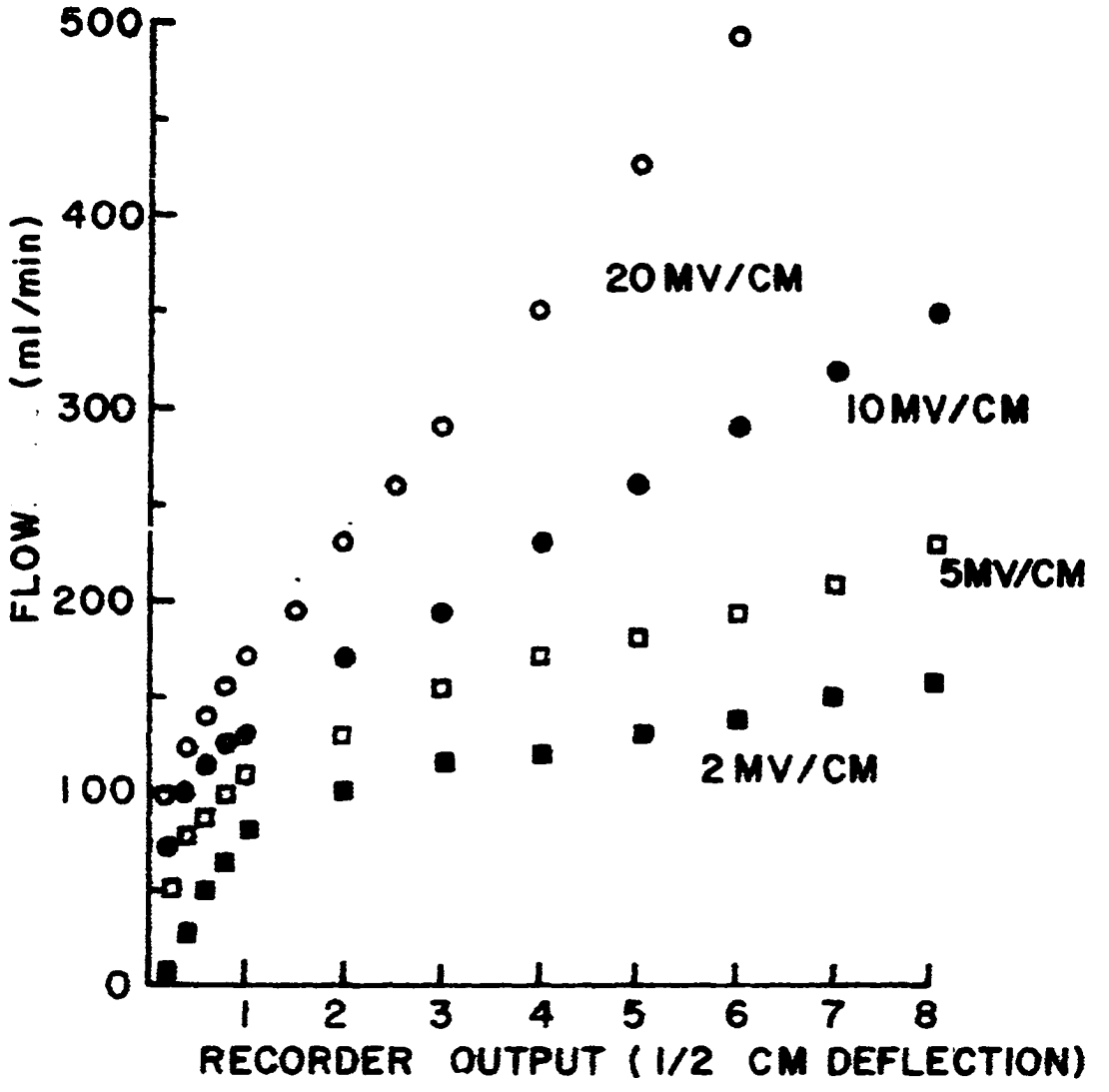

Figure 7. In vitro rotameter calibration curve for various sensitivity settings of the polygraph recorder

Figure 8. Block diagram of data record and playback system

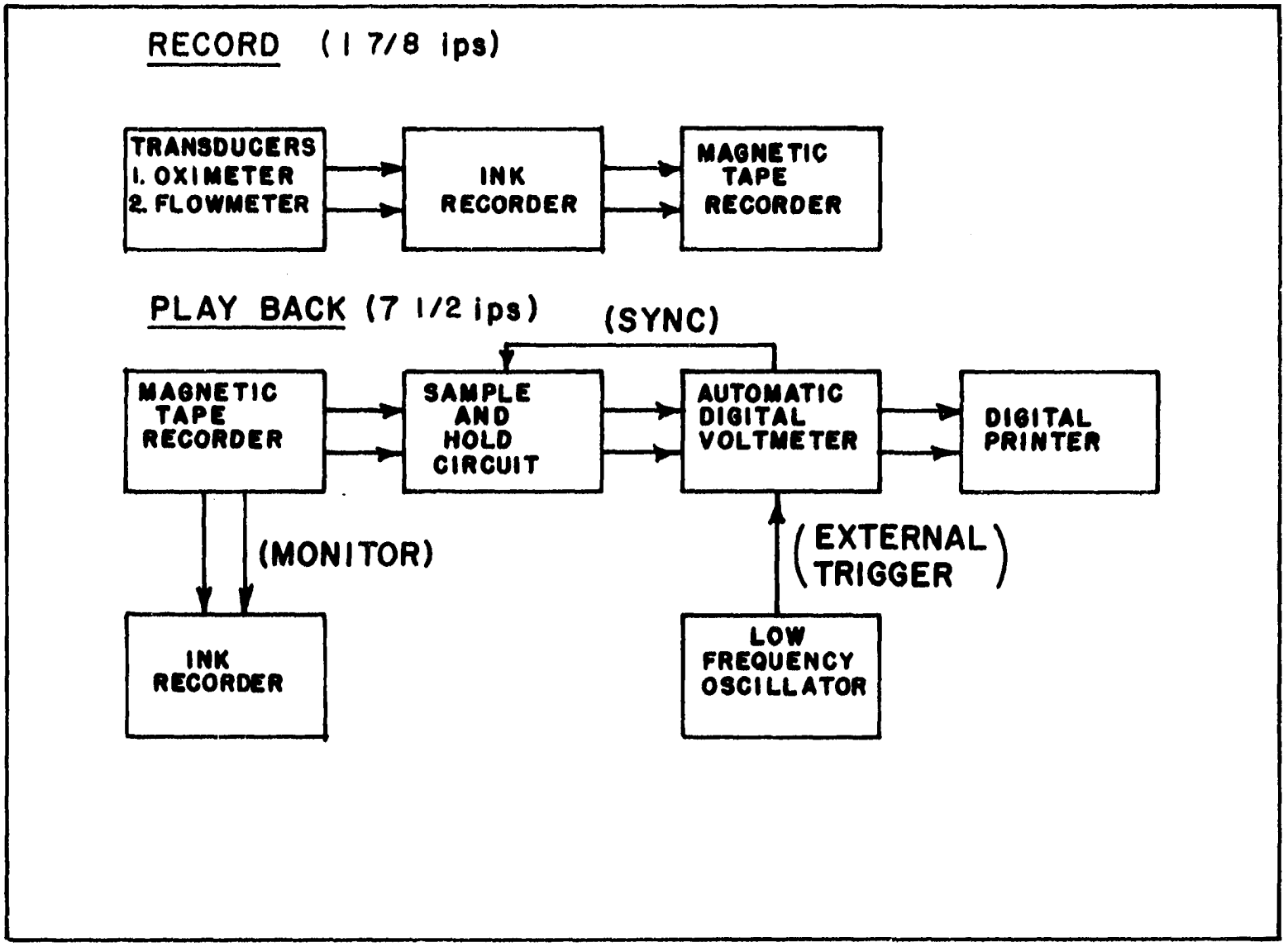
RECORD (1 7/8 ips)
TRANSDUCERS
1. OXIMETER
2. FLOWMETER
INK RECORDER
MAGNETIC TAPE RECORDER
PLAY BACK (7 1/2 ips)
(SYNC)
MAGNETIC TAPE RECORDER
SAMPLE AND HOLD CIRCUIT
AUTOMATIC DIGITAL VOLTMETER
DIGITAL PRINTER
(MONITOR)
(EXTERNAL TRIGGER)
INK RECORDER
LOW FREQUENCY OSCILLATOR

Figure 9. Sample and hold circuit

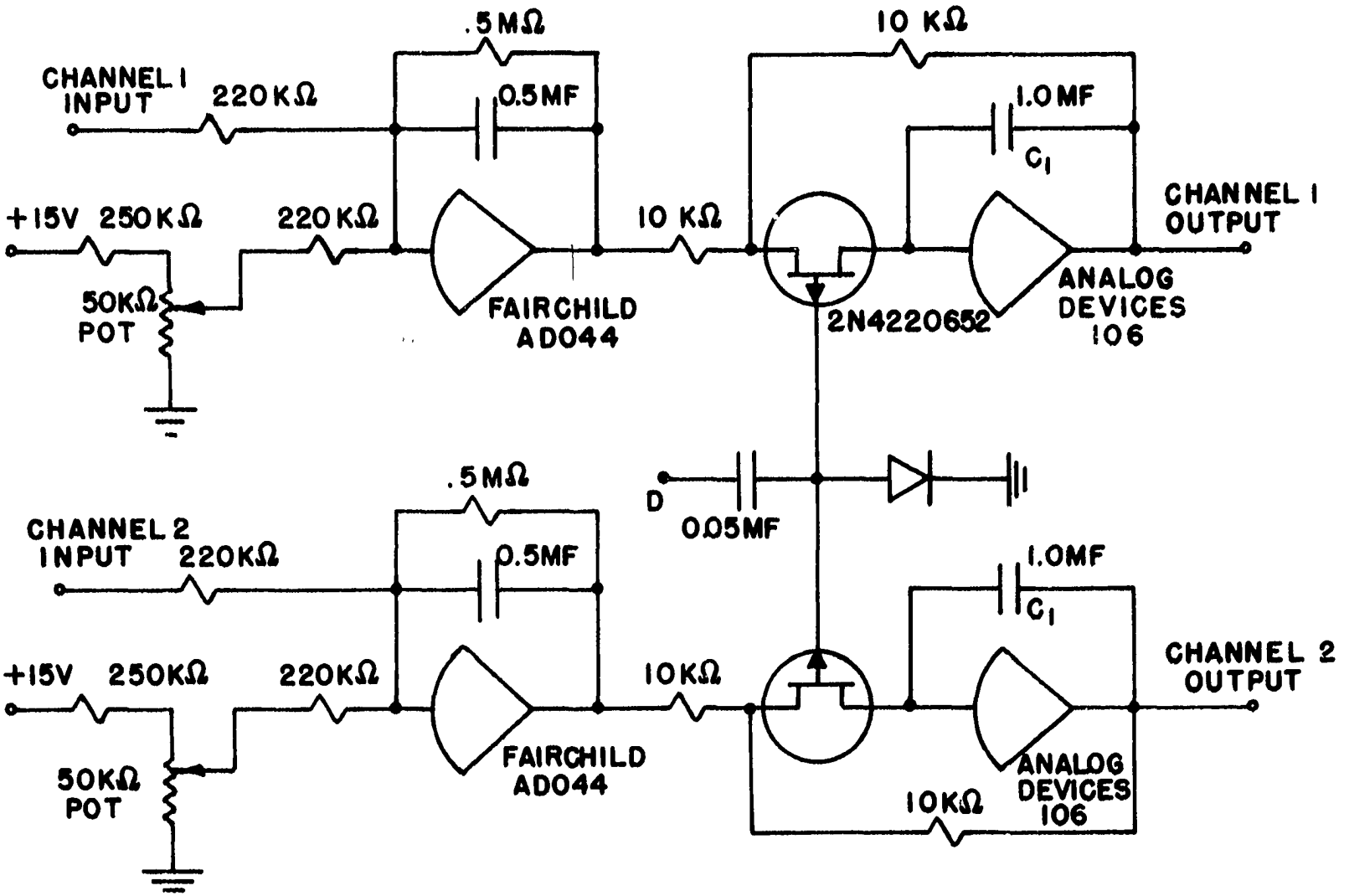
.5MΩ
10 KΩ
CHANNEL 1
INPUT
220KΩ
0.5MF
1.0MF
C1
+15V 250KΩ
220KΩ
10 KΩ
CHANNEL 1
OUTPUT
50KΩ
POT
FAIRCHILD
AD044
2N4220652
ANALOG
DEVICES
106
.5MΩ
D
0.05MF
CHANNEL 2
INPUT
220KΩ
0.5MF
1.0MF
C1
+15V
250KΩ
220KΩ
10KΩ
CHANNEL 2
OUTPUT
50KΩ
POT
FAIRCHILD
AD044
10KΩ
ANALOG
DEVICES
106

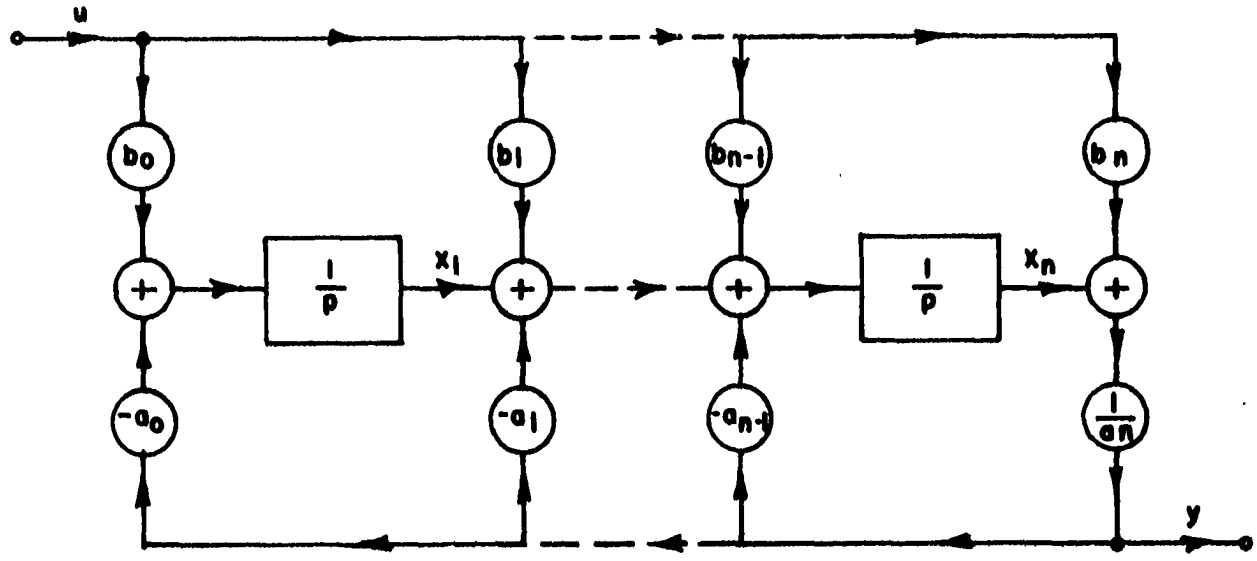

Figure 10. Realization of $\frac{(b_n p^n + \cdots + b_0)}{(a_n p^n + \cdots + a_0)}$, $a_n \neq 0$ (Zadeh and Desoer 90, p. 281)

Figure 11. Second order transfer function realization with $b_2 = 0$ and $a_2 = 1$

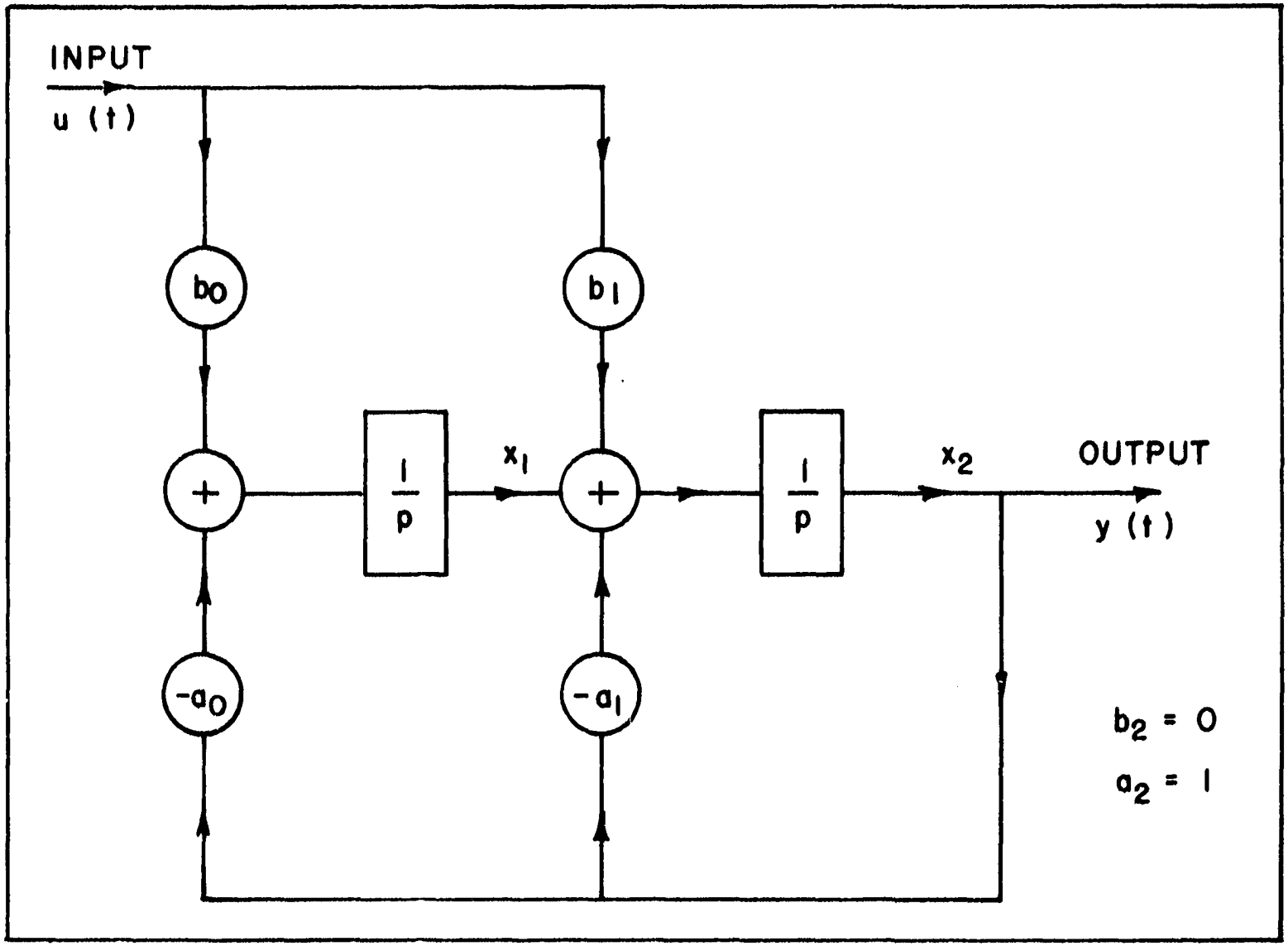
INPUT
u (t)
b_0
b_1
+
+
$\frac{1}{p}$
x_1
$\frac{1}{p}$
x_2
OUTPUT
y (t)
$-a_0$
$-a_1$
$b_2 = 0$
$a_2 = 1$

Figure 12. Equation 2.17

$$
\begin{bmatrix}
\int_0^T u_1^2(t)dt & \int_0^T u_1(t)u_2(t)dt & \int_0^T u_1(t)y_1(t)dt & \int_0^T u_1(t)y_2(t)dt & \int_0^T u_1(t)dt & \int_0^T u_1(t)\cdot t\,dt \\
\int_0^T u_2(t)u_1(t)dt & \int_0^T u_2^2(t)dt & \int_0^T u_2(t)y_1(t)dt & \int_0^T u_2(t)y_2(t)dt & \int_0^T u_2(t)dt & \int_0^T u_2(t)\cdot t\,dt \\
-\int_0^T y_1(t)u_1(t)dt & -\int_0^T y_1(t)u_2(t)dt & -\int_0^T y_1^2(t)dt & -\int_0^T y_1(t)y_2(t)dt & -\int_0^T y_1(t)dt & -\int_0^T y_1(t)\cdot t\,dt \\
-\int_0^T y_2(t)u_1(t)dt & -\int_0^T y_2(t)u_2(t)dt & -\int_0^T y_2(t)y_1(t)dt & -\int_0^T y_2^2(t)dt & -\int_0^T y_2(t)dt & -\int_0^T y_2(t)\cdot t\,dt \\
\int_0^T u_1(t)dt & \int_0^T u_2(t)dt & \int_0^T y_1(t)dt & \int_0^T y_2(t)dt & \int_0^T dt & \int_0^T t\,dt \\
\int_0^T t\cdot u_1(t)dt & \int_0^T t\cdot u_2(t)dt & \int_0^T t\cdot y_1(t)dt & \int_0^T t\cdot y_2(t)dt & \int_0^T t\cdot dt & \int_0^T t^2 dt
\end{bmatrix}
\begin{bmatrix} b_1 \\ b_0 \\ -a_1 \\ -a_0 \\ x_2(0) \\ x_1(0) \end{bmatrix}
=
\begin{bmatrix}
\int_0^T u_1(t)y(t)dt \\
\int_0^T u_2(t)y(t)dt \\
\int_0^T y_1(t)y(t)dt \\
\int_0^T y_2(t)y(t)dt \\
\int_0^T y(t)dt \\
\int_0^T t\,y(t)dt
\end{bmatrix}
$$

Figure 13. Recordings of systemic arterial pressure, input $\%HbO_2$, hind limb blood pressure, and hind limb blood flow rate during heavy vasomotor activity. The circulation time delay between the input $\%HbO_2$ and the output blood flow rate was removed manually prior to the computer processing. The time scale is 20 seconds

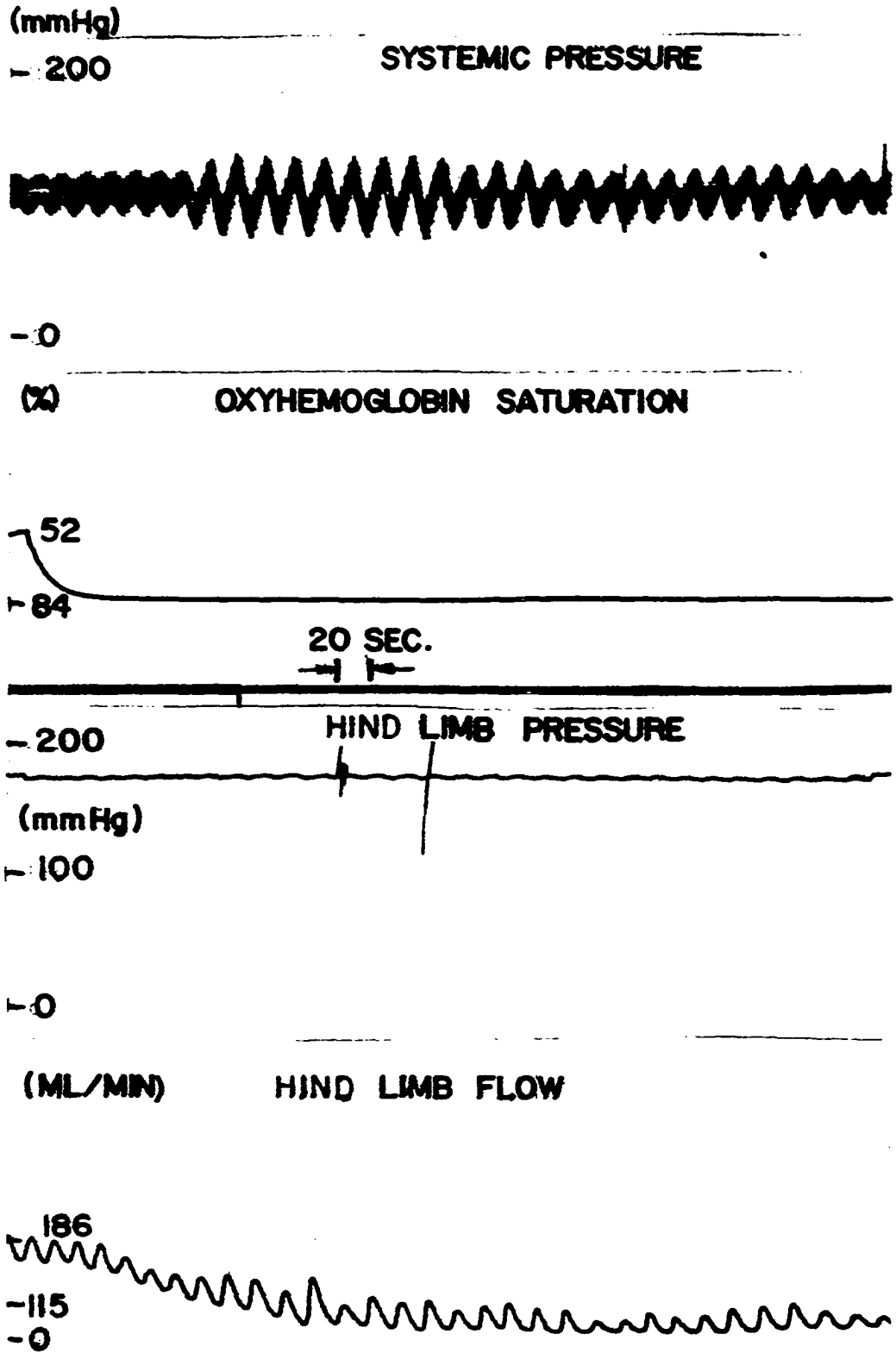
(mmHg)
200
SYSTEMIC PRESSURE
0
(%)
OXYHEMOGLOBIN SATURATION
52
84
20 SEC.
200
HIND LIMB PRESSURE
(mmHg)
100
0
(ML/MIN)
HIND LIMB FLOW
186
115
0

Figure 14. Recordings of systemic arterial pressure, input $\%HbO_2$, hind limb blood pressure, and hind limb blood flow rate during diminished vasomotor activity due to the use of a hydrostatic arterial reservoir (see text for explanation)

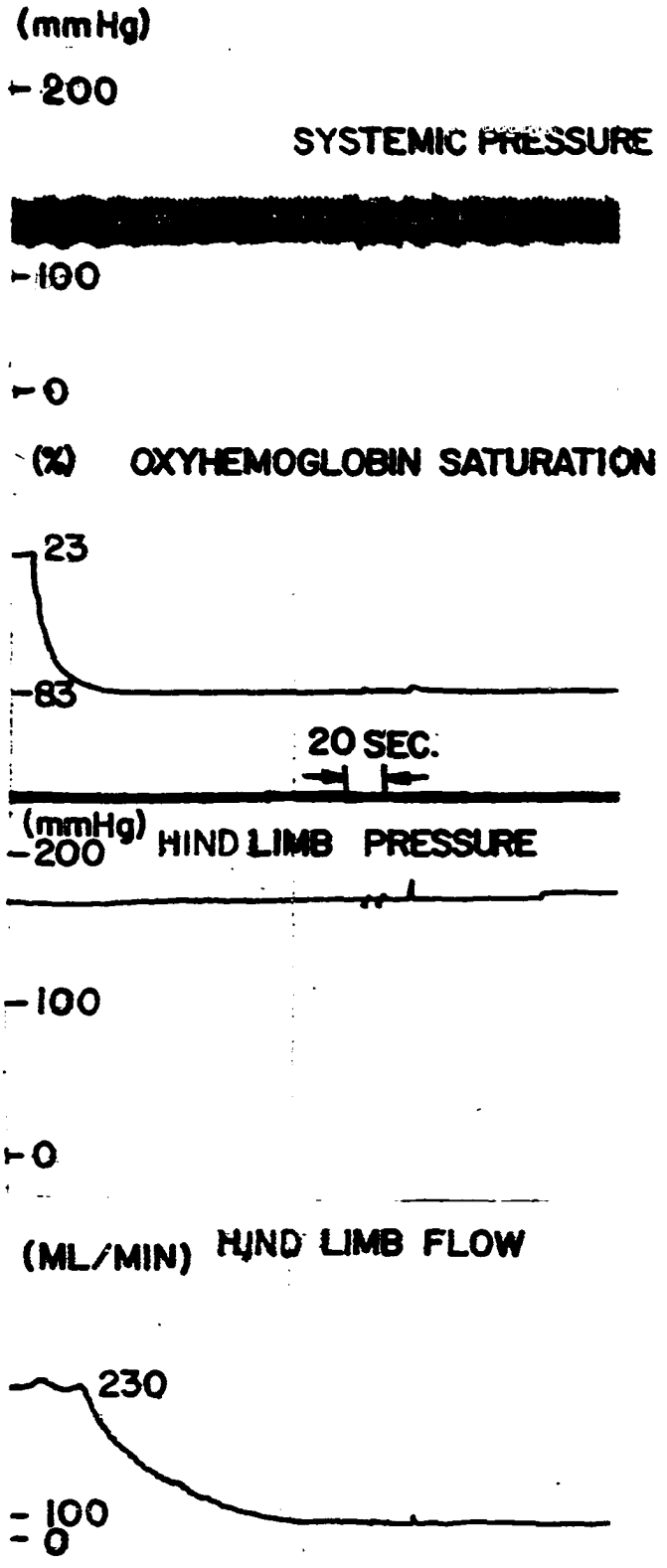
(mmHg)
200
SYSTEMIC PRESSURE
100
0
(%) OXYHEMOGLOBIN SATURATION
23
83
20 SEC.
(mmHg)
200
HIND LIMB PRESSURE
100
0
(ML/MIN) HIND LIMB FLOW
230
100
0

Figure 15. First order system identification for an input change in $\%HbO_2$ from 87 to 63%. The graphs show the actual input $\%HbO_2$(I), actual output flow rate (X), and simulated output (0) vs. time. The units of $\%HbO_2$ are in % and the flow rate units are in ml/min/kg body weight. These units apply to Figures 15 to 34. The time scale should be multiplied by 100. The first order transfer function is

$$\frac{\Delta FR}{\Delta \%HbO_2} = \frac{-2.00 \times 10^{-2}}{S + 7.71 \times 10^{-2}}$$

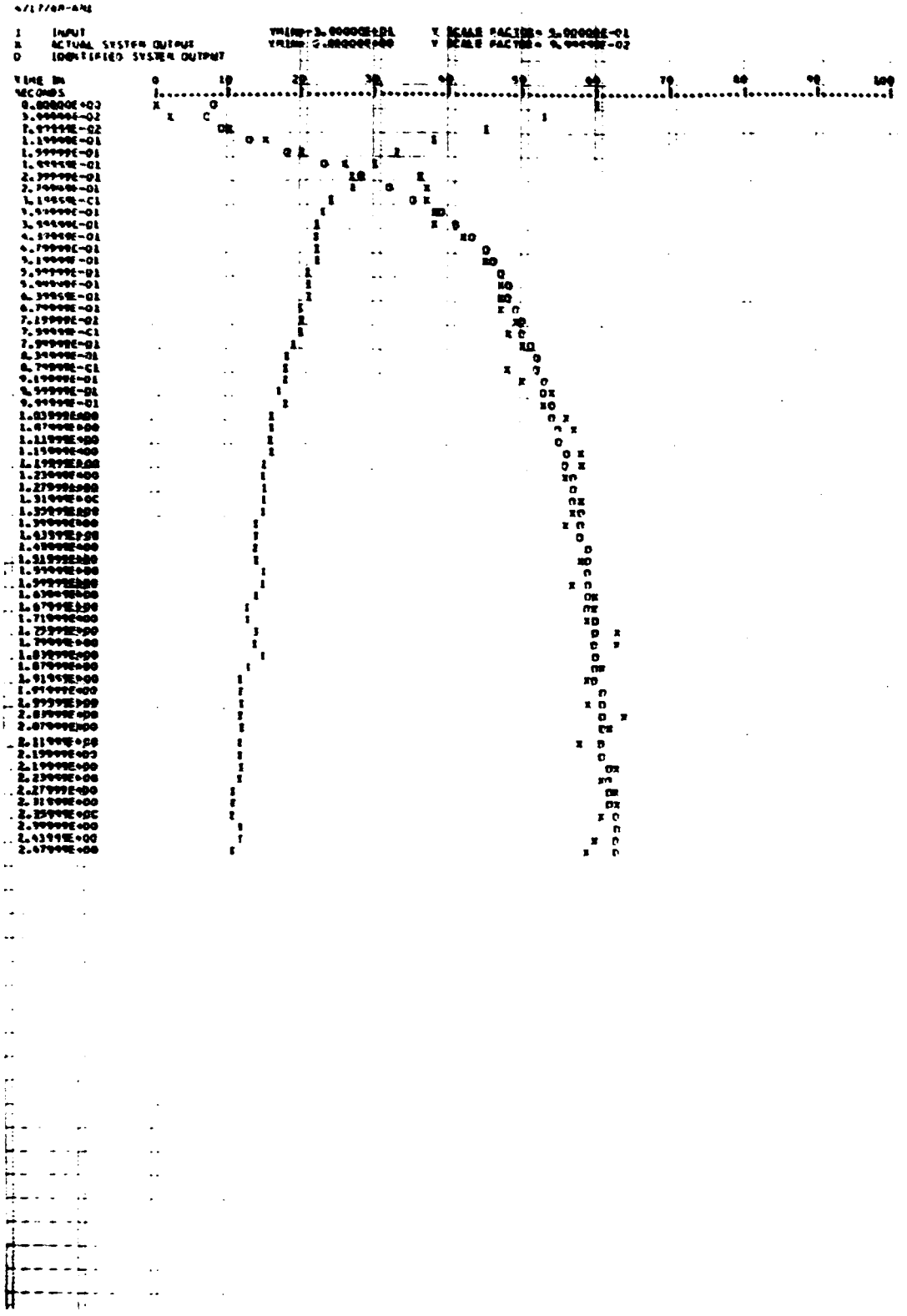
I INPUT
A ACTUAL SYSTEM OUTPUT
O IDENTIFIED SYSTEM OUTPUT
TIME IN SECONDS
0
10
20
30
40
50
60
70
80
90
100

Figure 16. Second order system identification for an input change in $\%HbO_2$ from 87 to 63%. The graphs show the actual input $\%HbO_2$(I), actual output flow rate (X), and simulated output (O) vs. time. The time scale should be multiplied by 100. The second order transfer function is

$$\frac{\Delta FR}{\Delta \%HbO_2} = \frac{-1.86 \times 10^{-2}(S - 2.17 \times 10^{-3})}{(s + 7.78 \times 10^{-2})(S - 2.16 \times 10^{-3})}$$

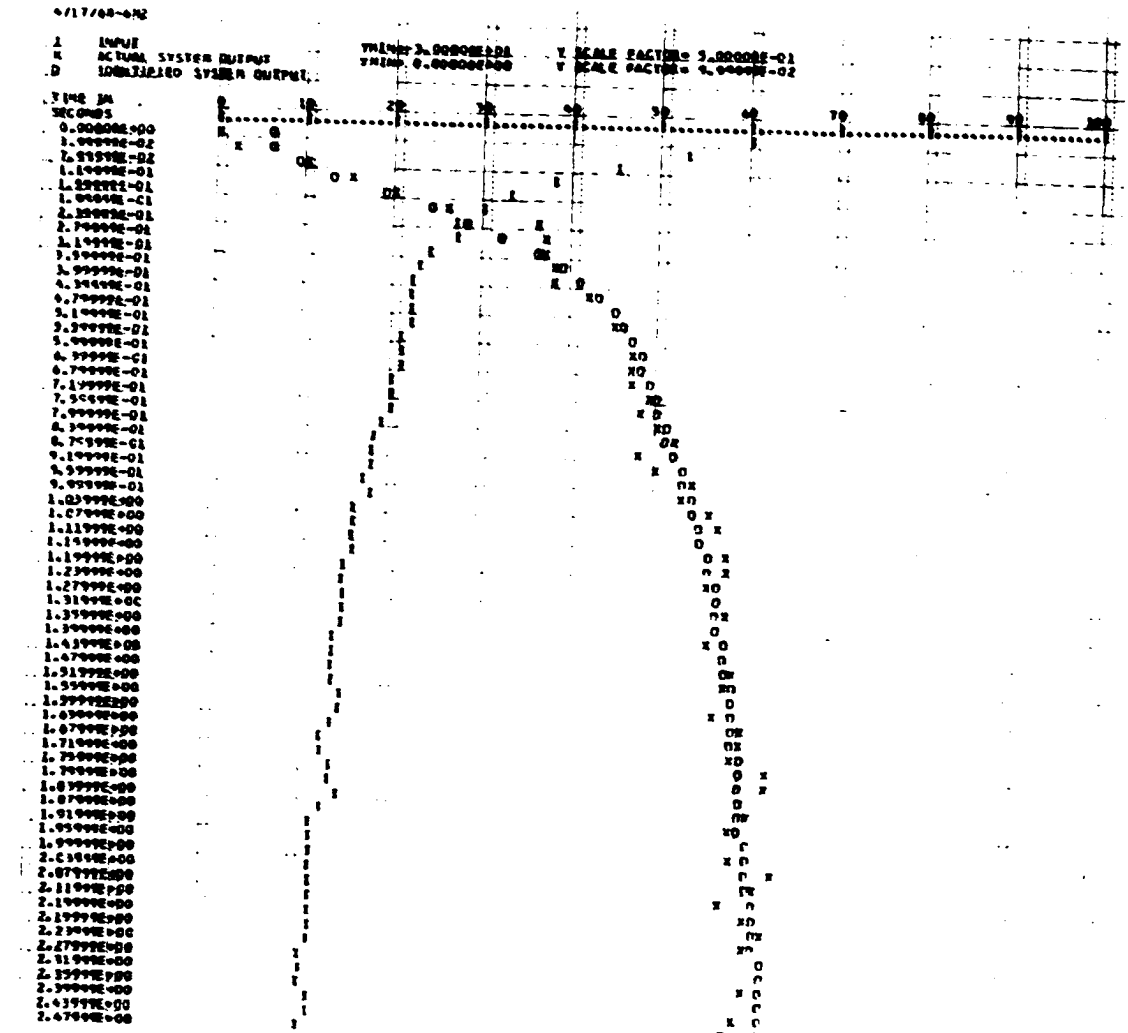
I INPUT
X ACTUAL SYSTEM OUTPUT
O LINEARIZED SYSTEM OUTPUT
TIME IN SECONDS

Figure 17. First order system identification for an input change in $\%HbO_2$ from 89 to 45%. The graphs show the actual output flow rate (X), and the simulated output (O) vs. time. The first order transfer function is

$$\frac{\Delta FR}{\Delta \%HbO_2} = \frac{-5.67 \times 10^{-3}}{S + 1.83 \times 10^{-2}}$$

3/6-2N1

X ACTUAL SYSTEM OUTPUT
O IDENTIFIED SYSTEM OUTPUT

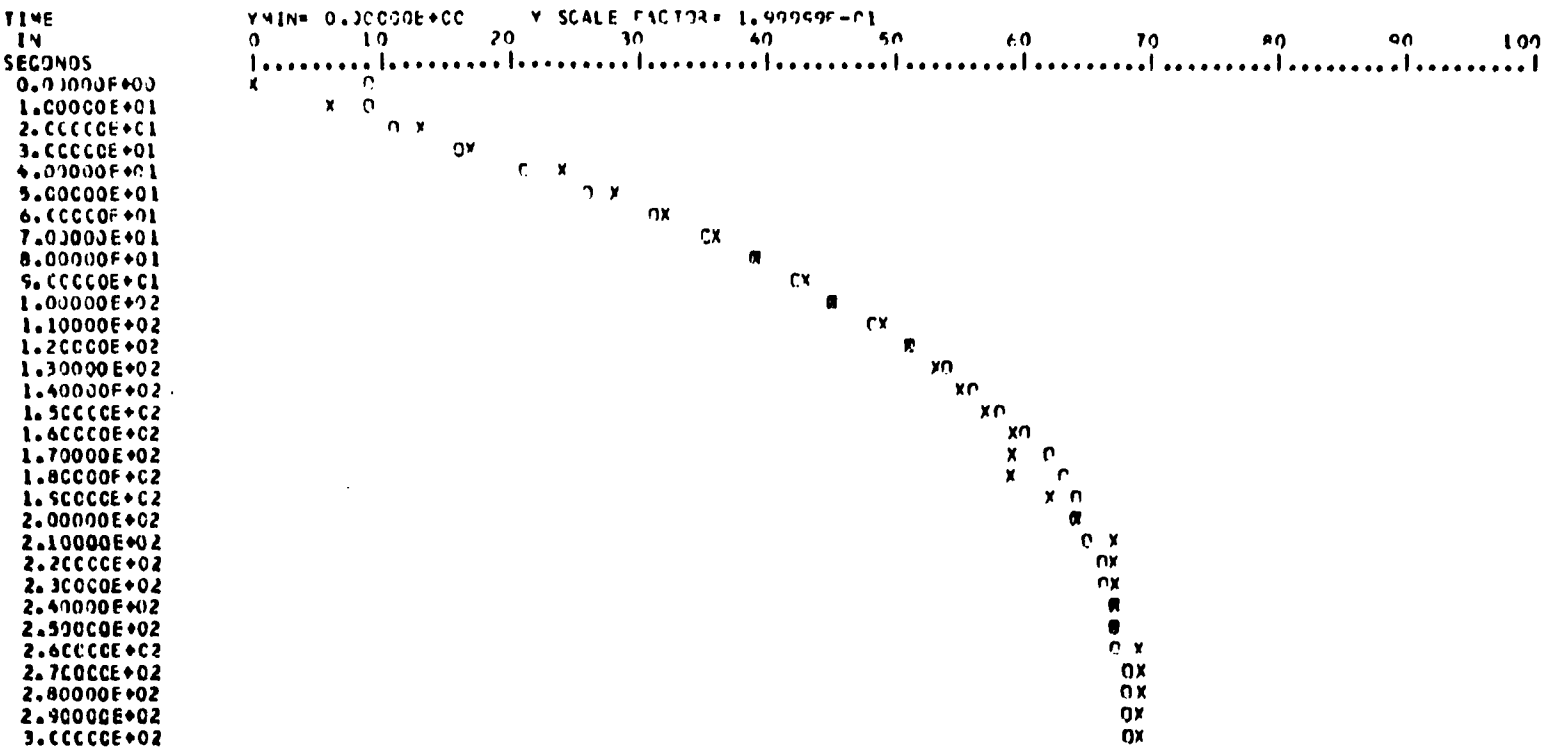

Figure 18. Second order identification for an input change in $\%HbO_2$ from 89 to 45%. The graphs show the actual output flow rate (X), and the simulated output (O) vs. time. The time scale should be multiplied by 100. The second order transfer function is

$$\frac{\Delta FR}{\Delta \%HbO_2} = \frac{9.26 \times 10^{-4}(S + 1.39 \times 10^{-2})}{(S - 4.17 \times 10^{-3})(S + 7.50 \times 10^{-3})}$$

3/6/6- 2N2

X ACTUAL SYSTEM OUTPUT
O IDENTIFIED SYSTEM OUTPUT

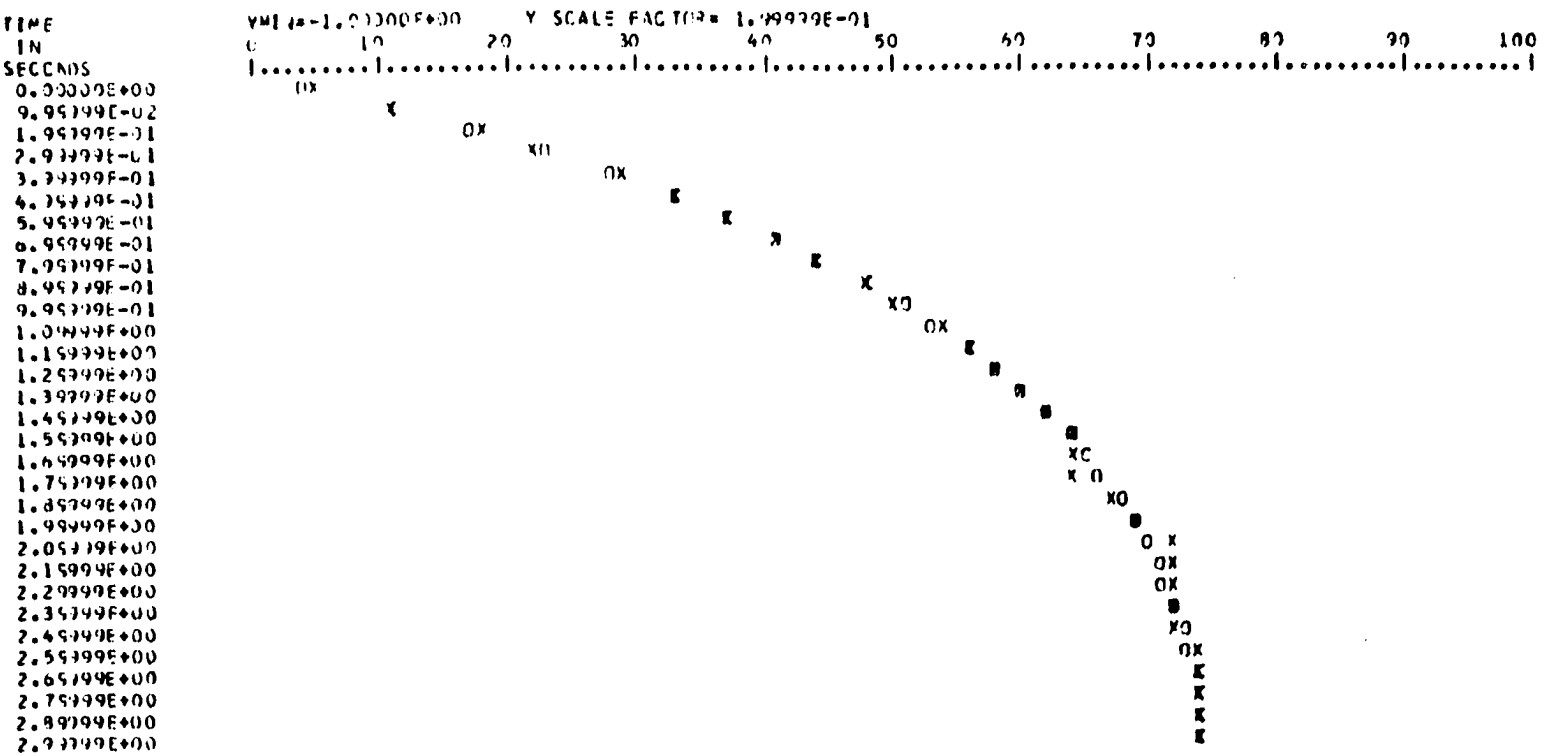

Figure 19. First order identification for an input change in $\%HbO_2$ from 86 to 32%. The graphs show the actual output flow rate (X), and the simulated output (O) vs. time. The first order transfer function is

$$\frac{\Delta FR}{\Delta \%HbO_2} = \frac{-3.97 \times 10^{-3}}{(S + 1.69 \times 10^{-2})}$$

2/7/68-20N1

X ACTUAL SYSTEM OUTPUT
O IDENTIFIED SYSTEM OUTPUT

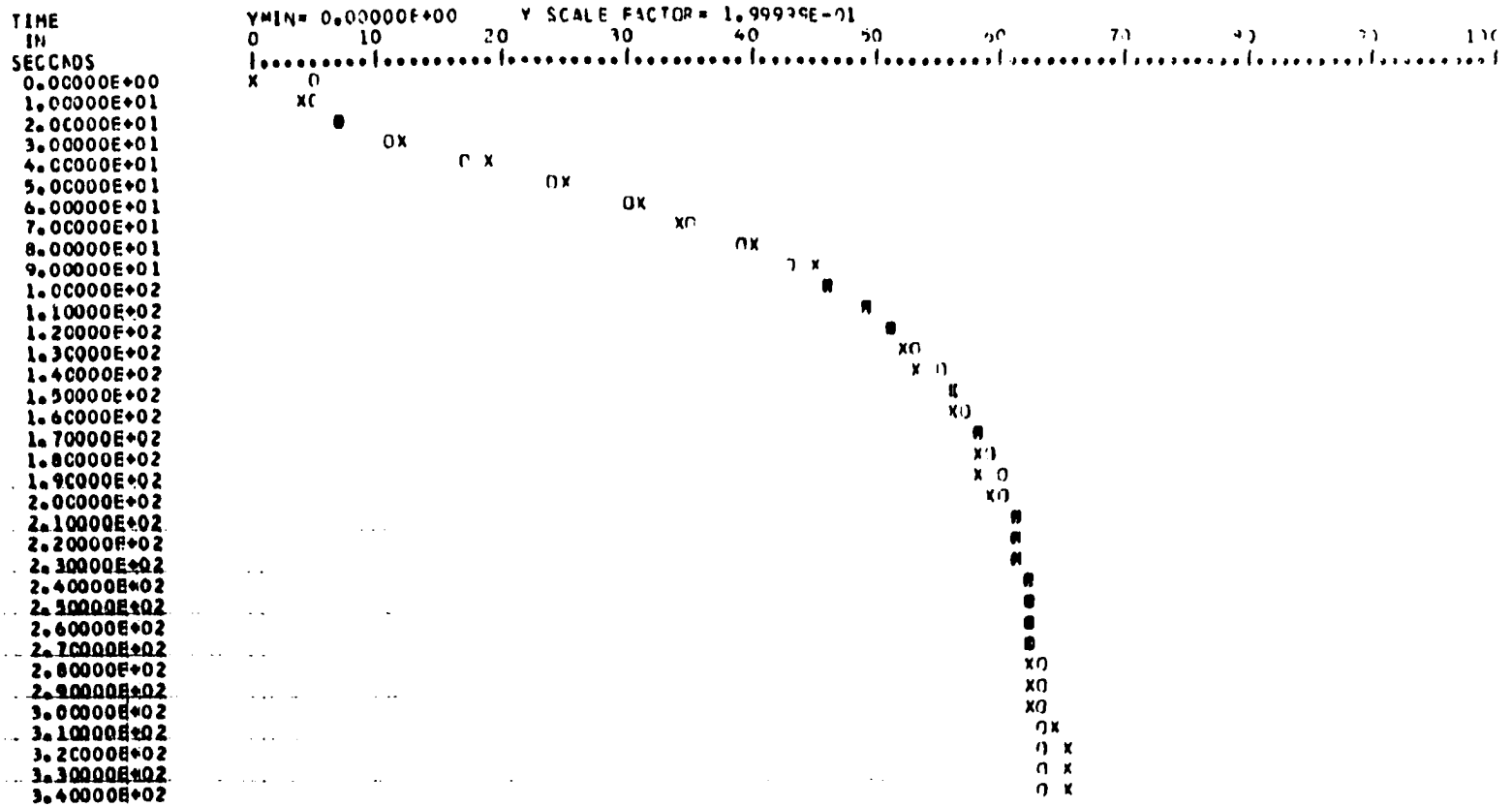

Figure 20. Second order identification for an input change in $\%HbO_2$ from 86 to 32%. The graphs show the actual output flow rate (X), and the simulated output (0) vs. time. The time scale should be multiplied by 100. The second order transfer function is

$$\frac{\Delta FR}{\Delta \%HbO_2} = \frac{-3.29 \times 10^{-3} (S - 7.72 \times 10^{-3})}{(S + 1.84 \times 10^{-2})(S - 6.29 \times 10^{-3})}$$

2/7/63-20N2

X ACTUAL SYSTEM OUTPUT
O IDENTIFIED SYSTEM OUTPUT

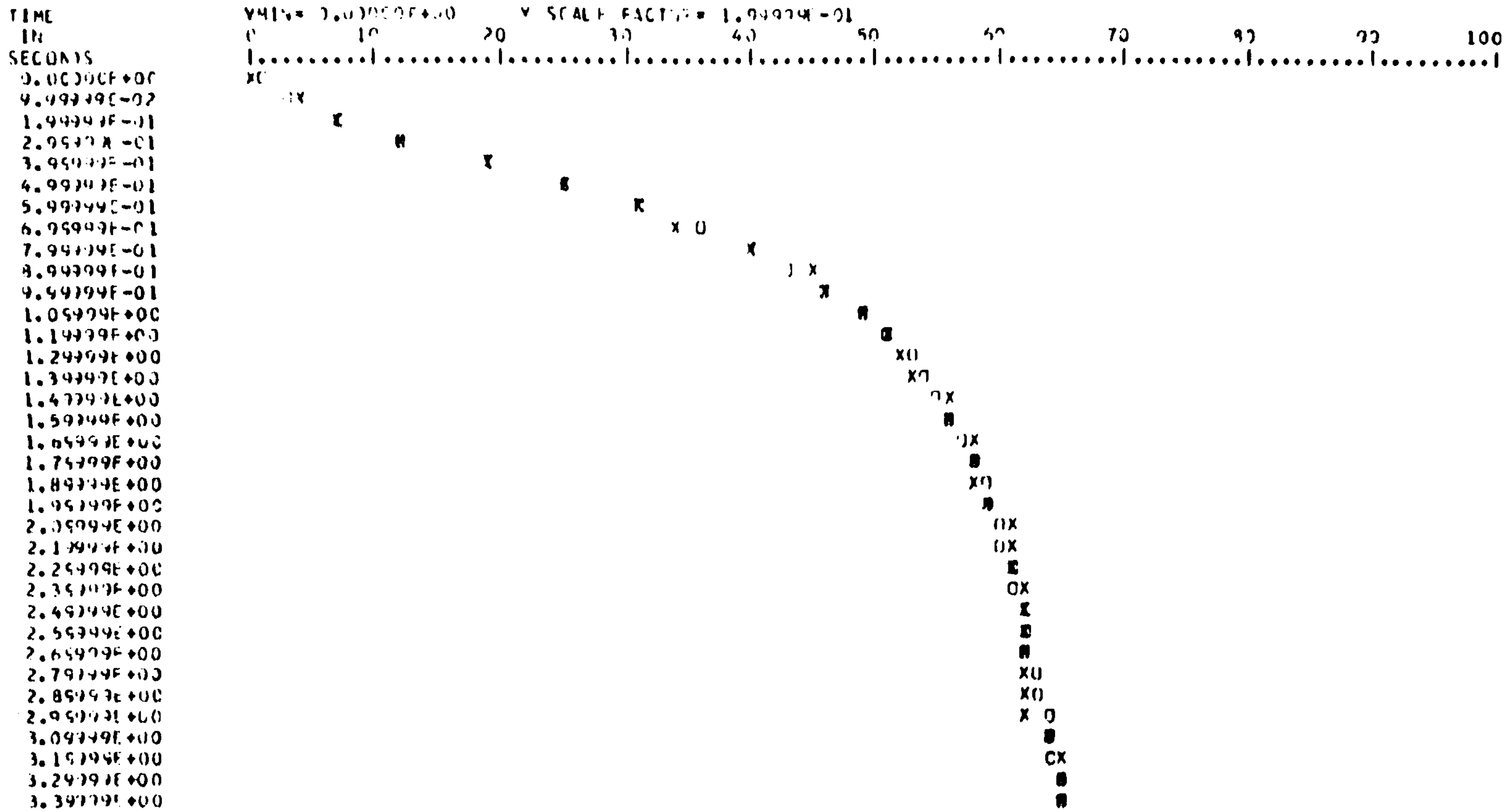

Figure 21. First order identification for an input change in $\%HbO_2$ from 53 to 86%. The graphs show the actual output flow rate (X), and the simulated output (O) vs. time. The first order transfer function is

$$\frac{\Delta FR}{\Delta \%HbO_2} = \frac{-4.35 \times 10^{-3}}{(S + 2.23 \times 10^{-2})}$$

3/6/68-1341

X ACTUAL SYSTEM OUTPUT
0 IDENTIFIED SYSTEM OUTPUT

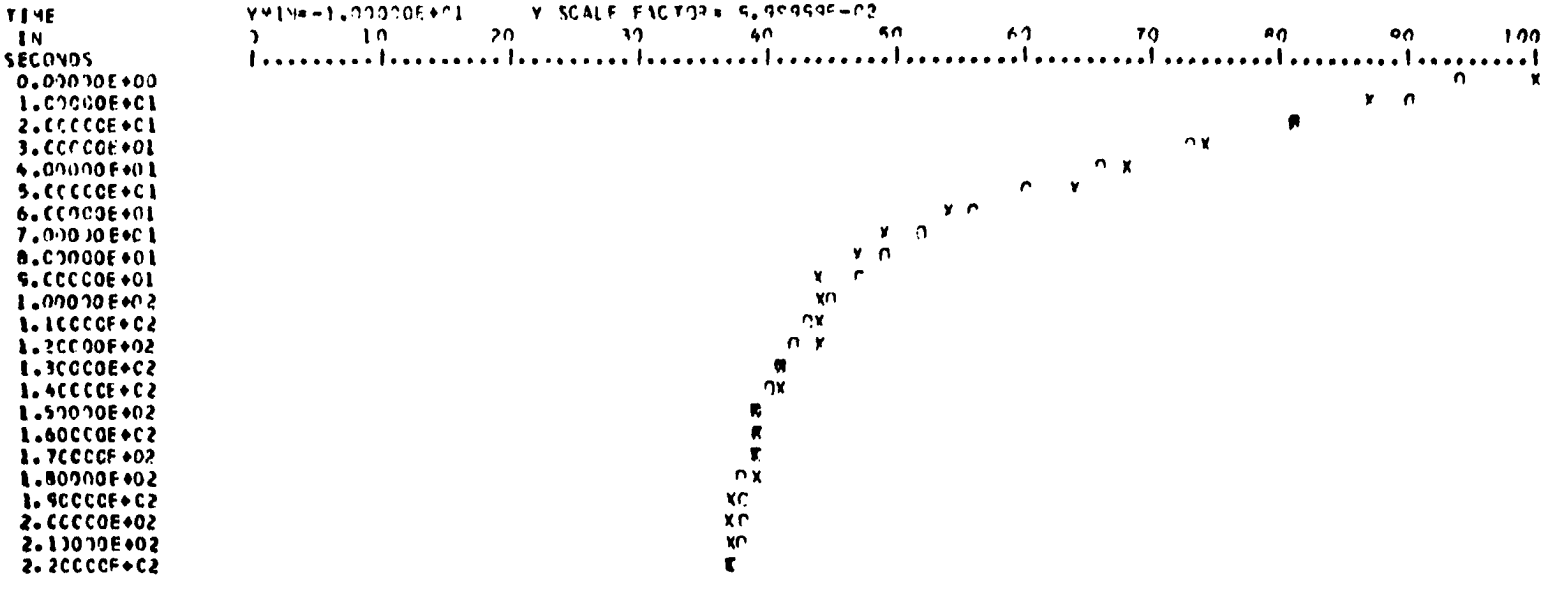

Figure 22. Second order identification for an input change in $\%HbO_2$ from 53 to 86%. The graphs show the actual output flow rate (X), and the simulated output (0) vs. time. The time scale should be multiplied by 100. The second order transfer function is

$$\frac{\Delta FR}{\Delta \%HbO_2} = \frac{-3.92 \times 10^{-3}(S - 1.09 \times 10^{-2})}{(S + 2.21 \times 10^{-2})(S - 9.90 \times 10^{-3})}$$

3/6/6-13N2

X ACTUAL SYSTEM OUTPUT
O IDENTIFIED SYSTEM OUTPUT

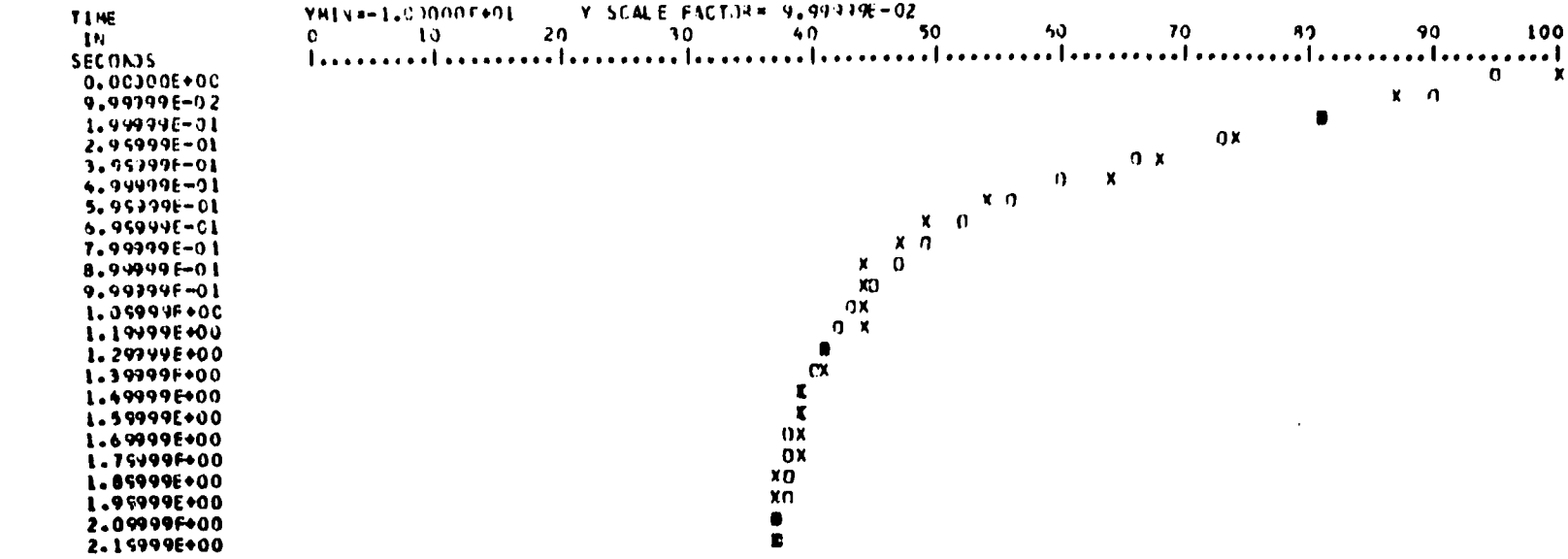

Figure 23. First order identification for an input change in $\%HbO_2$ from 26 to 87%. The graphs show the actual input $\%HbO_2$ (I), the actual output flow rate (X), and the simulated output (0) vs. time. The time scale should be multiplied by 100. The first order transfer function is

$$\frac{\Delta FR}{\Delta \%HbO_2} = \frac{-3.45 \times 10^{-4}}{(S + 1.01 \times 10^{-2})}$$

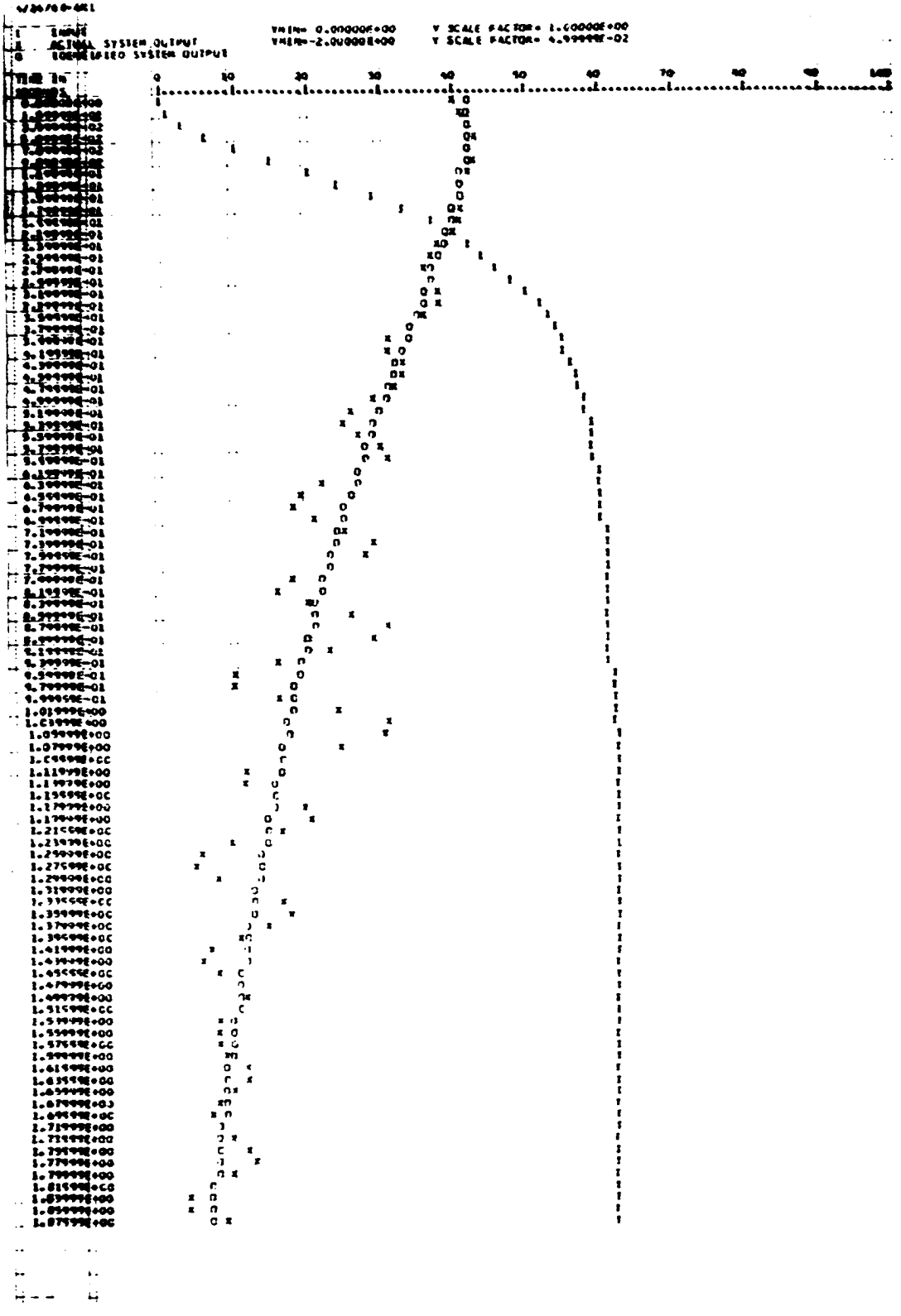
ACTUAL SYSTEM OUTPUT
YMIN= 0.000000E+00
Y SCALE FACTOR= 1.000000E+00
YMIN=-2.000000E+00
Y SCALE FACTOR= 4.999999E-02
0
10
20
30
40
50
60
70
80
90
100

Figure 24. Second order identification for an input change in $\%HbO_2$ from 26 to 87%. The graphs show the actual input $\%HbO_2$ (I), the actual output flow rate (X), and the simulated output (0) vs. time. The time scale should be multiplied by 100. The second order transfer function is

$$\frac{\Delta FR}{\Delta \%HbO_2} = \frac{-1.93 \times 10^{-4}(S + 1.75 \times 10^{-3})}{(S+3.32\times10^{-3}+j5.48\times10^{-3}) \cdot (S+3.32\times10^{-3}-j5.48\times10^{-3})}$$

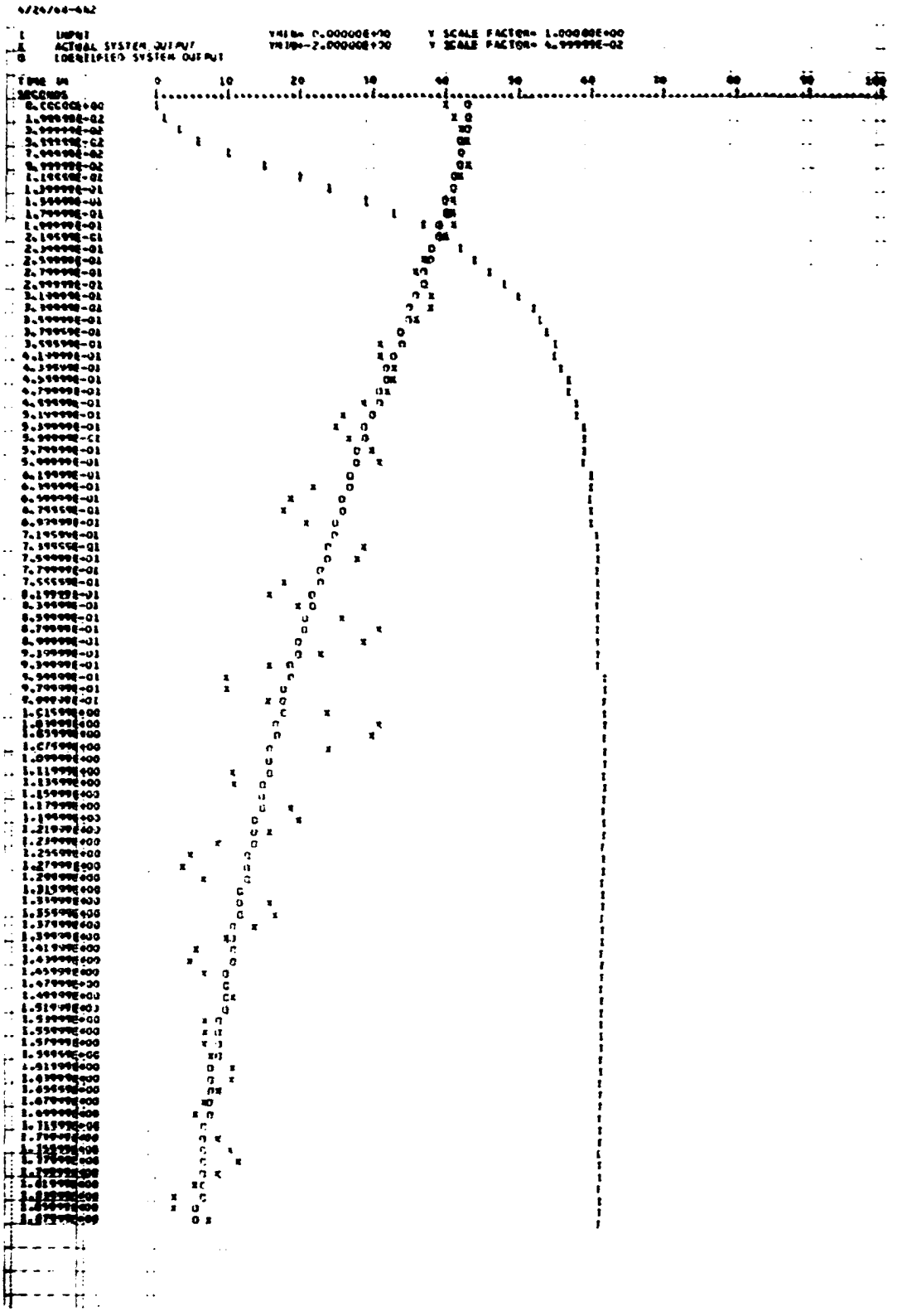
6/24/84-442
1 INPUT
A ACTUAL SYSTEM OUTPUT
B IDEALIZED SYSTEM OUTPUT
Y MIN= 0.000000E+00
Y MIN=-2.000000E+00
Y SCALE FACTOR= 1.000000E+00
Y SCALE FACTOR= 4.999999E-02
TIME IN SECONDS
0
10
20
30
40
50
60
70
80
90
100

Figure 25. First order identification for an input change in $\%HbO_2$ from 95 to 80%. The graphs show the actual output flow rate (X), and the simulated output (O) vs. time. The first order transfer function is

$$\frac{\Delta FR}{\Delta \%HbO_2} = \frac{-2.83 \times 10^{-3}}{s + 1.37 \times 10^{-2}}$$

2/28/68-4N1

X ACTUAL SYSTEM OUTPUT
0 IDENTIFIED SYSTEM OUTPUT

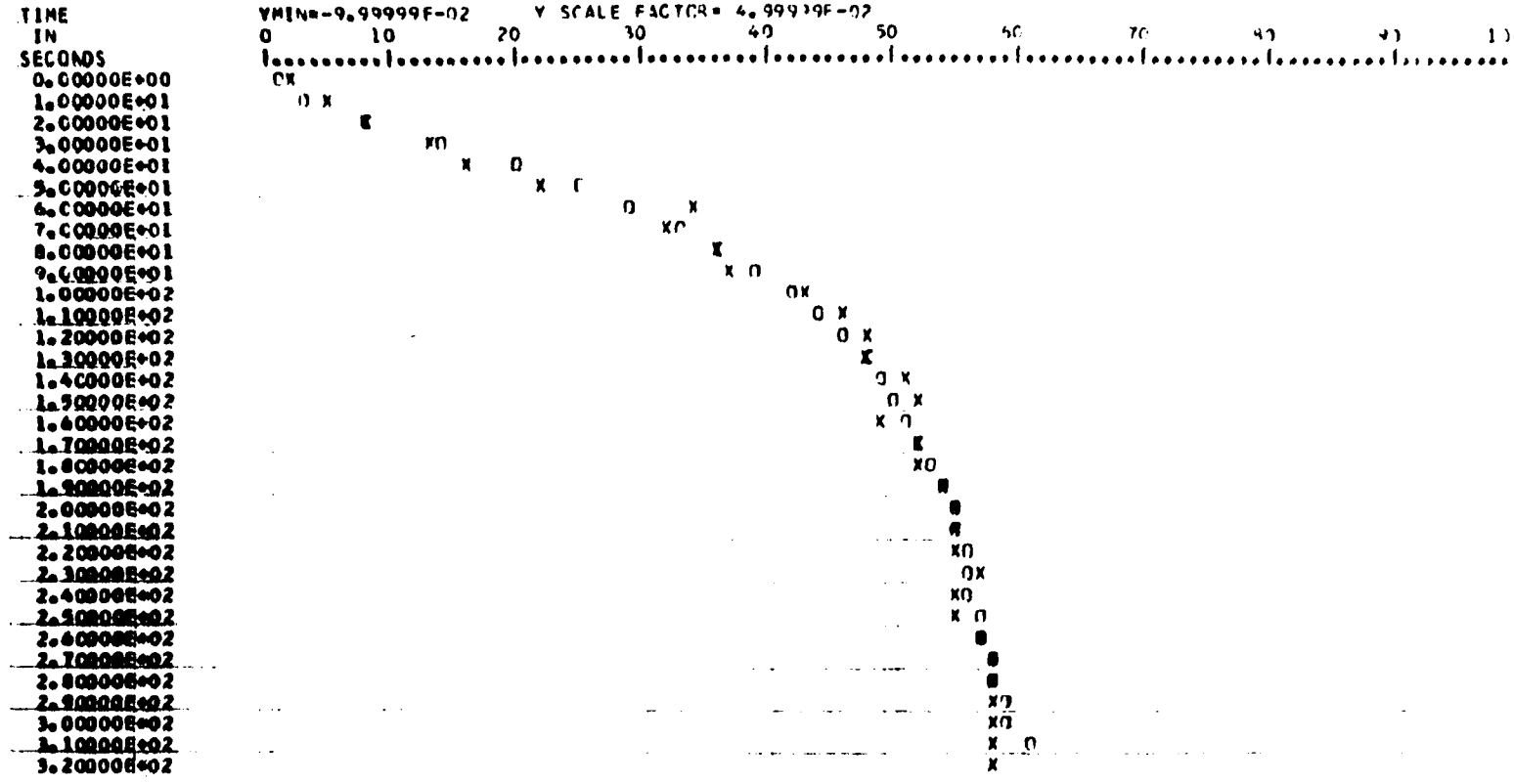

Figure 26. Second order identification for an input change in $\%HbO_2$ from 95 to 80%. The graphs show the actual output flow rate (X), and the simulated output (O) vs. time. The time scale should be multiplied by 100. The second order transfer function is

$$\frac{\Delta FR}{\Delta \%HbO_2} = \frac{-7.85 \times 10^{-4}(S + 1.72 \times 10^{-1})}{(S + 1.84 \times 10^{-2})(S + 3.63 \times 10^{-2})}$$

2/28/76- 452

X ACTUAL SYSTEM OUTPUT
O IDENTIFIED SYSTEM OUTPUT

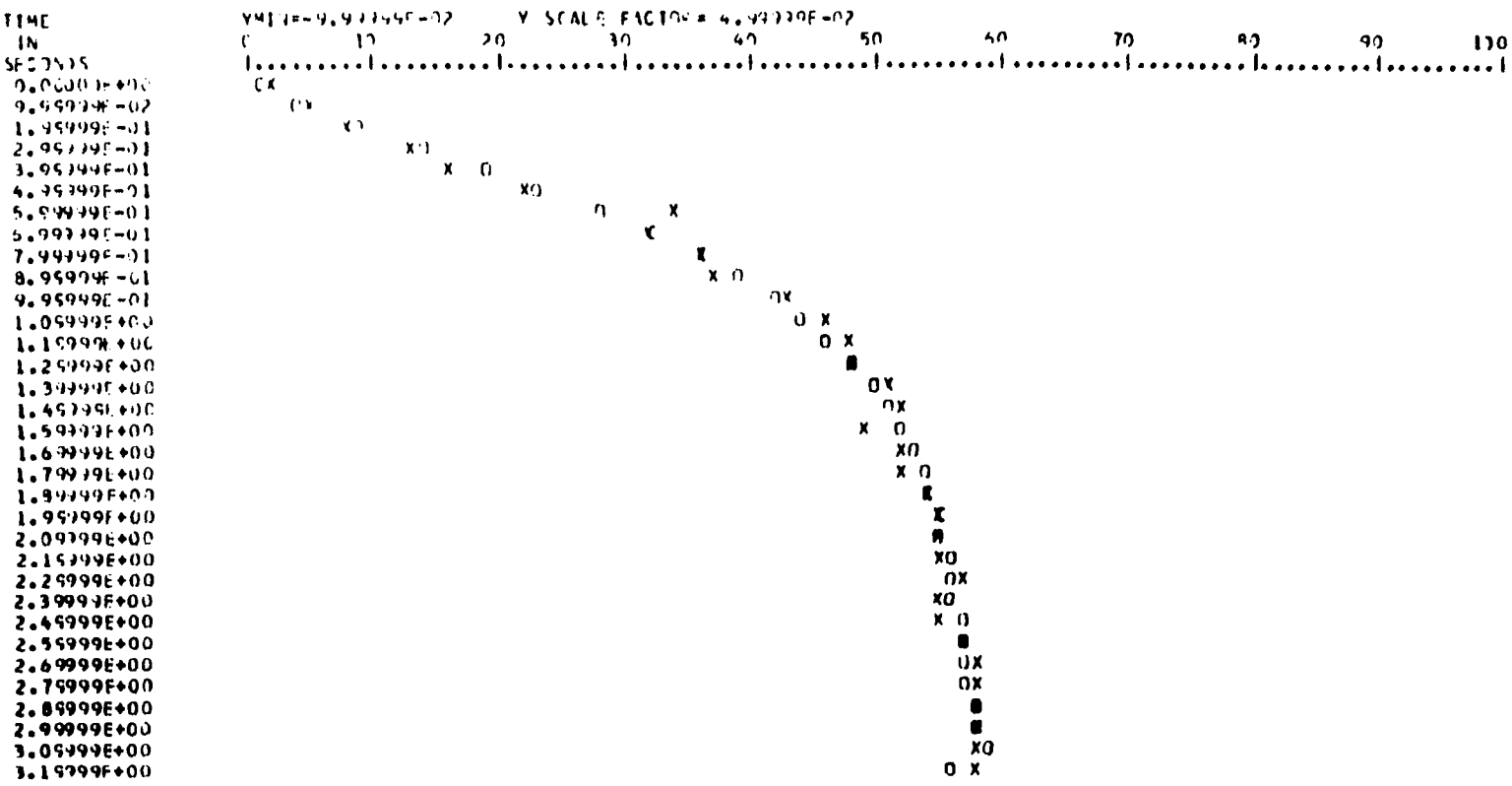

Figure 27. First order identification for an input change in $\%HbO_2$ from 84 to 71%. The graphs show the actual input $\%HbO_2$ (I), the actual output flow rate (X), and the simulated output (0) vs. time. The time scale should be multiplied by 100. The first order transfer function is

$$\frac{\Delta FR}{\Delta \%HbO_2} = \frac{-6.07 \times 10^{-3}}{S + 2.70 \times 10^{-2}}$$

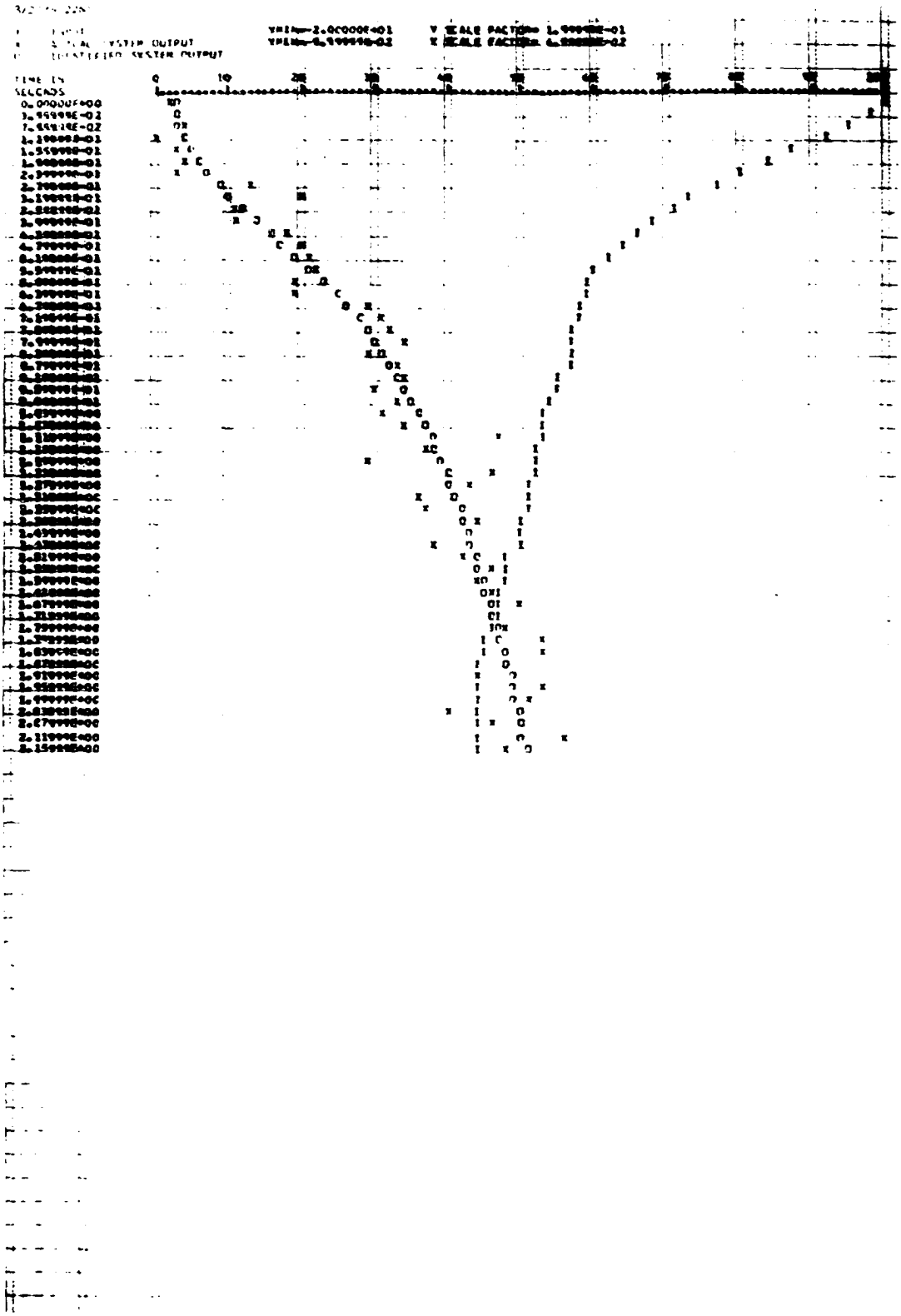

Figure 28. Second order identification for an input change in $\%HbO_2$ from 84 to 71%. The graphs show the actual input $\%HbO_2$ (I), the actual output flow rate (X), and the simulated output (0) vs. time. The time scale should be multiplied by 100. The second order transfer function is

$$\frac{\Delta FR}{\Delta \%HbO_2} = \frac{-3.94 \times 10^{-3}(S + 9.03 \times 10^{-3})}{(S + 2.23 \times 10^{-2})(S + 6.37 \times 10^{-3})}$$

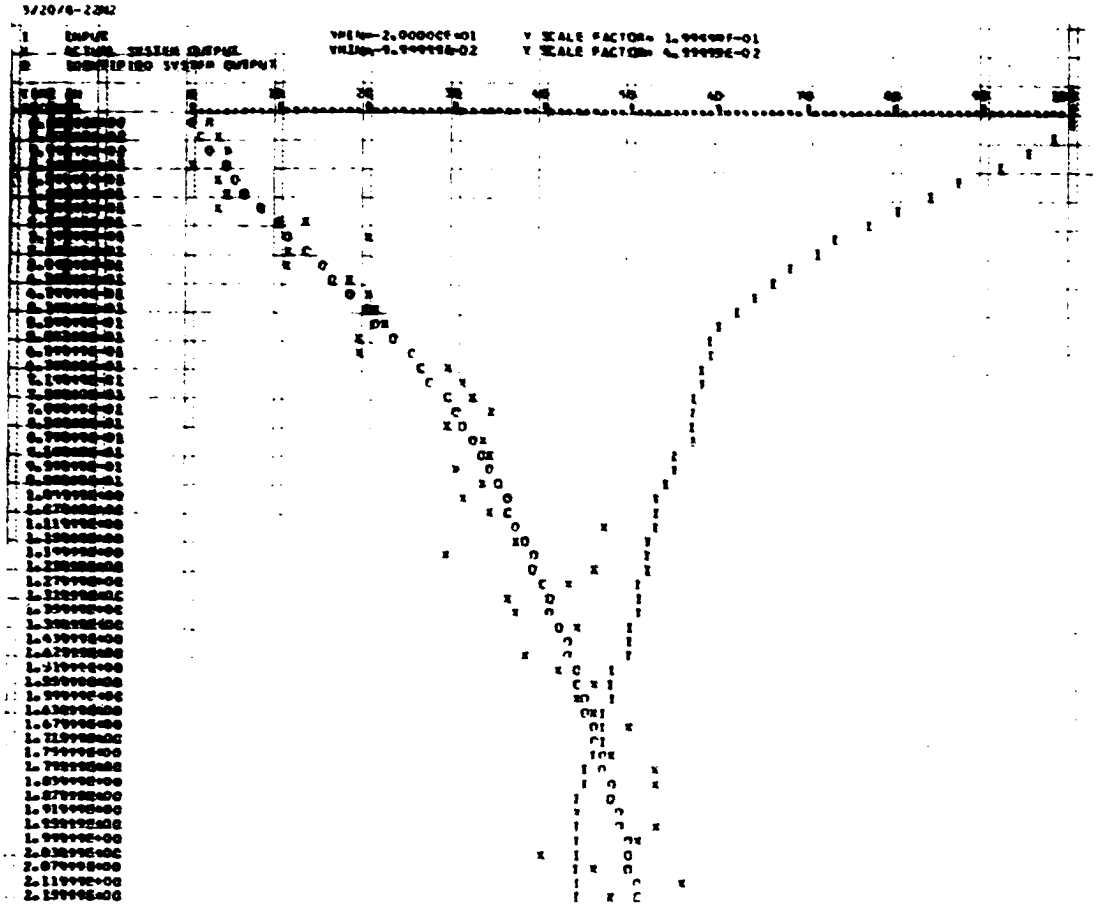

Figure 29. First order identification for an input change in $\%HbO_2$ from 63 to 88%. The graphs show the actual output flow rate (X) and the simulated output (0) vs. time. The first order transfer function is

$$\frac{\Delta FR}{\Delta \%HbO_2} = \frac{-2.84 \times 10^{-3}}{S + 8.11 \times 10^{-3}}$$

3/6/68-9N1
X ACTUAL SYSTEM OUTPUT
O IDENTIFIED SYSTEM OUTPUT
TIME IN SECONDS
YMIN=-1.000000E+01
Y SCALE FACTOR= 9.999999E-02
0
10
20
30
40
50
60
70
80
90
100

Figure 30. Second order identification for an input change in $\%HbO_2$ from 63 to 88%. The graph shows the actual output flow rate (X), and the simulated output (0) vs. time. The second order transfer function is

$$\frac{\Delta FR}{\Delta \%HbO_2} = \frac{-2.92 \times 10^{-3}(S + 8.26 \times 10^{-3})}{(S + 1.38 \times 10^{-2})(S + 4.49 \times 10^{-3})}$$

3/6/6- 942

X ACTUAL SYSTEM OUTPUT
0 IDENTIFIED SYSTEM OUTPUT

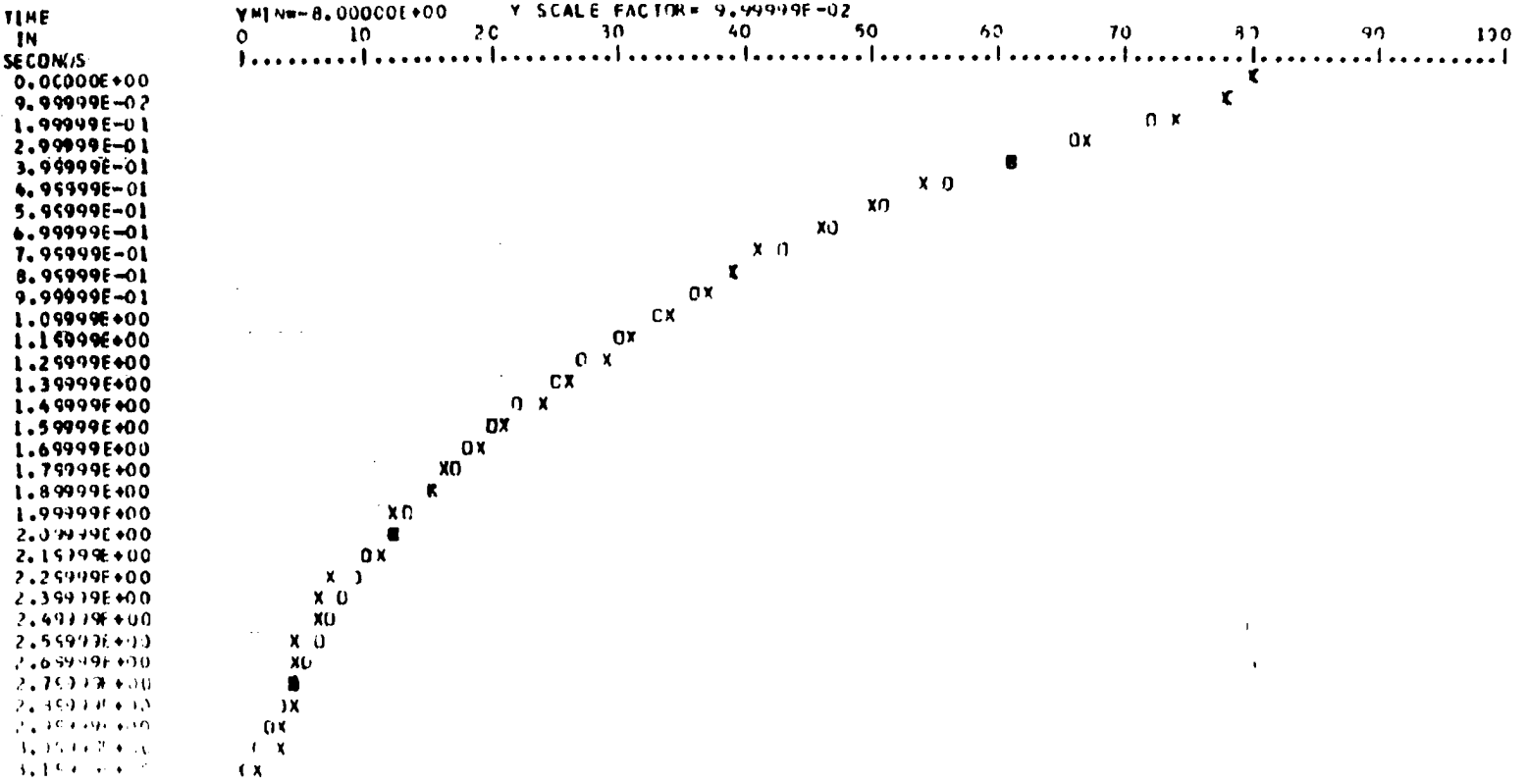

Figure 31. First order identification for an input change in $\%HbO_2$ from 57 to 61%. The graphs show the actual input $\%HbO_2$ (I), the actual output flow rate (X), and the simulated output (0) vs. time. The time scale should be multiplied by 100. The first order transfer function is

$$\frac{\Delta FR}{\Delta \%HbO_2} = \frac{-3.69 \times 10^{-3}}{S + 3.79 \times 10^{-3}}$$

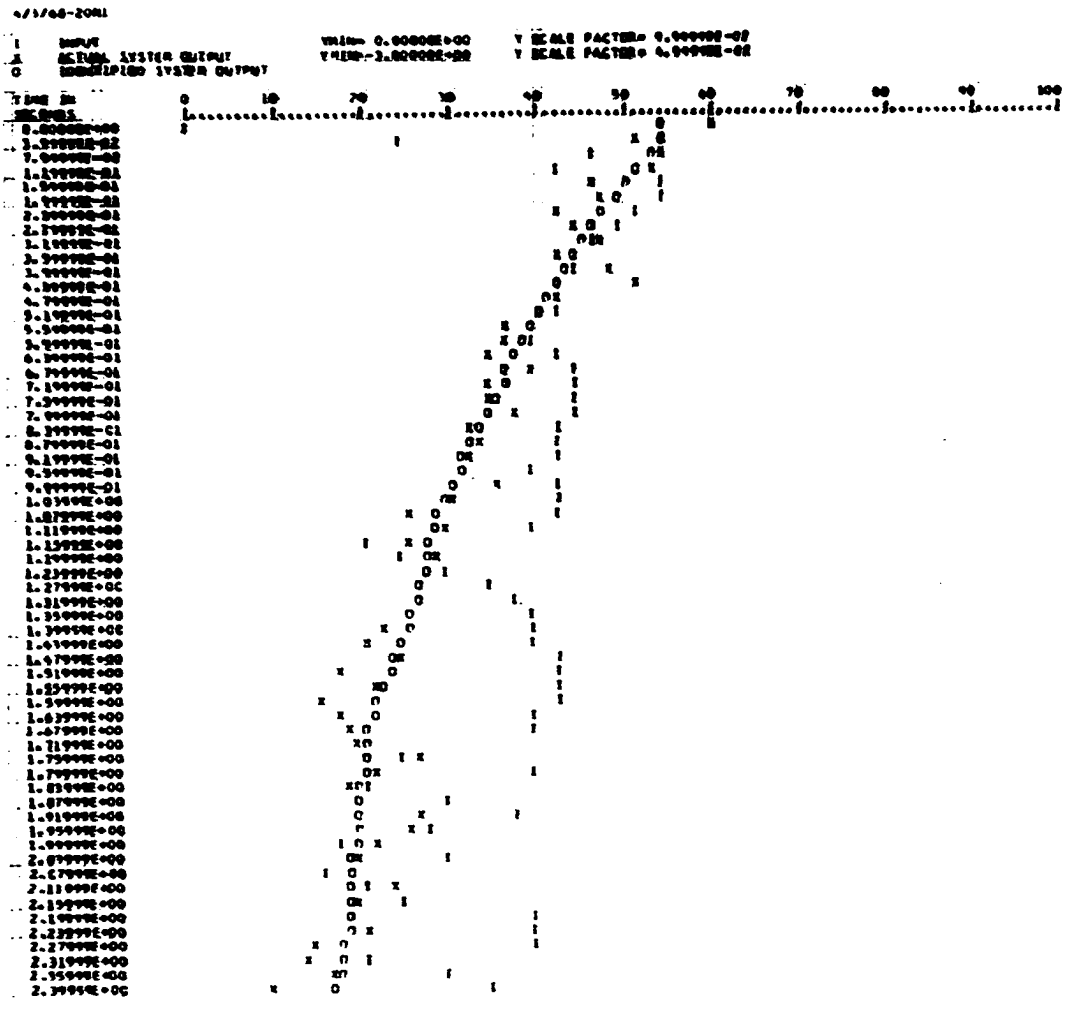

Figure 32. Second order identification for an input change in $\%HbO_2$ from 57 to 61%. The graphs show the actual input $\%HbO_2$ (I), the actual output flow rate (X), and the simulated output (0) vs. time. The time scale should be multiplied by 100. The second order transfer function is

$$\frac{\Delta FR}{\Delta \%HbO_2} = \frac{-3.86 \times 10^{-3}(S + 5.28 \times 10^{-3})}{(S+3.23\times10^{-3}+j4.83\times10^{-3})(S+3.23\times10^{-3}-j4.83\times10^{-3})}$$

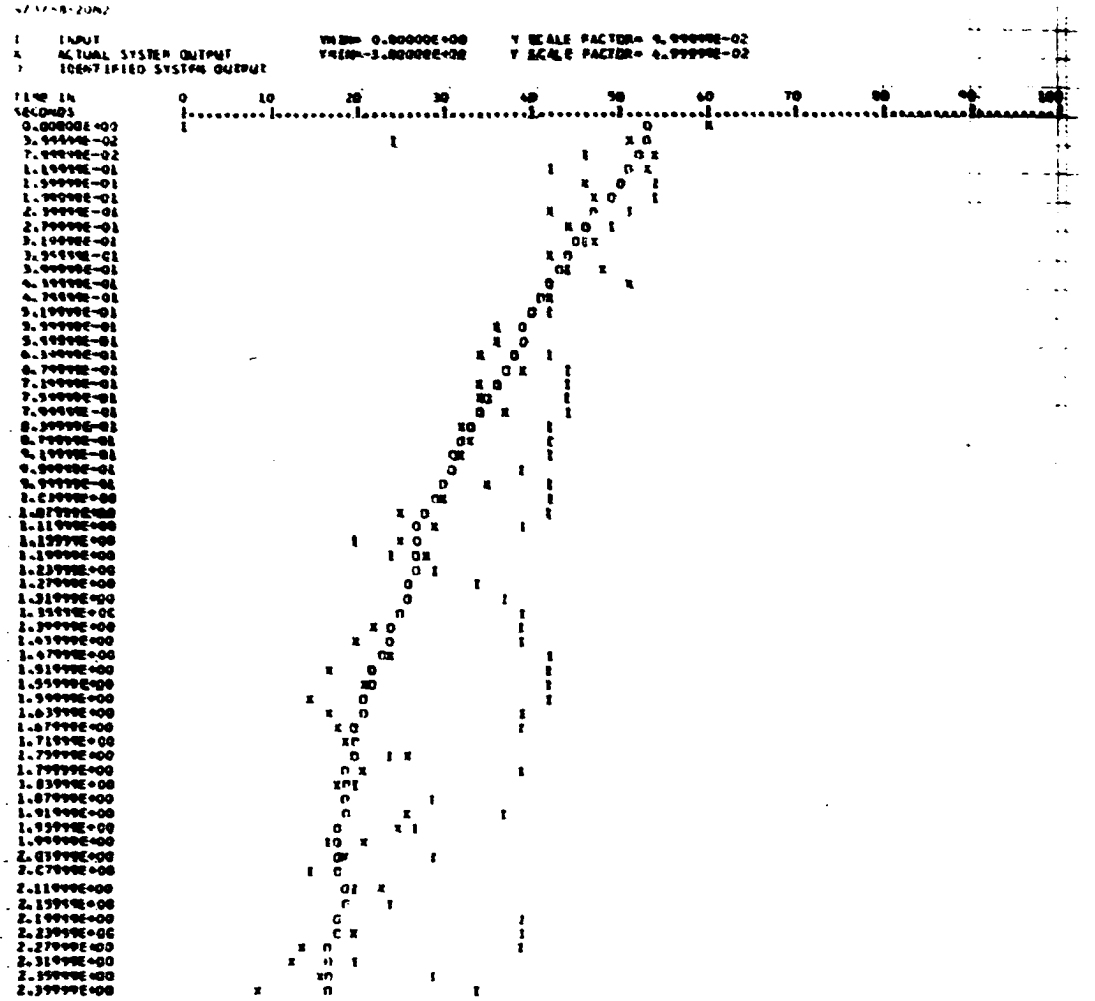
I INPUT
X ACTUAL SYSTEM OUTPUT
? IDENTIFIED SYSTEM OUTPUT
Y SCALE FACTOR= 4.999998E-02
Y SCALE FACTOR= 4.999998E-02
TIME IN SECONDS
0
10
20
30
40
50
60
70
80
90
100

Figure 33. First order identification for an input change in $\%HbO_2$ from 34 to 49%. The graphs show the actual input $\%HbO_2$ (I), the actual output flow rate (X), and the simulated output (0) vs. time. The time scale should be multiplied by 100. The first order transfer function is

$$\frac{\Delta FR}{\Delta \%HbO_2} = \frac{-2.21 \times 10^{-3}}{S + 4.32 \times 10^{-3}}$$

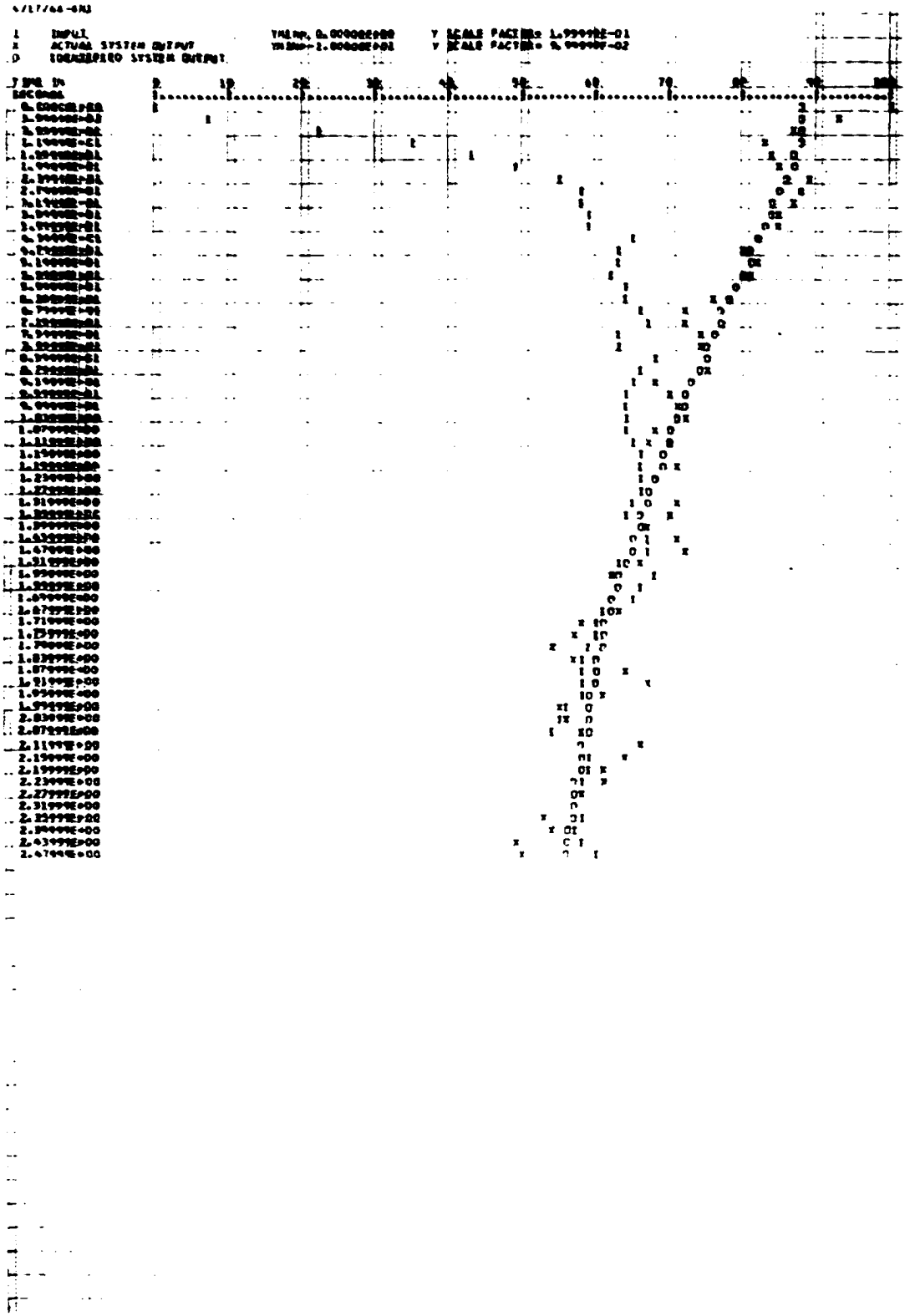

Figure 34. Second order identification for an input change in $\%HbO_2$ from 34 to 49%. The graphs show the actual input $\%HbO_2$ (I), the actual output flow rate (X), and the simulated output (0) vs. time. The time scale should be multiplied by 100. The second order transfer function is

$$\frac{\Delta FR}{\Delta \%HbO_2} = \frac{-2.27 \times 10^{-3}(S - 2.03 \times 10^{-2})}{(S + 1.31 \times 10^{-2})(S - 1.29 \times 10^{-2})}$$

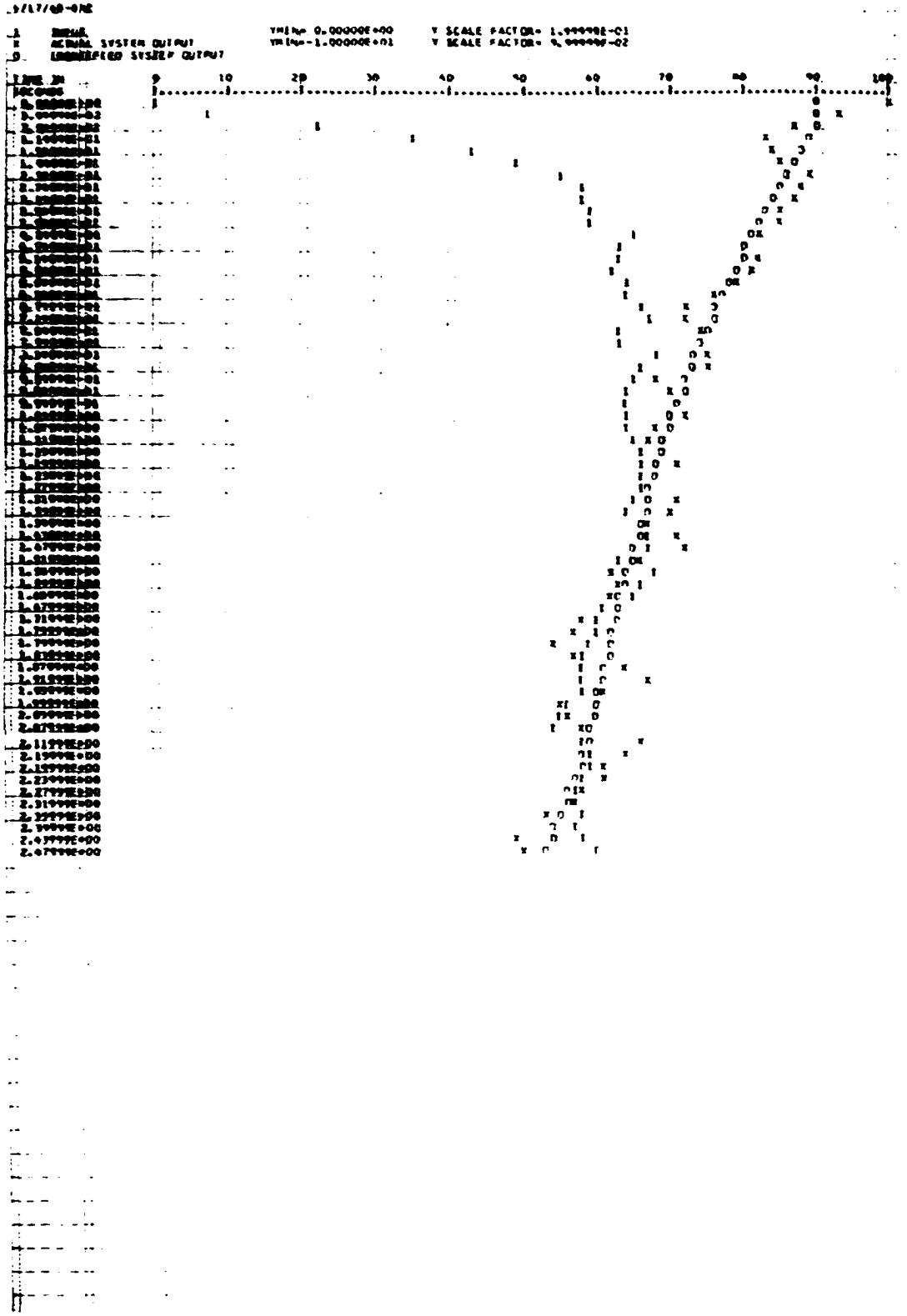

Figure 35. Number of observations vs. the time constant, τ

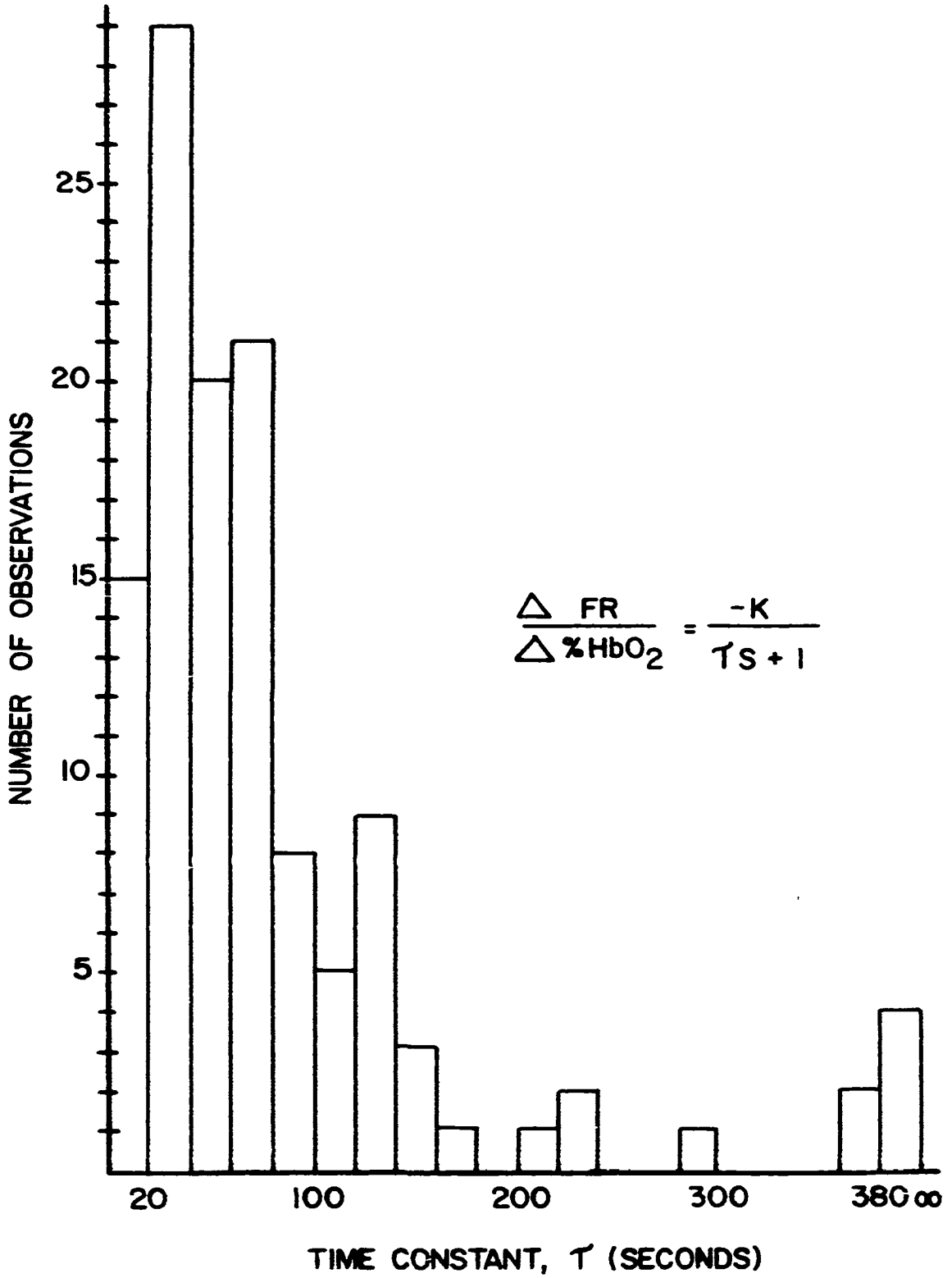
NUMBER OF OBSERVATIONS
25
20
15
10
5
20
100
200
300
380 ∞
TIME CONSTANT, τ (SECONDS)
Δ FR / Δ %HbO2 = -K / τS + 1

Figure 36. Number of observations vs. the gain constant, K

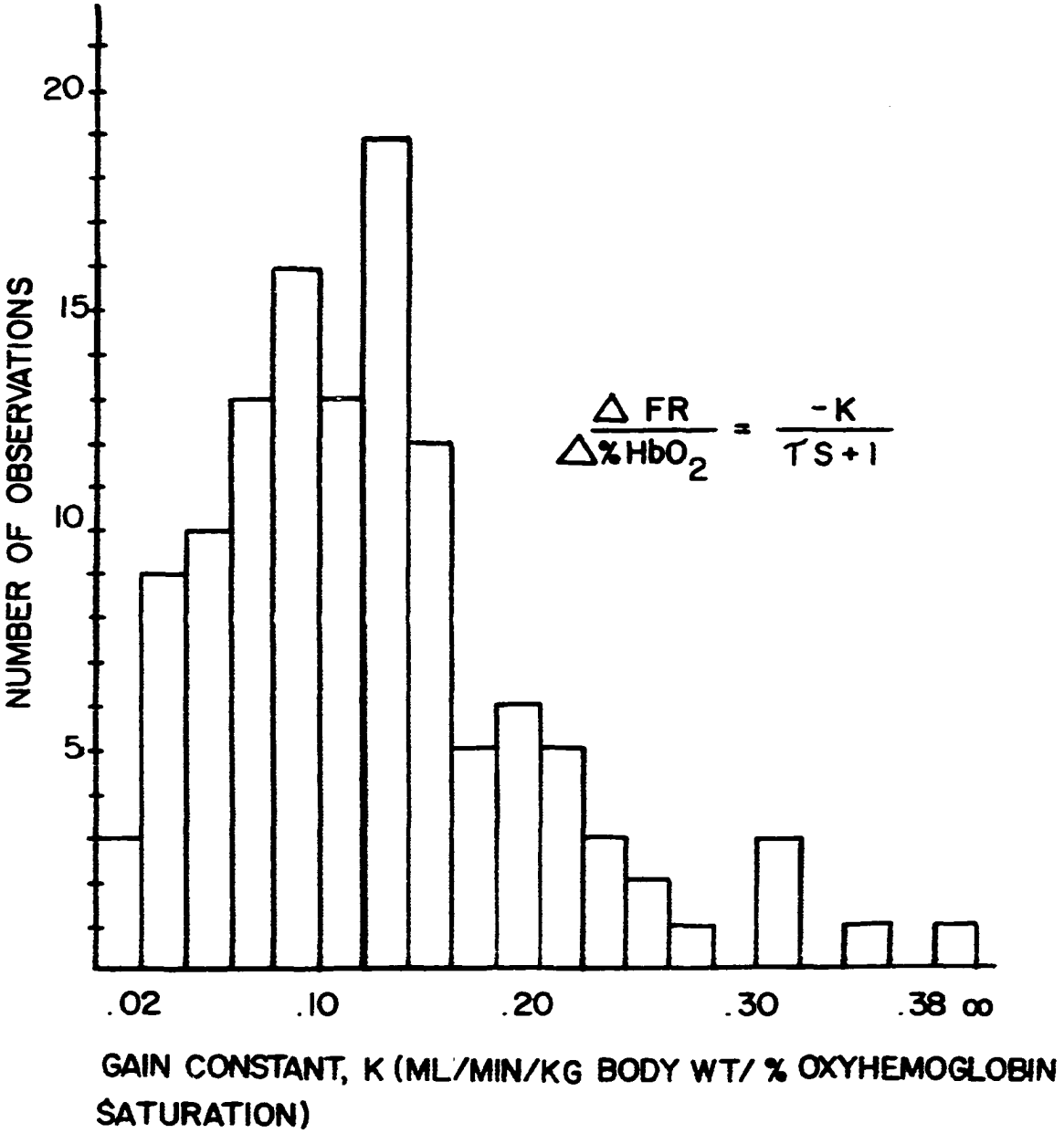
20
15
10
5
NUMBER OF OBSERVATIONS
$\frac{\Delta FR}{\Delta \%HbO_2} = \frac{-K}{TS+1}$
.02
.10
.20
.30
.38 ∞
GAIN CONSTANT, K (ML/MIN/KG BODY WT/ % OXYHEMOGLOBIN SATURATION)

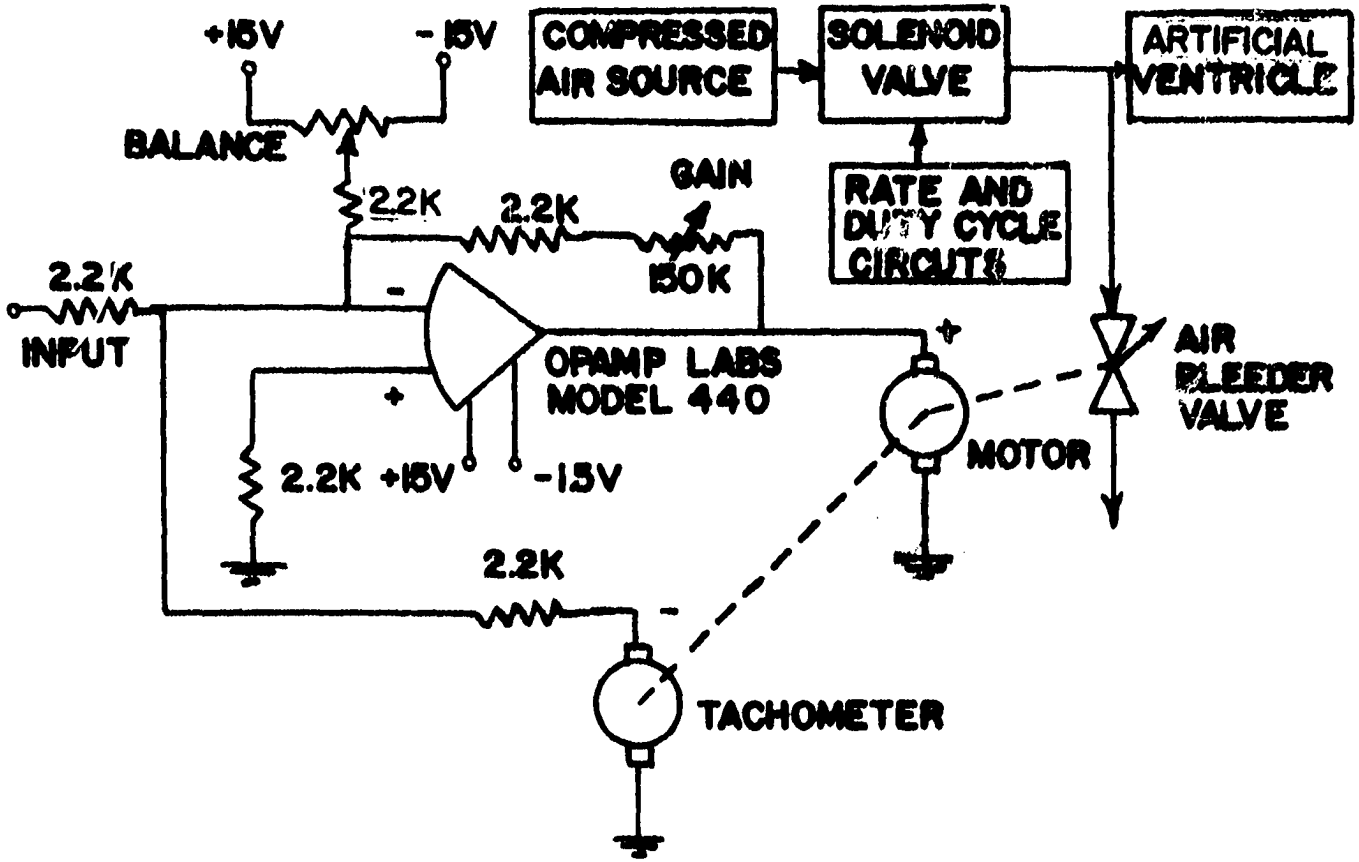

Figure 37. Schematic diagram of artificial ventricle power and control systems

Figure 38. Diagram of test circulation used to determine the transfer function of the artificial heart power and control systems

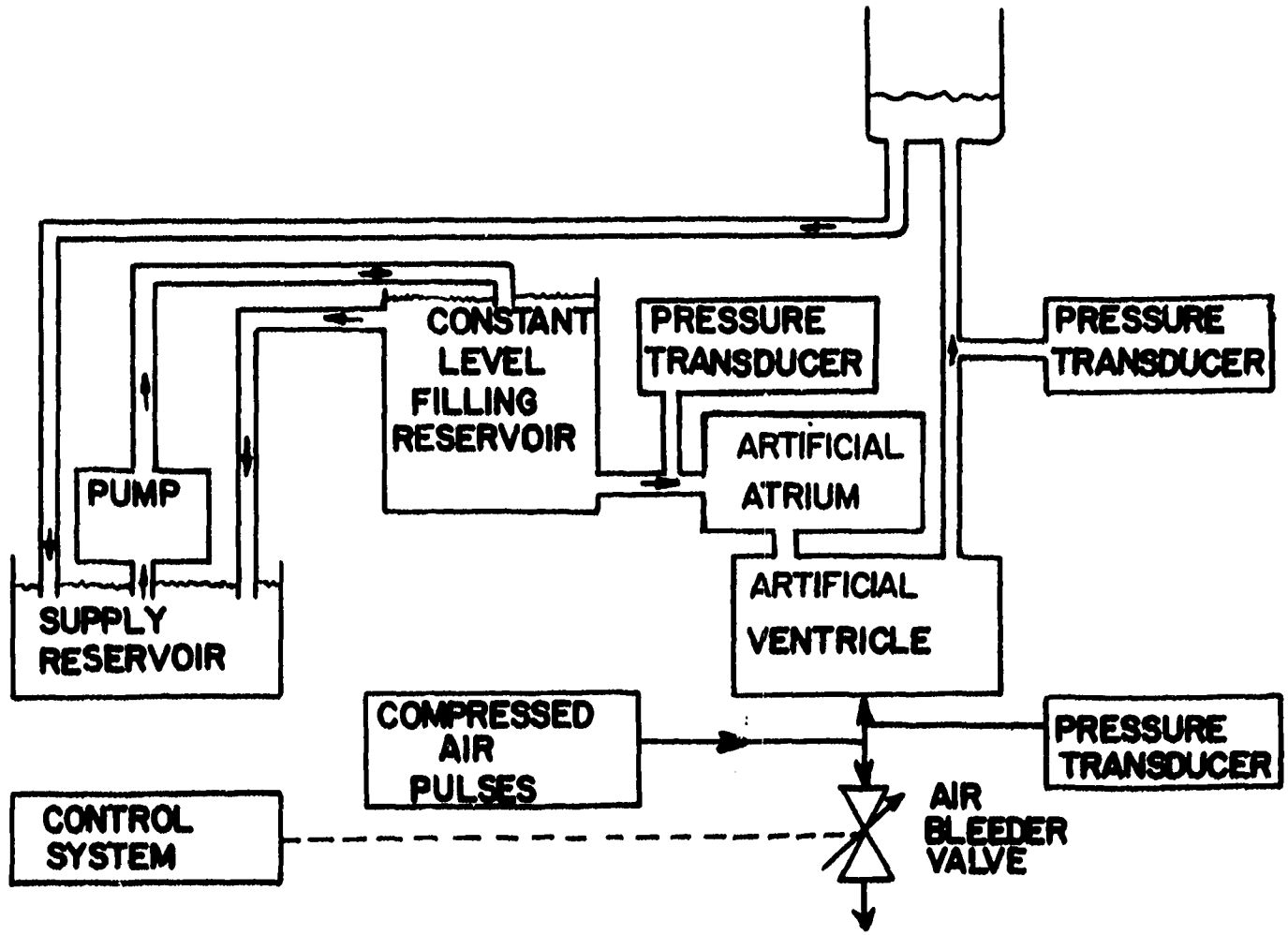
CONSTANT
LEVEL
FILLING
RESERVOIR
PRESSURE
TRANSDUCER
PRESSURE
TRANSDUCER
ARTIFICIAL
ATRIUM
PUMP
ARTIFICIAL
VENTRICLE
SUPPLY
RESERVOIR
COMPRESSED
AIR
PULSES
PRESSURE
TRANSDUCER
CONTROL
SYSTEM
AIR
BLEEDER
VALVE

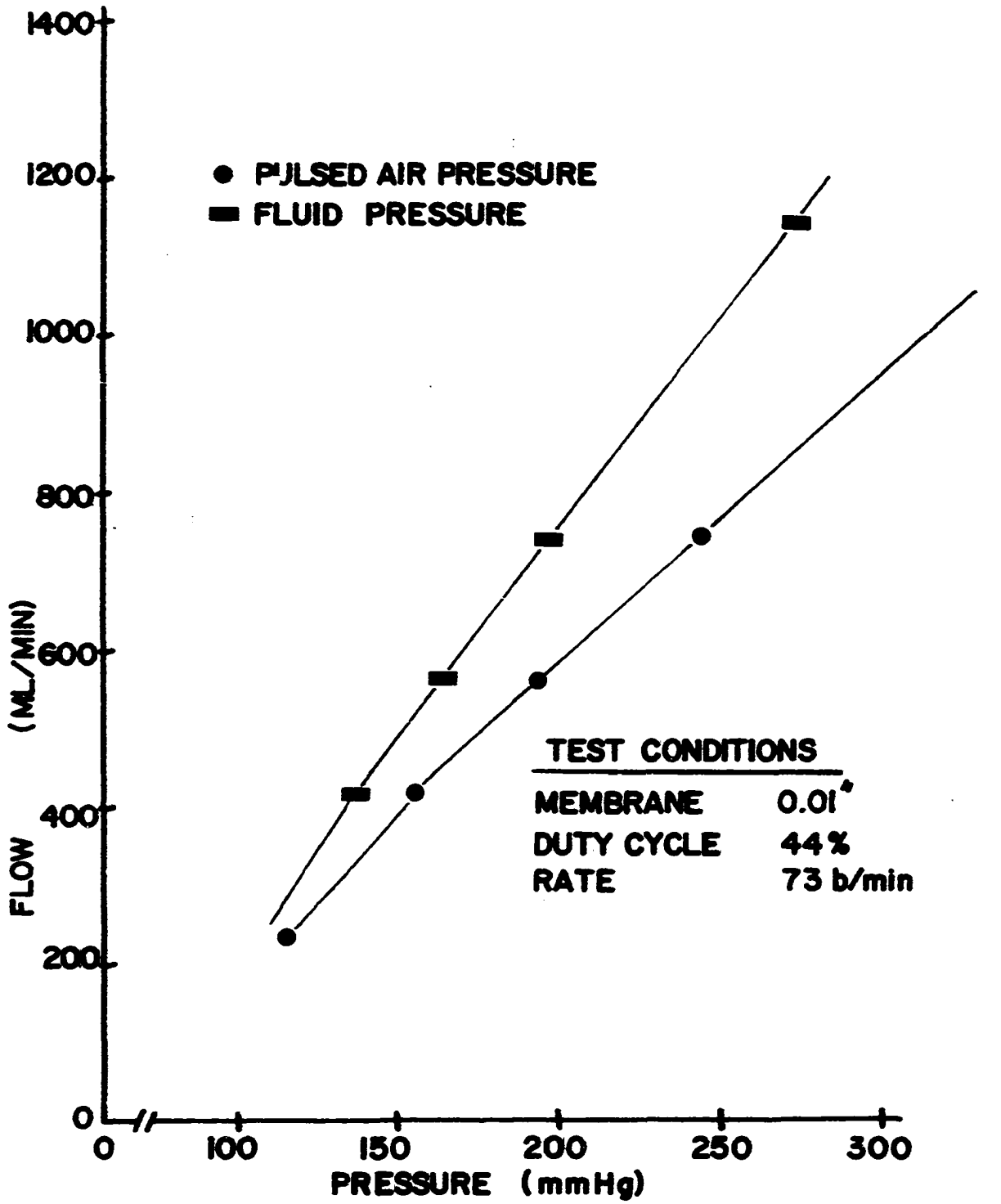

Figure 39. Artificial ventricle output vs. pressure

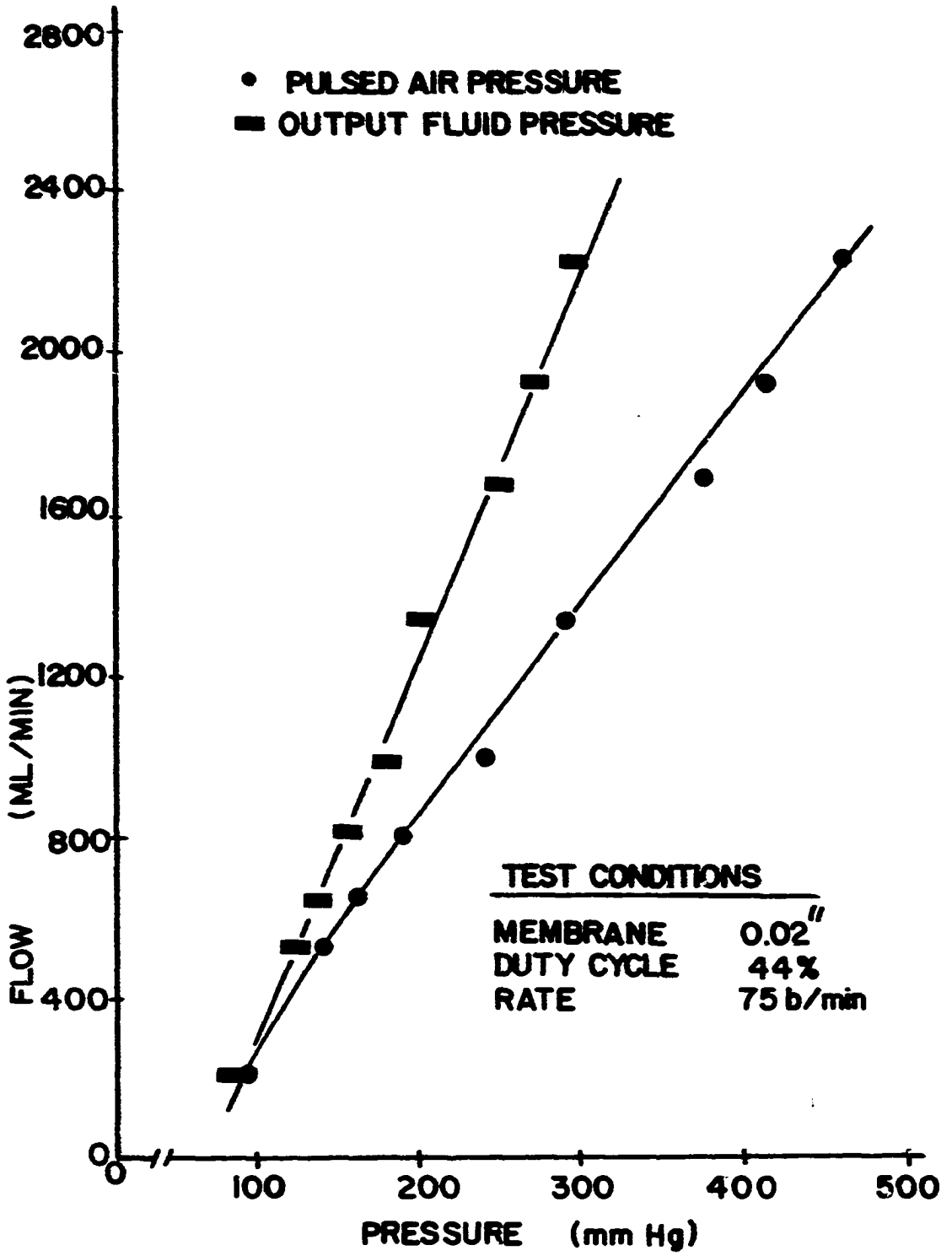

Figure 40. Artificial ventricle output vs. pressure

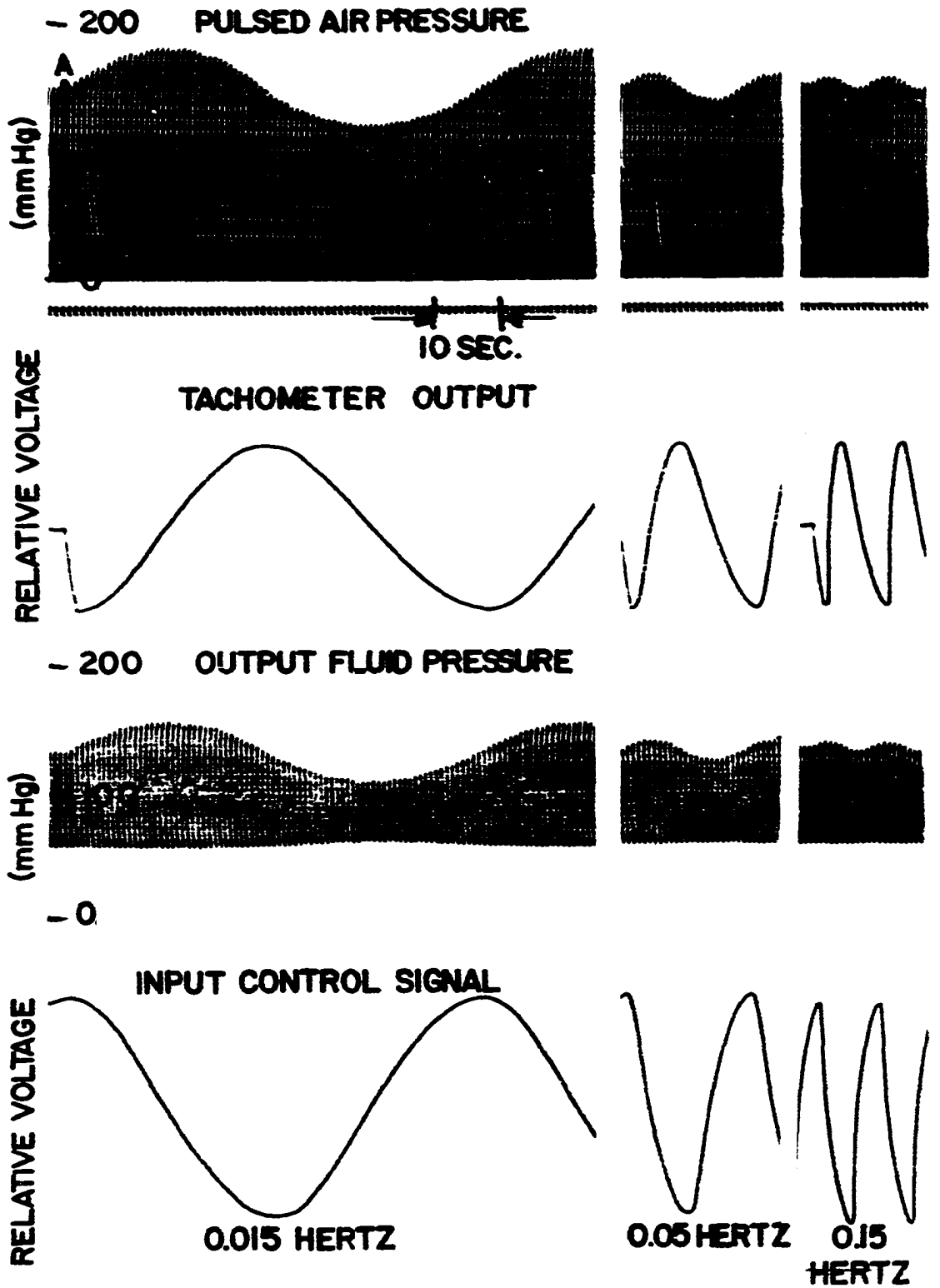

Figure 41. In vitro artificial heart transfer function data

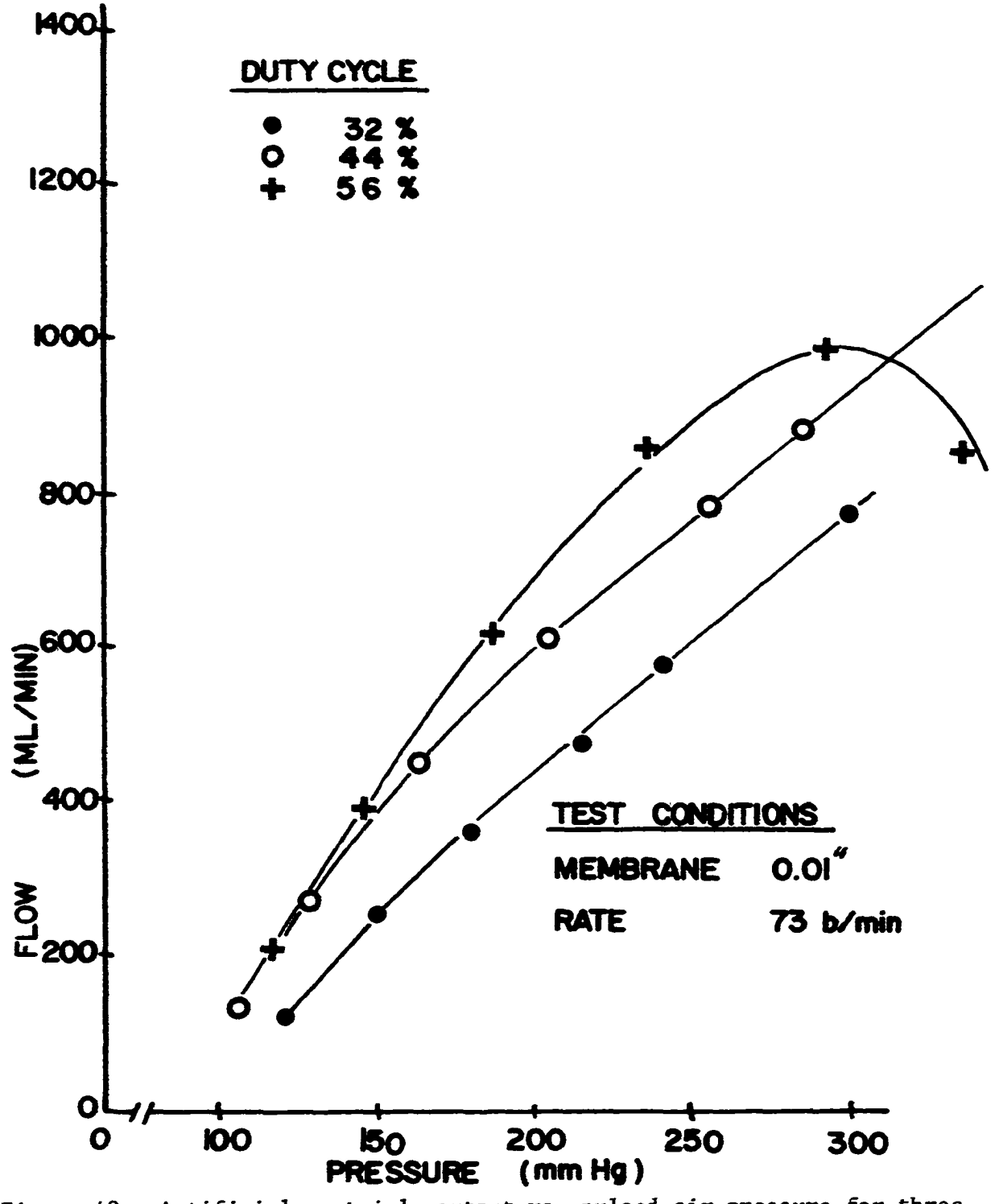

Figure 42. Artificial ventricle output vs. pulsed air pressure for three duty cycle values

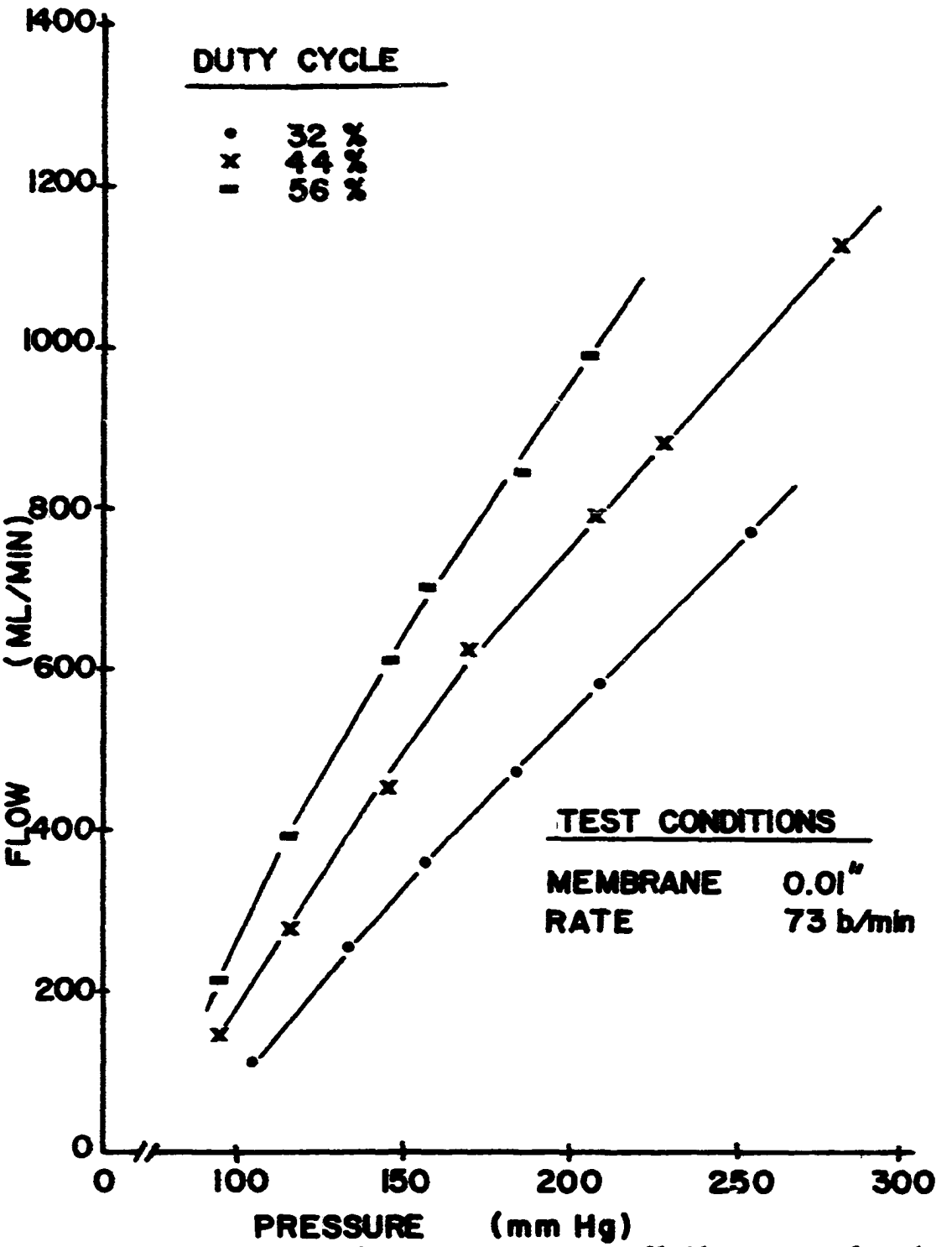

Figure 43. Artificial ventricle output vs. output fluid pressure for three duty cycle values

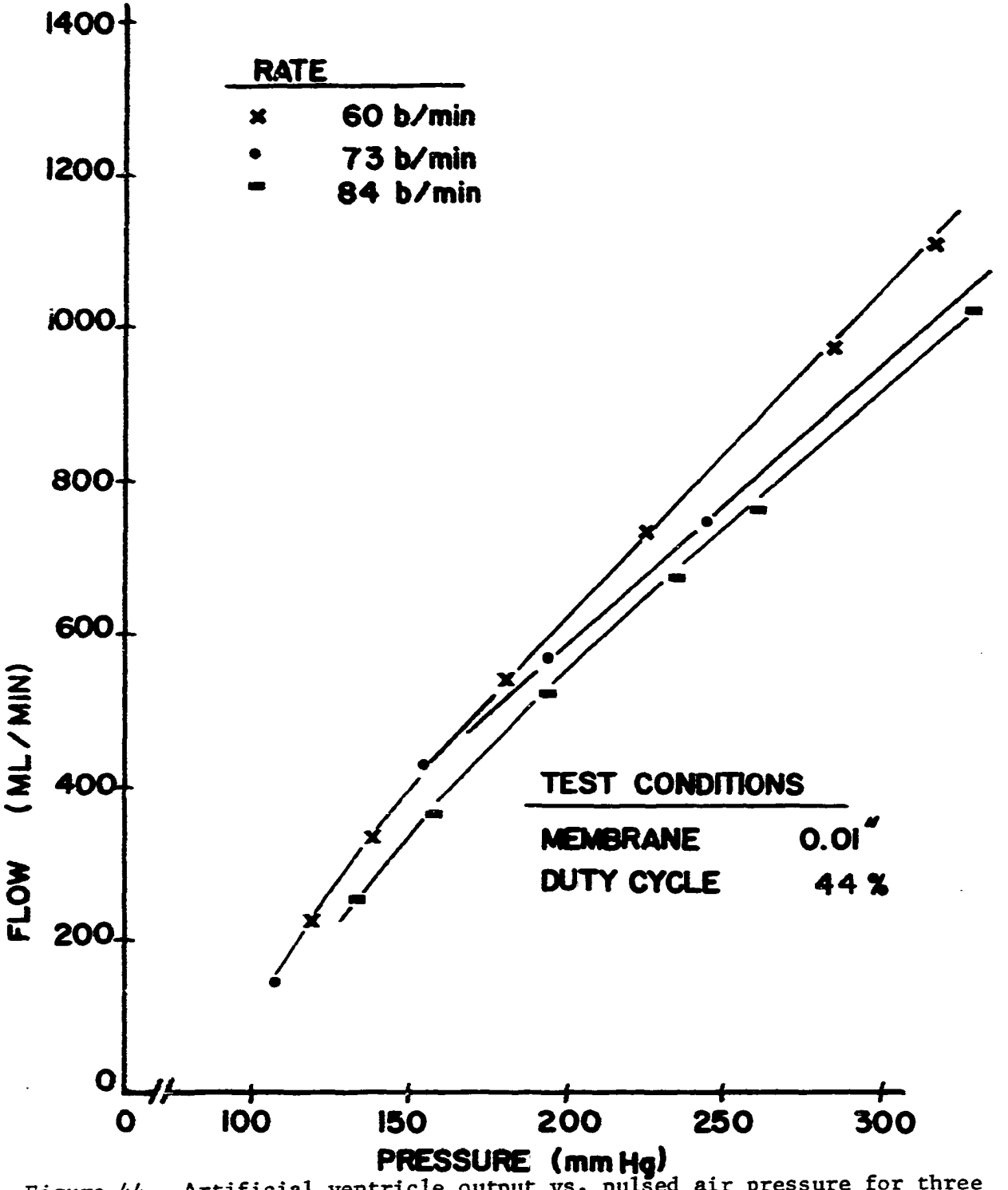

Figure 44. Artificial ventricle output vs. pulsed air pressure for three rate values

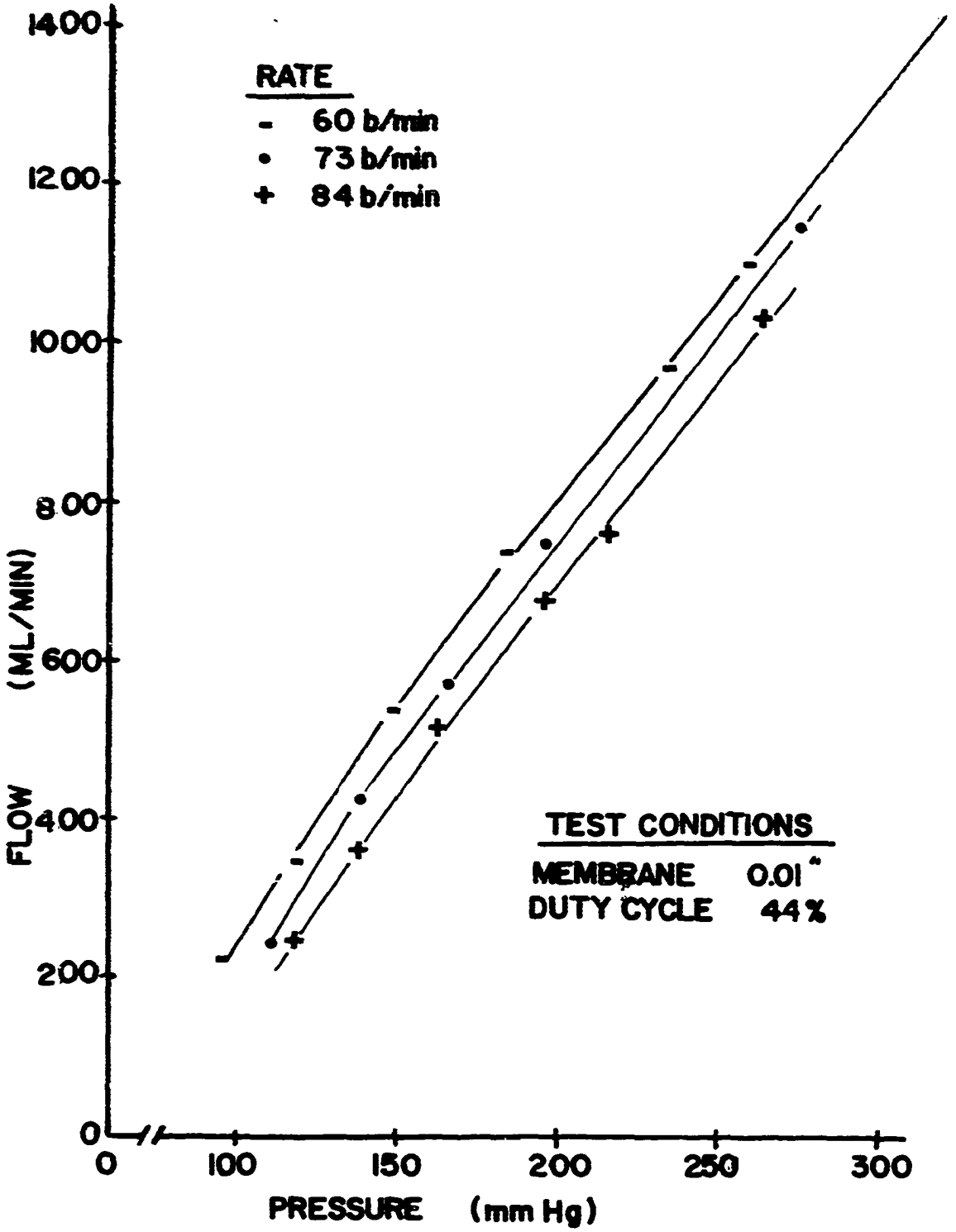

Figure 45. Artificial ventricle output vs. output fluid pressure for three rate values

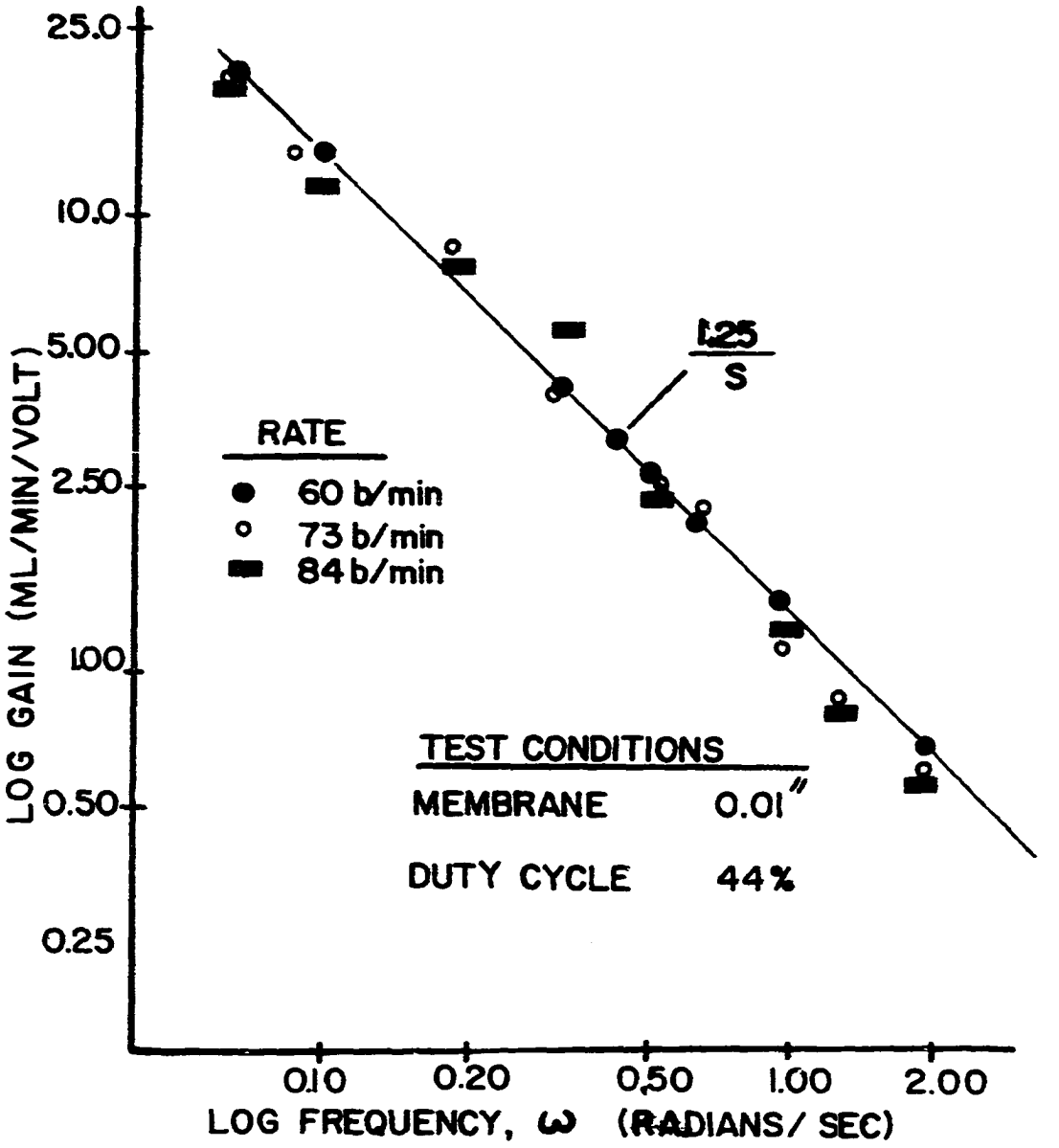

Figure 46. Bode amplitude plot for three rate values

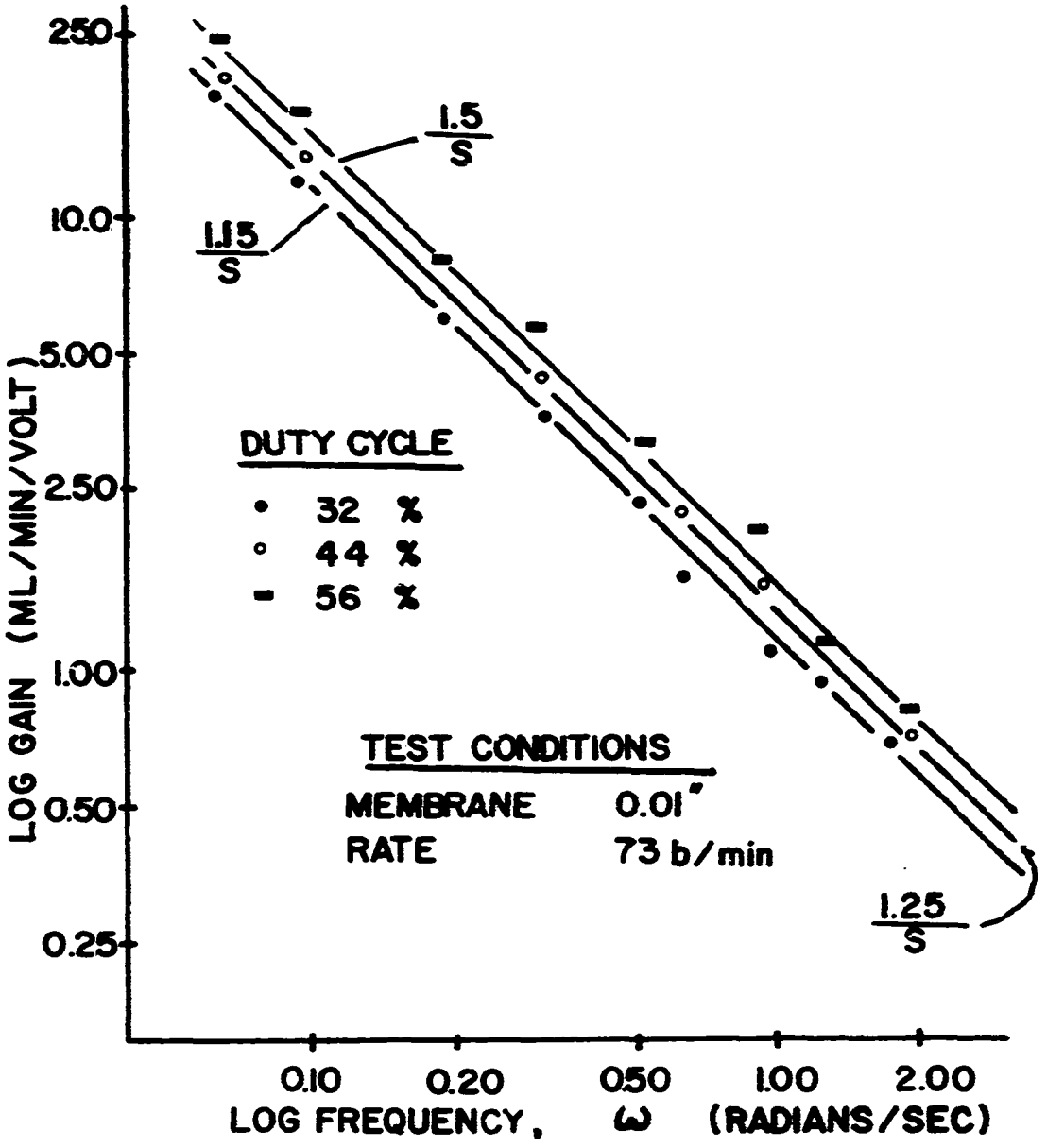

Figure 47. Bode amplitude plot for three duty cycle values

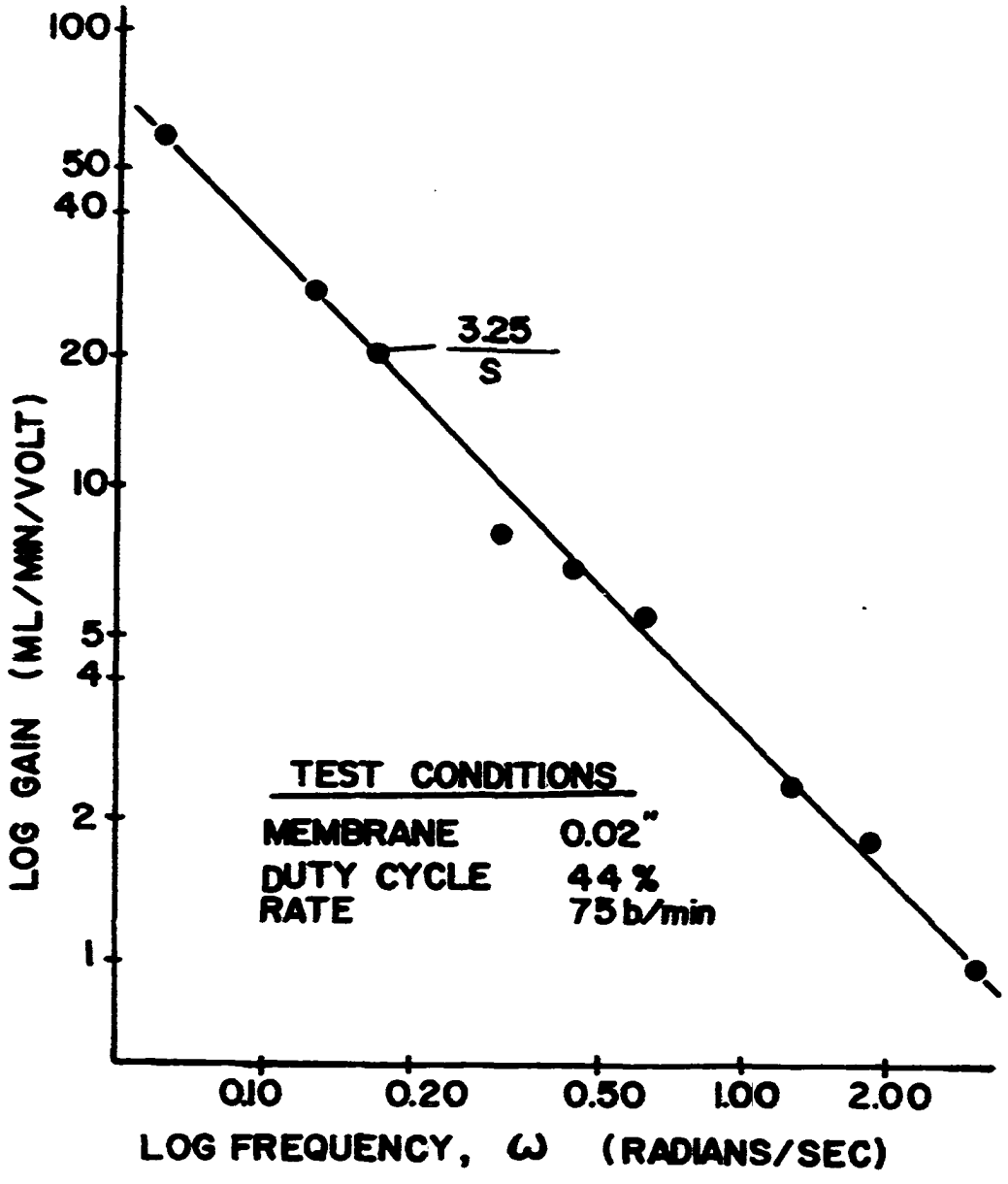

Figure 48. Bode amplitude plot

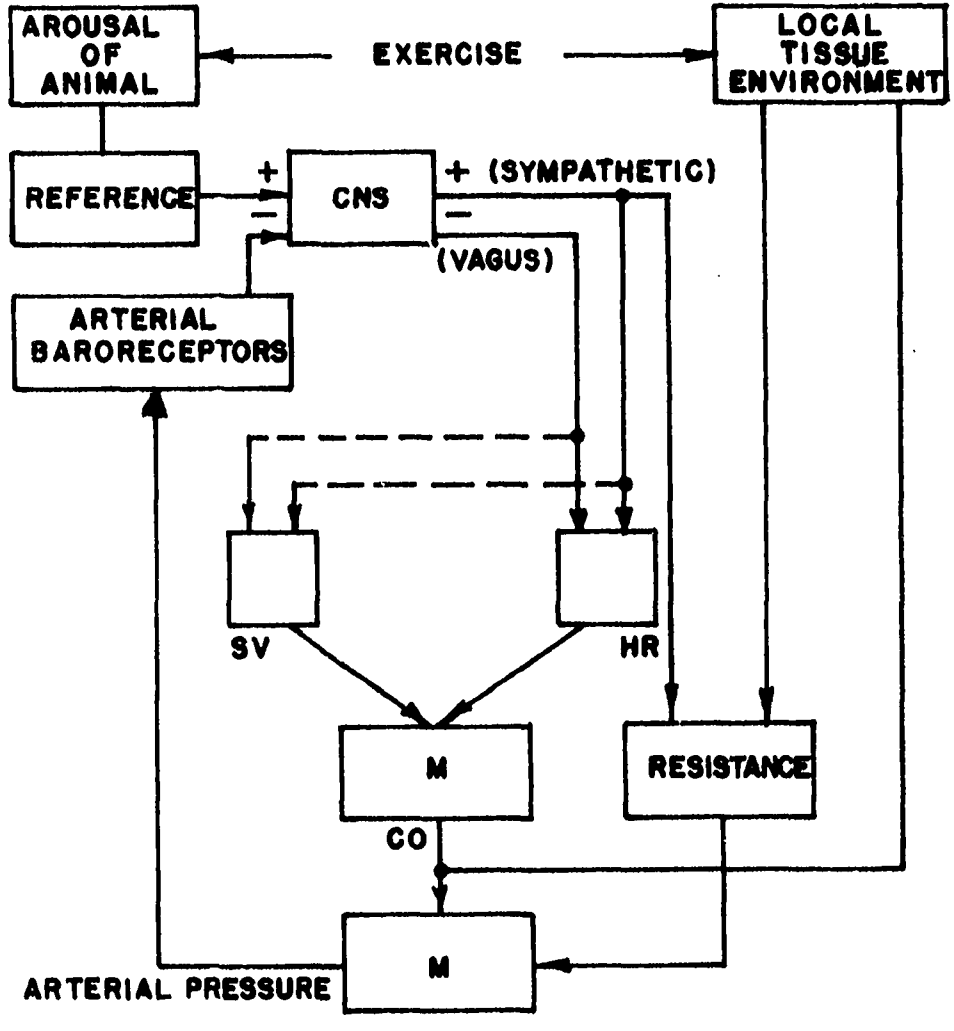

Figure 49. Block diagram of cardiac output control during exercise (Topham 78, p. 50)

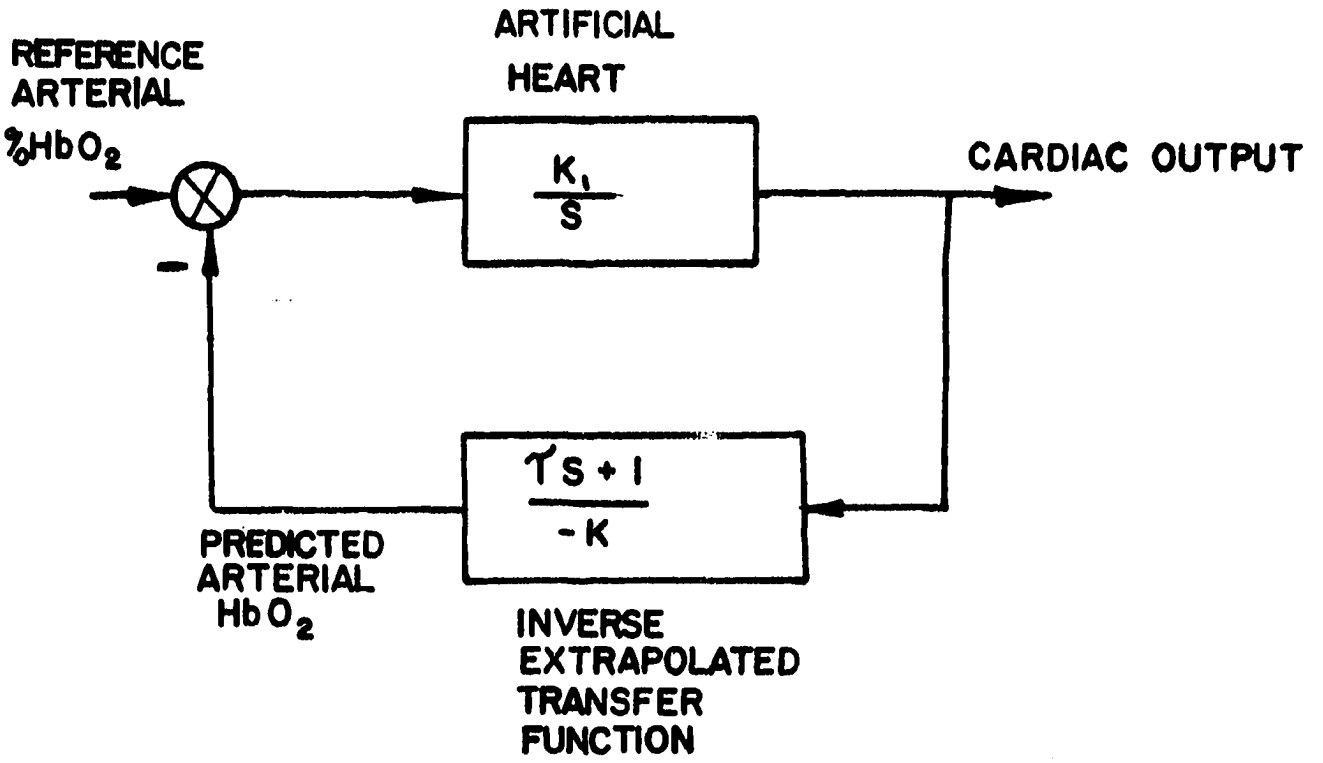

Figure 50. Closed loop artificial heart control system

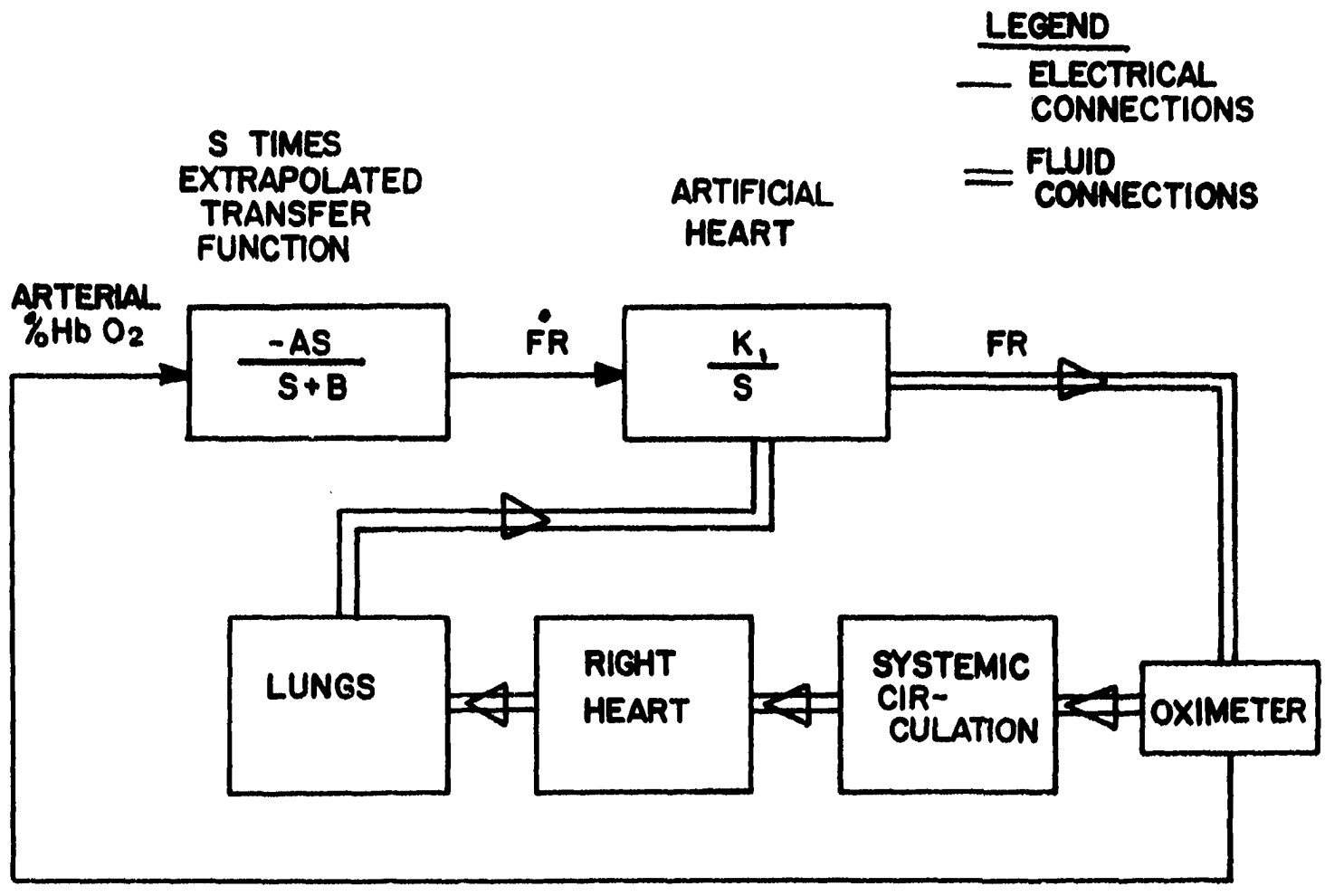

Figure 51. Open loop artificial heart control system

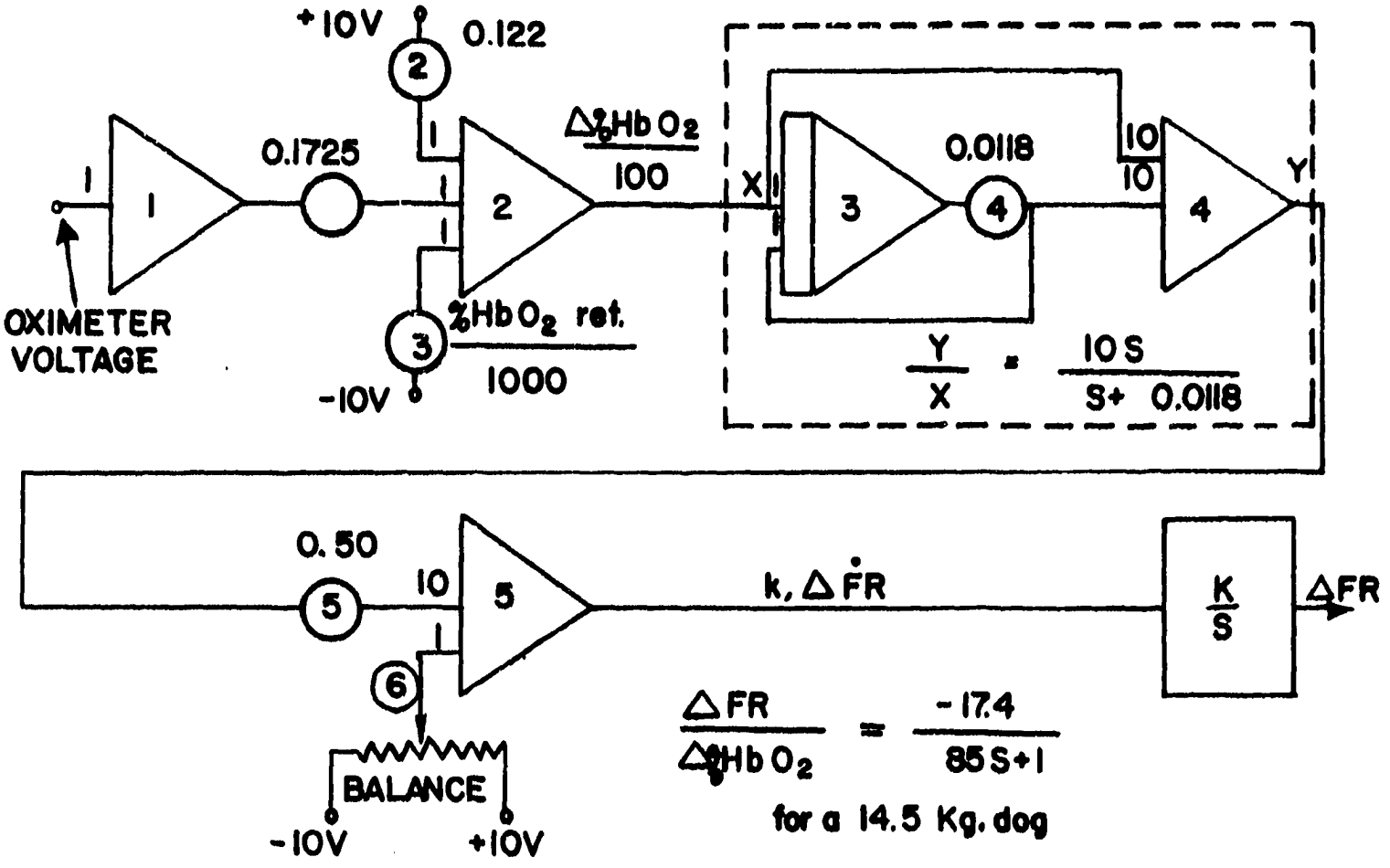

Figure 52. Schematic diagram of artificial heart control system

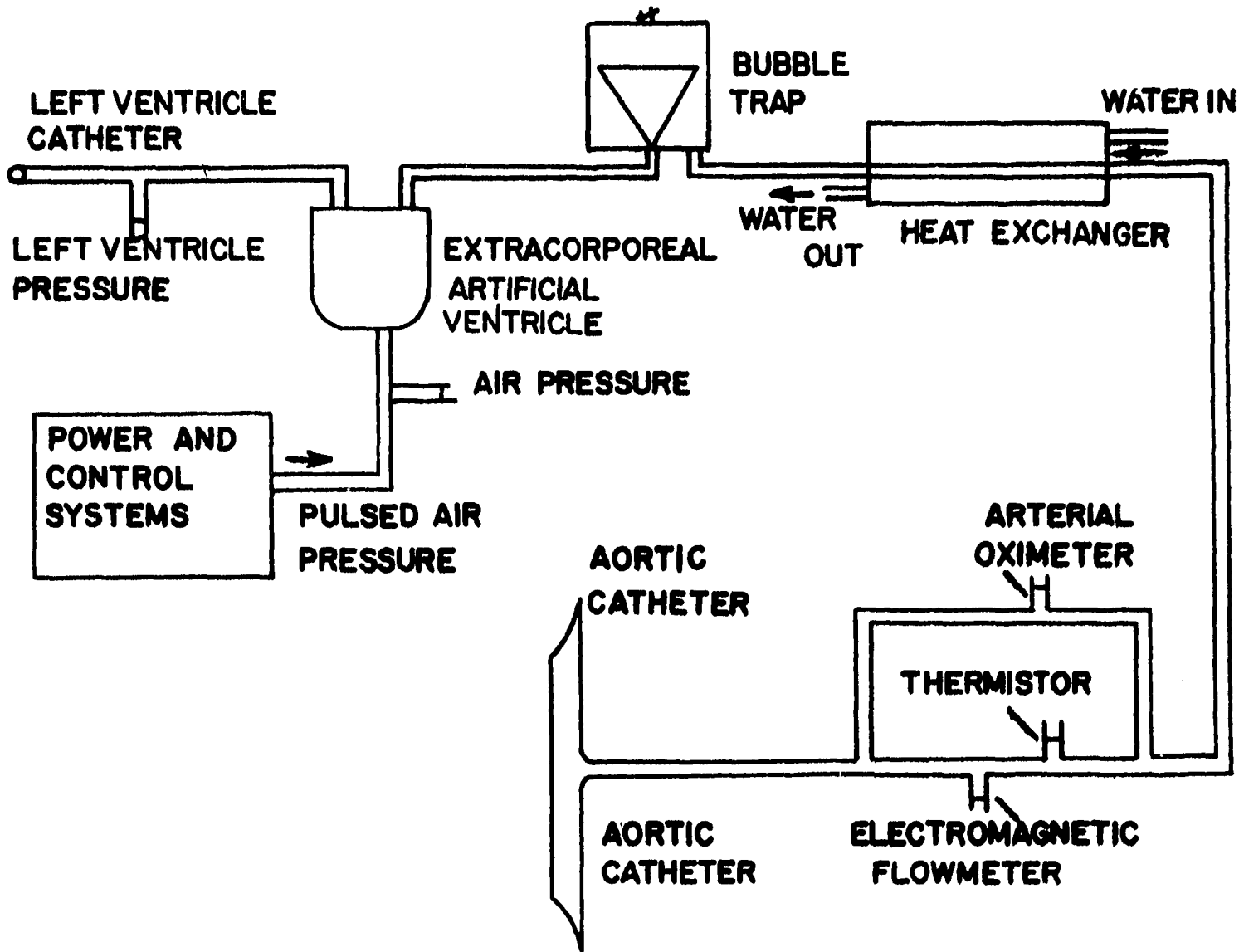

Figure 53. Schematic diagram of artificial heart perfusion system

Figure 54. A recording during an artificial heart experiment which illustrates the effect of changing the content of the inspired air from 100 percent oxygen to 10 percent oxygen and 90 percent nitrogen (arrow pointing down) and then back to 100 percent oxygen (arrow pointing up). Note that this figure is in three sections with the elapsed time indicated at the bottom of the figure

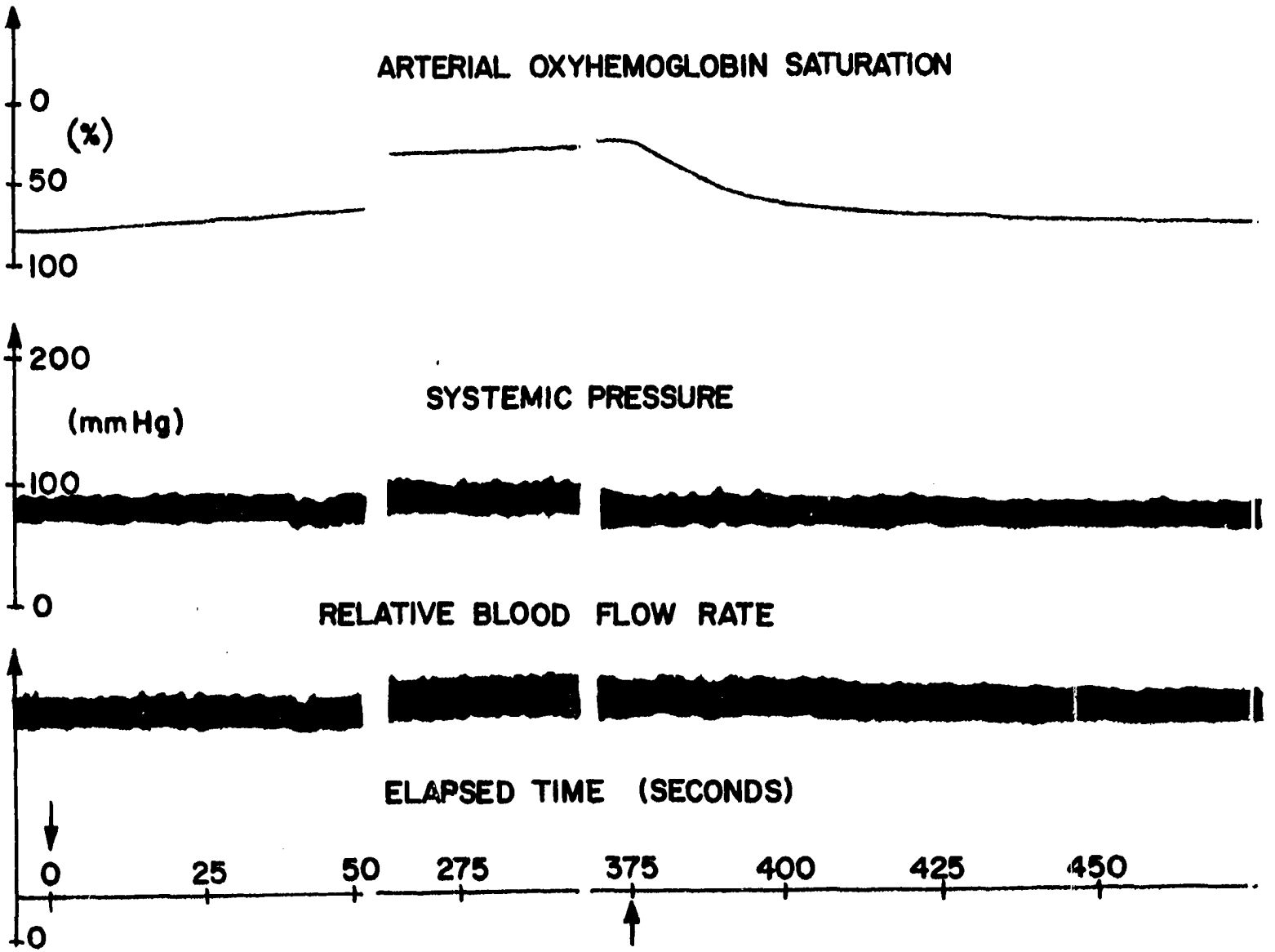
ARTERIAL OXYHEMOGLOBIN SATURATION
0
(%)
50
100
200
(mm Hg)
SYSTEMIC PRESSURE
100
0
RELATIVE BLOOD FLOW RATE
ELAPSED TIME (SECONDS)
0
25
50
275
375
400
425
450
0

BIBLIOGRAPHY

1. Akutsu, T., Takagi, H., Hardy, J. D. and Farish, C. A. A versatile control system for artificial hearts, its use with a left ventricular device. Conference on Engineering in Medicine and Biology Proceedings 20: 26.1. 1967.

2. Atsumi, Kazuhiko, Hori, Motokazu, Ikeda, Sadao, Sakurai, Yasuhisa, Fujimori, Yoshizo, and Kimoto, Seiji. Artificial heart incorporated in the chest. American Society for Artificial Internal Organs Transactions 9: 292-297. 1963.

3. Bayliss, W. M. On the local reactions of the arterial wall to changes of internal pressure. Journal of Physiology (London) 28: 220-231. 1902.

4. Berne, Robert M. and Levy, Matthew N. Cardiovascular physiology. Saint Louis, Missouri, The C. V. Mosby Company. 1967.

5. Brauer, Ralph W. Autoregulation of blood flow in the liver. In Johnson, Paul C. Autoregulation of blood flow. Pp. I-213 to I-221. New York, New York, The American Heart Association, Incorporated. 1964.

6. Burd, M. and Sear, B. High performance sample and holds. The Electronic Engineer 26: 60-64. 1967.

7. Burney, R. G., Pierce, W. S., Williams, K. R., Boyer, M. H. and Kirby, C. K. Studies on an artificial heart controlled by a venous pressure servomechanism. American Society for Artificial Internal Organs Transactions 9: 299-303. 1963.

8. Burns, Winton H., Loubier, R., and Bergstedt, R. The development of an electrohydraulic implantable artificial heart. American Society for Artificial Internal Organs Transactions 11: 265-268. 1965.

9. Burton, Alan C. Physiology and biophysics of the circulation. Chicago, Illinois, Year Book Medical Publishers, Incorporated. 1965.

10. Carrier, O., Jr., Walker, J. R., and Guyton, A. C. Comparative effects of pH and hypoxemia on minute coronary, mesenteric and skeletal muscle vessels. Angiology 17: 488-492. 1966.

11. Carrier, Oliver, Jr., Walker, James R., and Guyton, Arthur C. Role of oxygen in autoregulation of blood flow in isolated vessels. American Journal of Physiology 206: 951-954. 1964.

12. Cholvin, N. R., Erickson, H. H., Swift, C. S., and Pearson, P. T. Interdependence of venous pressure and oxyhemoglobin concentration in artificial heart control. International Conference on Medical and Biological Engineering Digest 7: 380. 1967.

13. Cholvin, Neal R., Erickson, Howard H., Swift, Curran S., and Pearson, Phillip T. Vascular responses to an automatically controlled artificial heart. Physiologist 9: 153. 1966.

14. Cholvin, Neal R., Swift, Curran S. and Erickson, Howard H. Progress report on the development of an artificial heart. American Veterinary Medical Association Journal 147: 1620-1627. 1965.

15. Clarke, W. Bromley, Lipicky, Raymond J., and Cohen, Gerald H. Model of the carotid sinus baroreceptor. Conference on Engineering in Medicine and Biology Proceedings 21: 3.9. 1968.

16. Coulam, Craig M., Warner, Homer R., Wood, Earl H., and Bassingthwaighte, James B. A transfer function analysis of coronary and renal circulation calculated from upstream and downstream indicator-dilution curves. Circulation Research 19: 879-890. 1966.

17. Crawford, Dewitt G., Fairchild, Hilton M. and Guyton, Arthur C. Oxygen lack as a possible cause of reactive hyperemia. American Journal of Physiology 197: 613-616. 1959.

18. Daly, M. de Burgh and Scott, Mary J. The cardiovascular responses to stimulation of the carotid body chemoreceptors in the dog. Journal of Physiology (London) 165: 179-197. 1962.

19. Daugherty, Robert M., Jr., Scott, Jerry B., Dabney, Joe M., and Haddy, Francis J. Local effects of O_2 and CO_2 on limb, renal, and coronary vascular resistances. American Journal of Physiology 213: 1102-1110. 1967.

20. Daugherty, Robert M., Jr., Scott, Jerry B., and Haddy, Francis J. Effects of generalized hypoxemia and hypercapnia on forelimb vascular resistance. American Journal of Physiology 213: 1111-1114. 1967.

21. Dedichen, Henrik, Race, David, and Schenk, Worthington G. Hemodilution and concomitant hyperbaric oxygenation. The Journal of Thoracic and Cardiovascular Surgery 53: 341-348. 1967.

22. Demaret, Kent. Why transplant patients die. Worcester, Massachusetts, The Worcester Evening Gazette. P. 7. January 2, 1969.

23. Detar, R. L. and Bohr, D. F. Oxygen and vascular smooth muscle contraction. American Journal of Physiology 214: 241-251. 1968.

24. Edgington, Glenn E. Reflection characteristics of hemodynamic systems under coherent optical radiation. Unpublished Ph.D. thesis. Ames, Iowa, Library, Iowa State University of Science and Technology. 1965.

25. Edgington, Glenn E. and Cholvin, Neal R. The reflection characteristics of hemodynamic systems at 632.8 mu. Rochester, Minnesota, International Business Machines Engineering Publications, Systems Development Division Laboratory. 1965.

26. Edwards, John F., Jr. and Bosher, Lewis H., Jr. Physiologically responsive closed loop servo in the control of cardiopulmonary bypass. American Society for Artificial Internal Organs Transactions 7: 175-179. 1961.

27. Enson, Yale, Jameson, A. Gregory and Cournand, Andre. In vivo studies with an intravascular and intracardiac reflection oximeter. Journal of Applied Physiology 17: 552-561. 1962.

28. Erickson, Howard H. Continuous measurement of oxyhemoglobin concentration by reflection oximetry and its use in controlling an artificial heart. Unpublished Ph.D. thesis. Ames, Iowa, Library, Iowa State University of Science and Technology. 1966.

29. Erickson, Howard H., Cholvin, N. R., Swift, C. S., Pearson, P. T., Workman, H. W., and Al-Nakeeb, S. Reflection oximetry: its use during cardiopulmonary bypass and artificial heart studies. International Conference on Medical and Biological Engineering Digest 7: 279. 1967.

30. Erickson, Howard H., Cholvin, Neal R., and Swift, Curran S. The use of oxyhemoglobin as a means of controlling an artificial heart. Conference on Engineering in Medicine and Biology Proceedings 19: 149. 1966.

31. Fairchild, Hilton M., Ross, Joe, and Guyton, Arthur C. Failure of recovery from reactive hyperemia in the absence of oxygen. American Journal of Physiology 210: 479-492. 1966.

32. Fleischli, G., and Bellville, J. W. Servo-analytic studies of cardiovascular control using sinusoidal norepinephrine infusions. San Diego Symposium for Biomedical Engineering Proceedings 42: 78-84. 1964.

33. Gorlin, Richard, and Lewis, Benjamin, M. Circulatory adjustments to hypoxia in dogs. Journal of Applied Physiology 7: 180-185. 1954.

34. Grodins, Fred S. Control theory and biological systems. New York, New York, Columbia University Press. 1963.

35. Guyton, Arthur C. Circulatory physiology: cardiac output and its regulation. Philadelphia, Pennsylvania, W. B. Saunders Company. 1963.

36. Guyton, Arthur C. Medical physiology. 2nd edition. Philadelphia, Pennsylvania, W. B. Saunders Company. 1966.

37. Guyton, Arthur C. and Harris, Jeff W. Pressoreceptor-autonomic oscillation: a probable cause of vasomotor waves. American Journal of Physiology 165: 158-166. 1951.

38. Guyton, Arthur C., Milhorn, Howard T., Jr., and Coleman, Thomas G. Simulation of physiological mechanisms. Part II. Simulation 9: 73-79. 1967.

39. Guyton, Arthur C., Ross, J. M., Carrier, Oliver and Walker, James R. Evidence for tissue oxygen demand as the major factor causing autoregulation. In Johnson, Paul C. Autoregulation of blood flow. Pp. I-60 to I-69. New York, New York, The American Heart Association, Incorporated. 1964.

40. Hall, C. William, Akers, W. W., O'Bannon, William, Liotta, Domingo, and De Bakey, Michael E. Intraventricular artificial heart. American Society for Artificial Internal Organs Transactions 11: 263-264. 1965.

41. Hastings, F. W., Holter, J. W., and Potter, W. H. A progress report on the development of a synthetic intracorporeal blood pump. American Society for Artificial Internal Organs Transactions 8: 116-117. 1962.

42. Hiller, Kirby W., Seidel, Wolfgang, and Kolff, Willem J. An electronic-mechanical control for an intrathoracic artificial heart. American Journal of Medical Electronics 2: 212-221. 1963.

43. Johnson, Paul C. Origin, localization, and homeostatic significance of autoregulation in the intestine. In Johnson, Paul C. Autoregulation of blood flow. Pp. I-225 to I-232. New York, New York, The American Heart Association, Incorporated. 1964.

44. Johnson, Paul C. Review of previous studies and current theories of autoregulation. In Johnson, Paul C. Autoregulation of blood flow. Pp. I-2 to I-9. New York, New York, The American Heart Association, Incorporated. 1964.

45. Kahler, Richard L., Goldblatt, Allan, and Braunwald, Eugene. The effects of acute hypoxia on the systemic venous and arterial systems and on myocardial contractile force. Journal of Clinical Investigation 41: 1553-1563. 1962.

46. Kapny, N. S. and Silbertrust, N. Fiber optics spectrophotometer for in vivo oximetry. Nature 204: 138-142. 1964.

47. Katona, Peter G. The cardiovascular system. In Stark, Lawrence, Young, Laurence R., Taub, Robert, Taub, Arthur, and Katona, Peter G., eds. Biological control systems — a critical review and evaluation. Washington, D.C., National Aeronautics and Space Administration, NASA Contractor Report NASA CR-577. 1966.

48. Katona, P., Barnett, G., and Jackson, W. Computer analysis of the blood pressure control of heart period. Cambridge, Massachusetts, Massachusetts Institute of Technology, Research Laboratory of Electronics, Information Exchange Group No. 3, Scientific Memo No. 38. 1966.

49. Koch, E. Die reflektrosiche selbststeuerung des kreislaufes. Ergeb. Kreislaufforsch. 1:1. 1931. Original not available for examination; cited in Warner, Homer R., Topham, W. Sanford, and Nicholes, Karl K. The role of peripheral resistance in controlling cardiac output during exercise. New York Academy of Sciences Annals 115: 669-679. 1964.

50. Kontos, Hermes A., Mauck, H. Page, Jr., Richardson, David W., and Patterson, John L., Jr. Mechanism of circulatory responses to systemic hypoxia in the anesthetized dog. American Journal of Physiology 209: 397-403. 1965.

51. Kwan-Gett, C. S., Crosby, M. J., Schoenberg, A., Jacobsen, S. C., and Kolff, W. J. Control systems for artificial hearts. American Society for Artificial Internal Organs Transactions 14: 284-290. 1968.

52. Lanig, R. B. Studies basic to considerations of artificial heart research and development program. Windsor Locks, Connecticut, Hamilton Standard Division, United Aircraft Corporation, Final report to National Heart Institute, National Institute of Health, Department of Health Education of Welfare, Bethesda, Maryland, Contract No. PH43-66-20. 1966.

53. Levison, W. H., Barnett, G. O., and Jackson, W. D. Nonlinear analysis of the baroreceptor reflex system. Circulation Research 17: 673-682. 1966.

54. Litwin, Jerzy, Dil, Abdul Habib, and Aviado, Domingo M. Effects of anoxia on the vascular resistance of the dog's hind limb. Circulation Research 8: 585-593. 1960.

55. Nicoll, Paul A. and Webb, Richard L. Vascular patterns and active vasomotion as determiners of flow through minute vessels. Angiology 6: 291-310. 1955.

56. Norton, S. Harry, Akutsu, Tetsuzo, and Kolff, Willem J. Artificial heart with anti-vacuum bellows. American Society for Artificial Internal Organs Transactions 8: 131-134. 1962.

57. Nosé, Yukihiko. Artificial heart inside the chest: past, present, and future. Institute of Electrical and Electronics Engineers International Convention Record, Symposium on Bio-Medical Engineering, Part 12: 11-19. 1965.

58. Olsson, Ray A. Kinetics of myocardial reactive hyperemia blood flow in the unanesthetized dog. In Johnson, Paul C. Autoregulation of blood flow. Pp. I-81 to I-86. New York, New York, The American Heart Association, Incorporated. 1964.

59. Penrose, R. A generalized inverse for matrices. Cambridge Philosophical Society Proceedings 51: 406-413. 1954.

60. Pierce, William S., Burnex, Robert G., Boyer, Mark H., Driscoll, Robert W., and Kirby, Charles K. Problems encountered in experiments during the development of our artificial intrathoracic heart. American Society for Artificial Internal Organs Transactions 8: 118-122. 1962.

61. Pierce, William S., Burney, Robert G., Williams, Kirkley R., and Kirby, Charles K. A servomechanism to control output of an artificial ventricle. Journal of Applied Physiology 18: 1029-1032. 1963.

62. Polanyi, Michael L. and Hehir, R. M. New reflection oximeter. Review of Scientific Instruments 31: 401-403. 1960.

63. Radio Corporation of America. RCA phototubes and photocells, technical manual PT-60. Lancaster, Pennsylvania, author. 1963.

64. Rapela, Carlos E. and Green, Harold D. Autoregulation of canine cerebral blood flow. In Johnson, Paul C. Autoregulation of blood flow. Pp. I-205 to I-211. New York, New York, The American Heart Association, Incorporated. 1964.

65. Ross, J. M., Fairchild, H. M., Weldy, J. F., and Guyton, A. C. Autoregulation of blood flow by oxygen lack. American Journal of Physiology 202: 21-24. 1962.

66. Roy, C. S. and Brown, J. G. The blood pressure and its variations in the arterioles, capillaries and smaller veins. Journal of Physiology (London) 2: 323-359. 1879.

67. Rust, B., Burrus, W. R., and Schneeberger, C. A simple algorithm for computing the generalized inverse of a matrix. Association for Computing Machinery 9: 381-387. 1966.

68. Sagawa, Kiichi, Taylor, A. E., and Guyton, A. C. Dynamic performance and stability of cerebral ischemic pressor response. American Journal of Physiology 201: 1164-1172. 1961.

69. Sagawa, K. and Watanabe, K. Summation of bilateral carotid sinus signals in the barostatic reflex. American Journal of Physiology 201: 1164-1172. 1961.

70. Scher, A. M. and Young, A. C. Servoanalysis of carotic sinus reflex effects on peripheral resistance. Circulation Research 12: 152-162. 1963.

71. Seidel, Wolfgang, Akutsu, Tetsuzo, Mirkovitch, Velimir, Brown, Frederick, and Koff, Willem J. Air-driven artificial hearts inside the chest. American Society for Artificial Internal Organs Transactions 7: 378-385. 1961.

72. Selkurt, Ewald E. Summary remarks on autoregulation of renal blood flow. In Johnson, Paul C. Autoregulation of blood flow. Pp. I-198 to I-199. New York, New York, The American Heart Association, Incorporated. 1964.

73. Shipley, R. E. and Wilson C. A simplified recording rotameter. Society for Experimental Biology and Medicine Proceedings 78: 724-728. 1951.

74. Smith, Elvin E. and Crowell, Jack W. Influence of hypoxia on mean circulatory pressure and cardiac output. American Journal of Physiology 213: 1067-1069. 1967.

75. Swift, Curran S. The design of an artificial ventricle and its power and control systems. Unpublished Ph.D. thesis. Ames, Iowa, Library, Iowa State University of Science and Technology. 1966.

76. Swift, Curran S., Cholvin, Neal R. and Erickson, Howard H. A control system for an artificial heart. Conference on Engineering in Medicine and Biology Proceedings 18: 56. 1965.

77. Swift, Curran S., Cholvin, Neal R. and Erickson, Howard H. A control system for an artificial heart. Medical Research Engineering 7: 10-13. 1968.

78. Topham, W. Sanford. An analog model of the control of cardiac output. Simulation 8: 49-53. 1967.

79. Topham, William S. Control of Cardiac output studies with computer techniques. Unpublished Ph.D. thesis. Salt Lake City, Utah, Library, University of Utah. 1965.

80. Walker, James R. The current status of autoregulation of blood flow. Texas Reports on Biology and Medicine 24: 418-425. 1966.

81. Walker, James R. The effects of blood-oxygen content on autoregulation in skeletal muscle. Unpublished Ph.D. thesis. Jackson, Mississippi, Library, University of Mississippi School of Medicine. 1966.

82. Walker, James R. and Guyton, Arthur C. Influence of oxygen saturation on pressure-flow curve of dog hindleg. American Journal of Physiology 212: 506-509. 1967.

83. Warner, H. R. The frequency-dependent nature of blood pressure regulation by the carotid sinus — studies with an electronic analog. Circulation Research 6: 35-40. 1958.

84. Warner, H. R. A study of the mechanism of pressure wave distortion by arterial walls using an electrical analog. Circulation Research 5: 79-84. 1957.

85. Warner, H. R. The use of an analog computer for analysis of control mechanisms in the circulation. Institute of Radio Engineers Proceedings 47: 1913-1916. 1959.

86. Warner, H. R. and Cox, A. A mathematical model of heart rate control by sympathetic and vagus efferent information. Journal of Applied Physiology 17: 349-355. 1962.

87. Warner, Homer R., Topham, W. Sanford, and Nicholes, Karl K. The role of peripheral resistance in controlling cardiac output during exercise. New York Academy of Sciences Annals 115: 669-679. 1964.

88. Wieting, David W., Hall, C. William, Kreisle, Leonardt F., Liotta, Domingo, and De Bakey Michael E. Design of a system for analyzing flow behavior of prosthetic human heart valves. Houston, Texas, Texas Medical Center, Cardiovascular Research Center Bulletin 5: 41-56. 1966.

89. Wildevuur, C. R. H., Mrava, G. L., Crosby, M. J., Wright, J. I., Hladky, H. L., Andresen, G. J., Pierson, R. M., Kon, T., and Nosé, Y. An artificial heart sensitive to atrial volume. American Society for Artificial Internal Organs Transactions 14: 276-283. 1968.

90. Zadeh, Lotfi A. and Desoer, Charles A. Linear system theory: the state space approach. New York, New York, McGraw-Hill Book Company, Incorporated. 1963.

ACKNOWLEDGMENTS

The author would like to express his sincere appreciation to the many people who contributed to this research. I especially wish to thank the following: Dr. Neal R. Cholvin, co-major professor, for providing guidance and encouragement for the research, the many hours spent in the surgery room, and for helping greatly in the preparation of this dissertation; to Dr. Harry W. Hale, co-major professor, for his encouragement, counsel and assistance in my graduate program; to Dr. William H. Brockman for his guidance and counsel in the research; to Drs. Phillip T. Pearson, Shaheen Al-Nakeeb, Charles E. Bonney and Robert W. Carithers for the surgical preparation of the animals; to Mr. Dennis J. Duven for the preparation of the computer program; to Dr. David Cox for his assistance in the statistical analysis of the data; to Dr. Curran S. Swift for the use of his artificial heart system, to Dr. Glen A. Richardson for making time available for this dissertation preparation; to Mr. Steven Johnson, Mr. Michael Brown, Mr. Robert Akins and Mrs. Barbara Royer for their technical assistance; to Mr. Paul Amazeen for his photographic work; to Mr. David Maki and Miss Marilyn Clem for the illustrations; and to Mrs. Marjorie Wibholm for the final preparation of this dissertation.

A special appreciation is due to his family - his parents for their continued support and encouragement, his wife, Carol, and son Glenn, who made the many sacrifices during his graduate study and to whom this dissertation is dedicated.

This investigation was supported by a National Defense Education Act Title IV Fellowship and a Public Health Service Predoctoral Fellowship.